Suite 1414, Executive Plaza, 555 Sparkman Drive, Huntsville, Alabama 35805, (205) 837-8510

DEFINITION OF GROUND TEST FOR VERIFICATION OF LARGE SPACE STRUCTURE CONTROL

FINAL REPORT
NOVEMBER 1984

Sponsored By:

George C. Marshall Space Flight Center
Marshall Space Flight Center, Alabama 35812

Under:

Contract NO. NAS8-34700

Contributors:
Dr. George B. Doane III
Dr. John R. Glaese
Danny Tollison
Thomas Howsman
Sally Curtis
Betsy Banks

Edited By:
Sally Curtis

Prepared By:

Control Dynamics Company
555 Sparkman Drive, Suite 1414
Huntsville, AL 35805

ABSTRACT

This paper discusses the work performed under contract No. NAS8-34700. The body of the paper deals mainly with descriptions of the tasks undertaken in a chronological order, with references made to detailed theories contained in the monthly reports. Those reports referenced are located in their corresponding appendices so that this document may stand alone.

The main tasks discussed in this report include control theory and design, dynamic system modelling, and simulations of test scenarios. Other miscellaneous projects also in this paper include two papers presented and co-authored by Marshall Space Flight Center and Control Dynamics, and supervision of hardware construction.

TABLE OF CONTENTS

INTRODUCTION

This contract, throughout the years of its existence, has been associated with several different and varying tasks. These tasks have ranged from evaluating test articles and testing locations to control system design to system modeling to test simulations. These tasks and others all maintain the goal of supporting Marshall Space Flight Center (MFSC) in its effort to achieve a successful ground test experiment of a large space structure (LSS).

This final report deals with the time period ranging from October 1982 until the contract's official end in July 1984. A report dealing with the first year of the contract has previously been delivered in the form of an oral presentation to MSFC and can be found in Appendix A.

LEVEL of EFFORT

The first project in the reporting time frame was the generation of a planar model of the ground test experiment structure. This was done by adapting an in-house modal analysis code (Gimbalflex) to allow placement of sensors and actuators at certain locations on the structure. At this point certain system characteristics had to be assumed as they were not as well known as they are currently. Figure 1 depicts the planar model and Attachment 1 from the 13th Monthly Report (MR) (found in Appendix B) delves more carefully into the theory behind this model.

The next step in the development of this model was to adapt it for use with the control pole placement algorithm. This amounted to removing the uncontrollable rigid body mode from the model. This uncontrollable mode was due to the pointing of the gimbal. The method to eliminate this mode is discussed in Attachment 1 from MR #14 (Appendix C).

Control system design for the planar model was also initiated during this time. A digital controller was being planned utilizing the Control Pole Placement technique. One assumption made in dealing with this design was the existence of rate of state feedback.

Once this controller and other control algorithms were developed, it became necessary to conduct speed tests on the HP9845C to determine if the 20ms sample period requirement could be met. It was discovered that it could not be met with the given equipment. A study was then made of additional hardware/software necessary to meet the speed requirement. The results of this study yielded several alternatives varying in cost and can be found in the 16th MR (Appendix D).

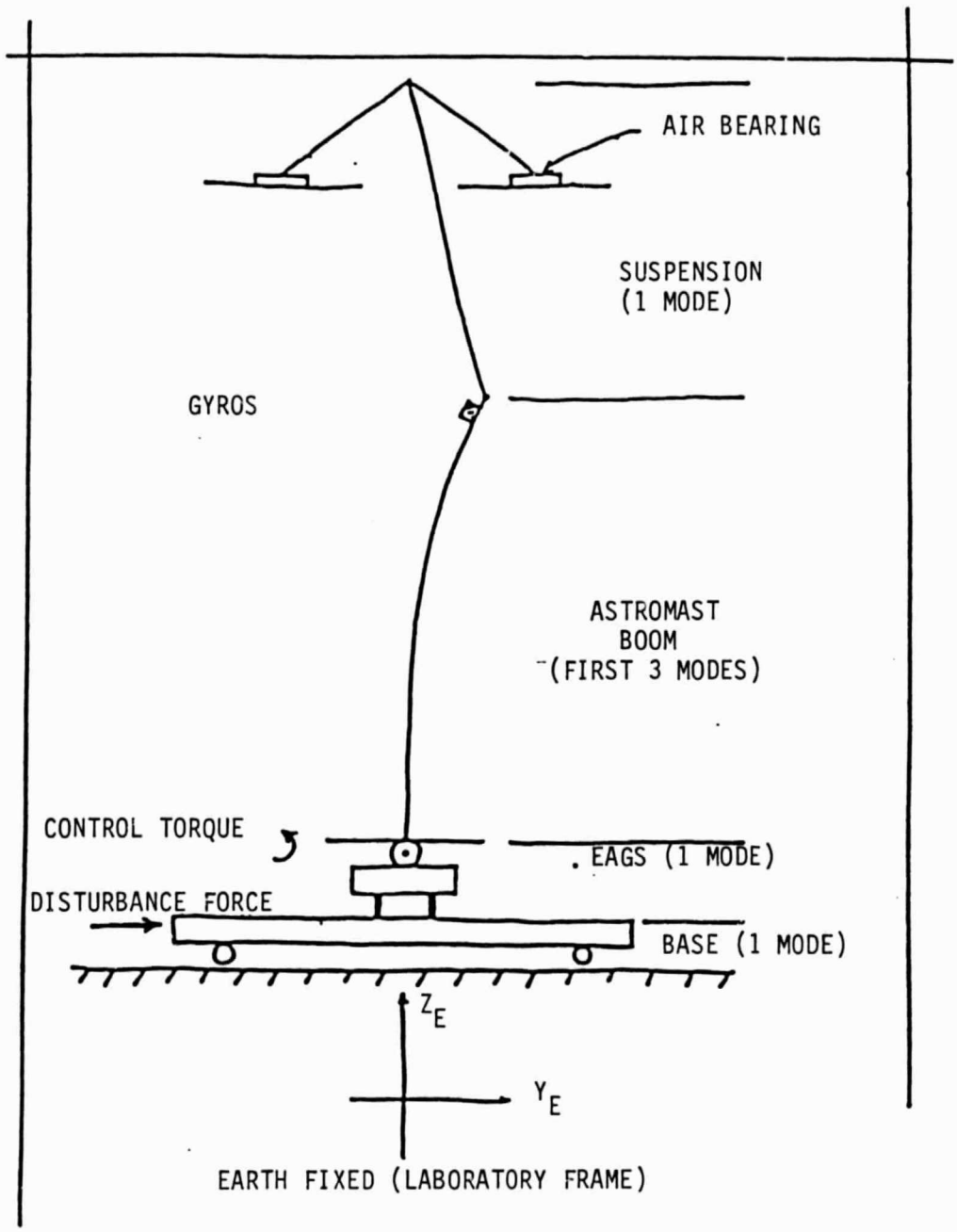

FIGURE 1. Planar Version of the LSS-GTV Structure.

Next, an analysis was made concerning the support of the tip instrument package mount. The following recommendations were made:

1. The tip support mechanism should be capable of exerting a constant, but adjustable force on the tip of the structure. The magnitude of this force should be variable over the range from a value corresponding to all the weight of the equipment above the roll gimbal down to as near to zero as practical (most likely around 5 pounds).
2. The mount used to attach the tip instrument package to the mast should incorporate the possibility of attaching weights to it. These weights could be used not only to balance the instrument package with respect to the mast but also to cause known and adjustable degrees of unbalance. This unbalance could be used to couple inertially the different modes of oscillation; i.e. in plane, out of plane, and torsional.

Figure 2 depicts the system design at the time of the above recommendations.

In order to design an accurate control system, a good dynamic model is necessary. At this stage it was deemed necessary to construct a better model of the ASTROMAST than had previously existed. The beam was modeled as 273 point masses (three for each of the 91 sections), each mass having three translational degrees of freedom with the exception of the three masses representing the tip section. They were restrained in one degree of freedom by being attached to the tip mass instrument package. This yielded a system of 816 second order equations of the form:

$$M\ddot{x} + Kx = 0,$$

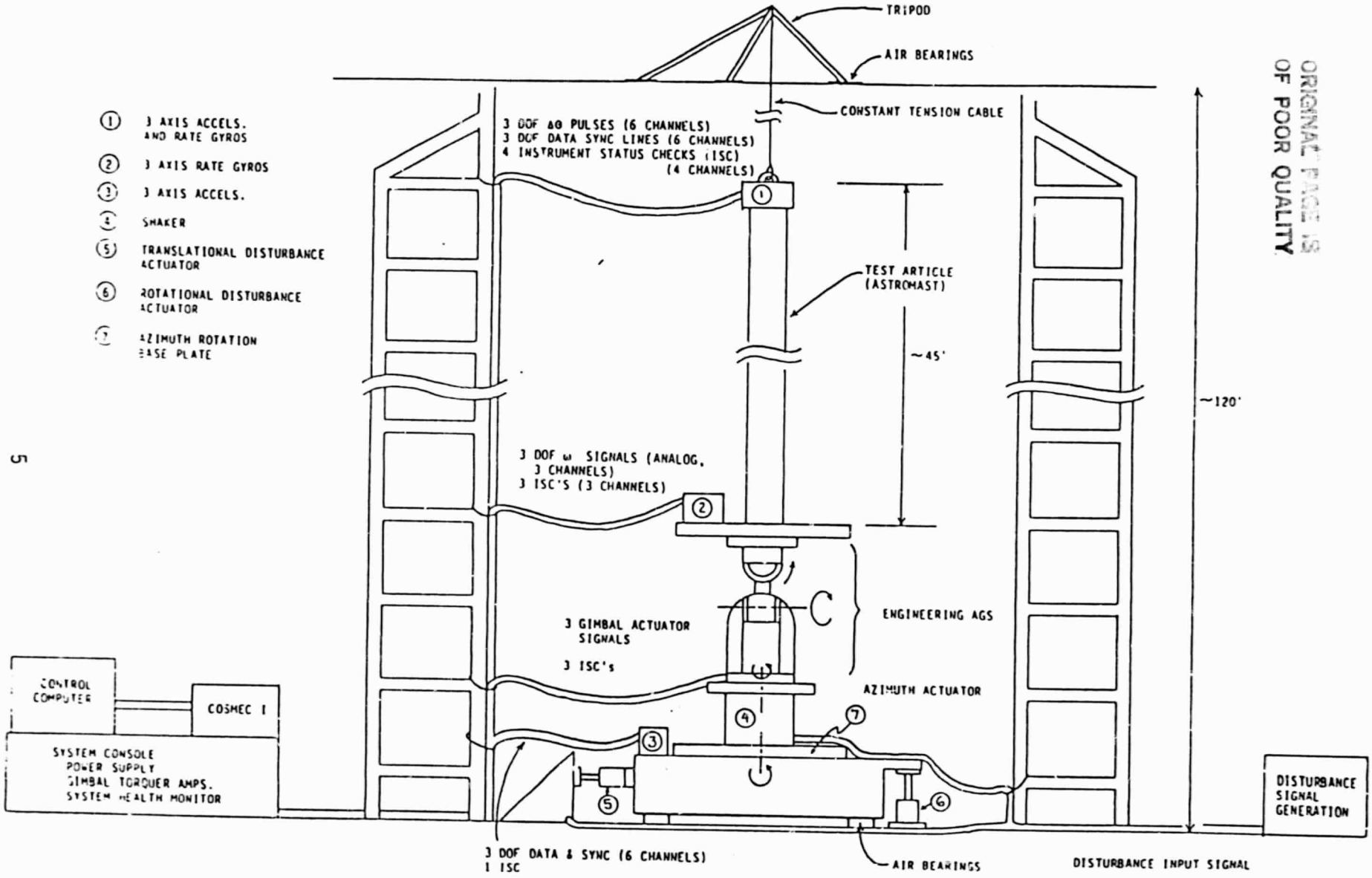

FIGURE 2. NASA LSS Ground Test Verification Facility

where M is a diagonal matrix of order 816 and K is a symmetric, 14 banded matrix, also of order 816.

It can be easily seen that the problem of determining the modal frequencies of the system can be reduced to that of determining the values of ω (frequency) such that

$$\det[\, K - M\,\omega^2] = 0.$$

This approach was straightforward; however, computational problems remained in finding the determinant of an 816th order matrix. Several methods were attempted which took into account the sparseness, bandedness, and symmetry of the problem. While these methods did reduce the problem somewhat, the problem was still extensive.

At this point a less complex model was developed. This method involved dividing the ASTROMAST into several lumped masses joined by massless rods. This is a standard practice in dealings with beam structures as developed by N.O. Myklestad and M.A. Prohl. The number of lumped masses was varied, until the value of 91 was eventually decided upon. Each section was described by a point and field matrix relating deflections, slopes, moments, shears, angles, and torsions at each lumped mass. The matrices were then consecutively multiplied to relate base and tip conditions. Because of the symmetry of the ASTROMAST, the torsional and translational modes could be uncoupled to obtain these frequencies separately. The theory behind this method can be found in the 21st MR (Appendix E). The values obtained using this method are listed in Table 1. Independent checks for both torsional and translational frequencies were calculated and they compared favorably. (Torsional check may also be found in Appendix E.)

TABLE 1
MODEL FREQUENCIES

Bending Frequencies	Torsional Frequencies
0.62 Hz	6.88 Hz
3.92 Hz	———
11.18 Hz	———

Once this model of the mast was built, it could then be incorporated into a modal synthesis technique to build up a model of the entire test system. The results of this model are located in Appendix F.

Using the above results, Dr. Henry Waites of MSFC and Dr. George Doane and Danny Tollison of Control Dynamics wrote and presented a paper at the AIAA Guidance and Control Conference at Gatlinburg, Tennessee during August of 1983. This paper was entitled: "Definition of Ground Test for Large Space Structure Control Verification". This paper described the experiment itself, the equipment to be used, the above modal results and a comparison of these results with the experimental results. The comparison results are shown below in Table 2. A copy of this paper is located in Appendix G.

At this point the work shifted back to control related tasks. A review was made of Dr. Henry Waites' technical papers on controlling large space structures. Three techniques were studied:

1. observer techniques,
2. closed-loop pole placement techniques, and
3. a disturbance isolation technique.

	Experimental (Hz)	Analytical (Hz)	% Difference
Bending*	0.56	0.62	11
	3.4	3.9	16
	----	11	--
Torsion	--	6.9	--
	21	21	0.0
	29	34	19

* Two modes at each frequency

Table 2. Summary of Modal Frequencies from Model and Test Results for the Cantilivered ASTROMAST Beam.

Of these three methods, the Pole Placement Method is expected to be the most practical and useful. For a more thorough examination of these methods, see the 23rd MR (Appendix H).

Another important aspect of this contract was simulation work. A simulation existed written in APL on the NASA computer, but one needed to exist at Control Dynamics in FORTRAN. This simulation would eventually be used to run test scenarios of the actual test set-up. The simulation contains transformation matrices from the tip and base instrument packages to the laboratory reference frame, the strapdown algorithm, torque controllers, Dr. Waites' controllers, and the results from modal analysis techniques.

The first step in this process was to convert the APL simulation to FORTRAN and resolve any discrepancies which might appear between the two versions. Next, various details were added to achieve a more realistic test scenario; uncertainties were added to the gyros and accelerometers, and accelerometer readings were added at the tip and base to allow for corrections due to constant accelerations due only to gravity.

Dr. Waites of MSFC and Danny Tollison of Control Dynamics wrote and presented another paper entitled: "Ground Test Experiment for Large Space Structures" at the 16th Southeastern Symposium on System Theory at Mississippi State University. For more information on this paper see the 28th MR (Appendix I). A major modification initialed by MSFC, of the test structure appeared in this paper: the entire structure had been flipped up-side down. This can be seen in Figure 3. Several reasons existed which brought about this change; a main reason was the complexity and cost of the tip support system. The revised structure reduced this to a more manageable problem.

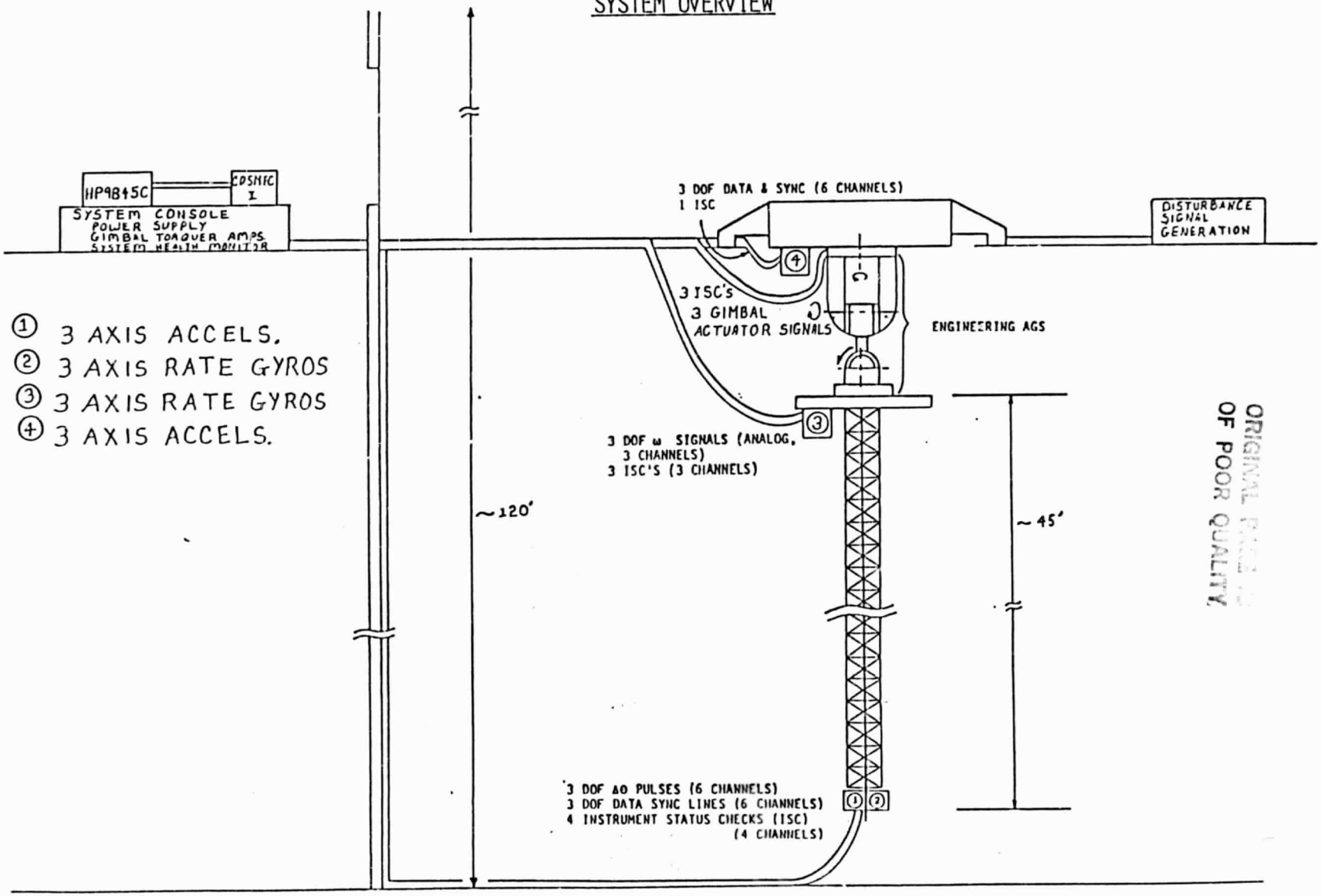

Figure 3. Modified Test Facility

Again, the dynamics came into question. A better model was again needed not only for the control system, but also to be modified to obtain LSS characteristics (densely packed frequencies between .1 and .2 Hz). For this model the test structure was approximated as a continuous beam with several equivalent finite elements.

At first, a model was made consisting only of the ASTROMAST in a cantilevered state. The first few frequencies (bending-torsional) obtained with this method agreed to within 5% of the experimental values shown in Table 3.

Next, the remaining elements of the test structure were added to obtain a total model: shake table, AGS, roll gimbal, ASTROMAST and tip package. This model yielded five rigid body modes including pendulum modes at .15 Hz. Table 4 contains the next five modal frequencies.

As can be seen from the tables, the frequencies are not densely packed. A couple of methods to try and achieve this characteristic were brought under consideration:

1. Add weighted flexible stringers alongside the ASTROMAST.
2. Add a flexible cruciform shape onto the bottom of the tip mass.

Neither of these methods were implemented under this contract. However, the second method was used in the follow-on contract.

Some remaining tasks to be dealt with on this contract included modifying the Work Breakdown Structure. As the project advanced and the testing phase approached, it was seen that changes to the WBS were necessary. These changes were initiated during this contract, but was not concluded until the next contract came into effect.

Two hardware tasks existed on this contract. Control Dynamics was to oversee these tasks. The first task involved the construction of an air

bearing for the roll gimbal. This was deemed necessary when the structure was turned up-side-down, as the shaft in the roll gimbal was no longer restrained and could dislodge itself. The air bearing would hold it in place. The second task involved constructing a new tip instrument package bracket out of aluminum, as the previous bracket was made from steel and was too massive for its purpose.

TABLE 3. CANTILEVERED ASTROMAST FREQUENCIES

MODE	MODEL VALUES (Hz)	EXPERIMENTAL VALUES	% DIFFERENCE
1st BENDING	0.543	0.555	-2.16
2nd BENDING	3.411	3.430	-.55
1st TORSION	4.016	4.015	.02
3rd BENDING	9.65	8.83	9.3
2nd TORSION	12.83	12.23	4.97

TABLE 4. SYSTEM FREQUENCIES

MODE #	FREQUENCY (Hz)
6	1.12
7	1.19
8	1.34
9	2.99
10	3.87

Conclusions

During this contract Control Dynamics supported Marshall Space Flight Center in many capacities in promoting and achieving the goals involved with this project. The diversity of the tasks involved demonstrated the capabilities this company has available; the construction of an excellent structural model of the test structure (as seen when comparing the experimental and analytical results), the review, analysis, and design of controllers to be used in controlling the test structure, the development of a simulation to use in running test scenarios, and various miscellaneous tasks such as having the air bearing and tip bracket constructed. Control Dynamics hopes to be further involved with this innovative project in the future.

D2

APPENDIX A. ORAL PRESENTATION OF FIRST YEAR FINAL REPORT

TWELVE MONTH REVIEW
OF CONTRACT TITLED
DEFINITION OF GROUND TEST FOR VERIFICATION
OF
LARGE SPACE STRUCTURE CONTROL
NAS 8-34700

BY

CONTROL DYNAMICS CO.
555 SPARKMAN DRIVE, SUITE 1414
HUNTSVILLE, ALABAMA 35805

OCT. 18, 1982

OVERALL OBJECTIVES AND PLANS

OBJECTIVES

SUPPORT MSFC IN OBTAINING SELF-CONTAINED IN-HOUSE CAPABILITY TO TEST LARGE SPACE STRUCTURES AND THEIR CONTROL PRIOR TO FLIGHT

BY SO DOING ASSIST MSFC IN DEVELOPING A NATIONALLY RECOGNIZED FACILITY

PLANS

INTENT IN FY82

ASSIST IN DEFINING A GROUND TEST FACILITY TO DEMONSTRATE AND VALIDATE LSS CONTROL THEORY

ASSIST IN THE DESIGN OF AN EXPERIMENT THAT HAS SUFFICIENT FIDELITY (WITHIN PHYSICAL AND RESOURCE CONSTRAINTS) TO ASSURE HIGH PROBABILITY OF FLIGHT TEST SUCCESS

RECOMMENDATIONS FOR FY83

CONTINUE MAINTAINING DR. WAITES WBS ETC. DOCUMENTATION

REFINE AND UPDATE THE DYNAMIC MODEL OF THE EXPERIMENT AS TEST DATA BECOME AVAILABLE

- MAJOR SYSTEM ELEMENTS ARE THE ENGINEERING AGS AND THE 512 INCH 5 POUND ASTROMAST

CONTINUE ACTIVITY IN STRAPDOWN ALGORITHMS

- TWO GYRO PACKAGES
- TWO SETS OF ACCELEROMETERS
- COSMIC AND FACILITY COMPUTER

DESIGN DIGITALLY IMPLEMENTED CONTROL LAWS

- DR. WAITES' POLE PLACEMENT TECHNIQUES
- OTHERS SUCH AS THE CONTROL DYNAMICS LAW DEVELOPED FOR SPERRY/MSFC

ACCOMPLISHMENTS

PREVIOUSLY REPORTED

ASSESSMENT AND RECOMMENDATION AS TO APPROPRIATE MSFC FACILITY
RECOMMENDED TEST FACILITY CONFIGURATION
STUDIED AND DEVELOPED TOOLS TO IMPLEMENT DR. WAITES' TECHNIQUES

ACCOMPLISHMENTS SINCE LAST REPORT

RESEARCH ON THE ASTROMAST PER SE
DEVELOPMENT OF OVERALL SYSTEM MODEL

DEVELOPMENT OF UNIQUE STRAPDOWN ALGORITHM

ASTROMAST PER SE

512 INCHES LONG
3×10^6 LB-IN^2
WEIGHS 5 LBS

HAVE AND ARE TREATING AS A SIMPLE LOADED BEAM

MODELED BY LUMPED MASSES AND LUMPED SPRINGS
MODELED BY MODAL SYNTHESIS

EARLY EXPERIMENTATION TREATED AS

BASE FIXED
TIP SUPPORTED BY A "STRING"
TIP LOADED BY A 15 POUND INSTRUMENT CLUSTER
BEAM INTERNALLY STRESSED I.E. COMPRESSED
VERTICAL ORIENTATION WITH "G"

CONTROL DYNAMICS
HUNTSVILLE, ALABAMA

GTV-LSS CONTROL

GEORGE B. DOANE III
OCTOBER 18, 1982

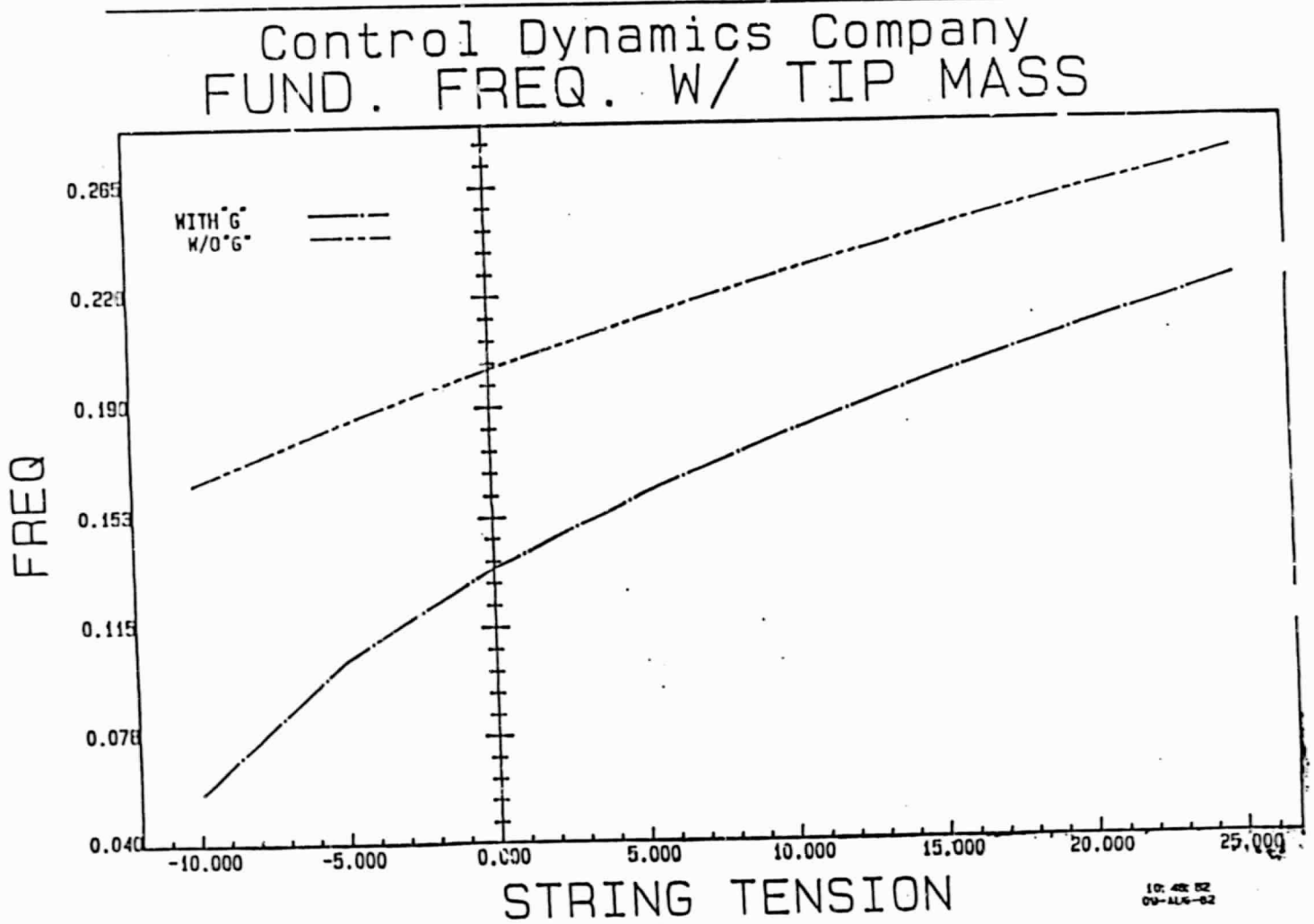

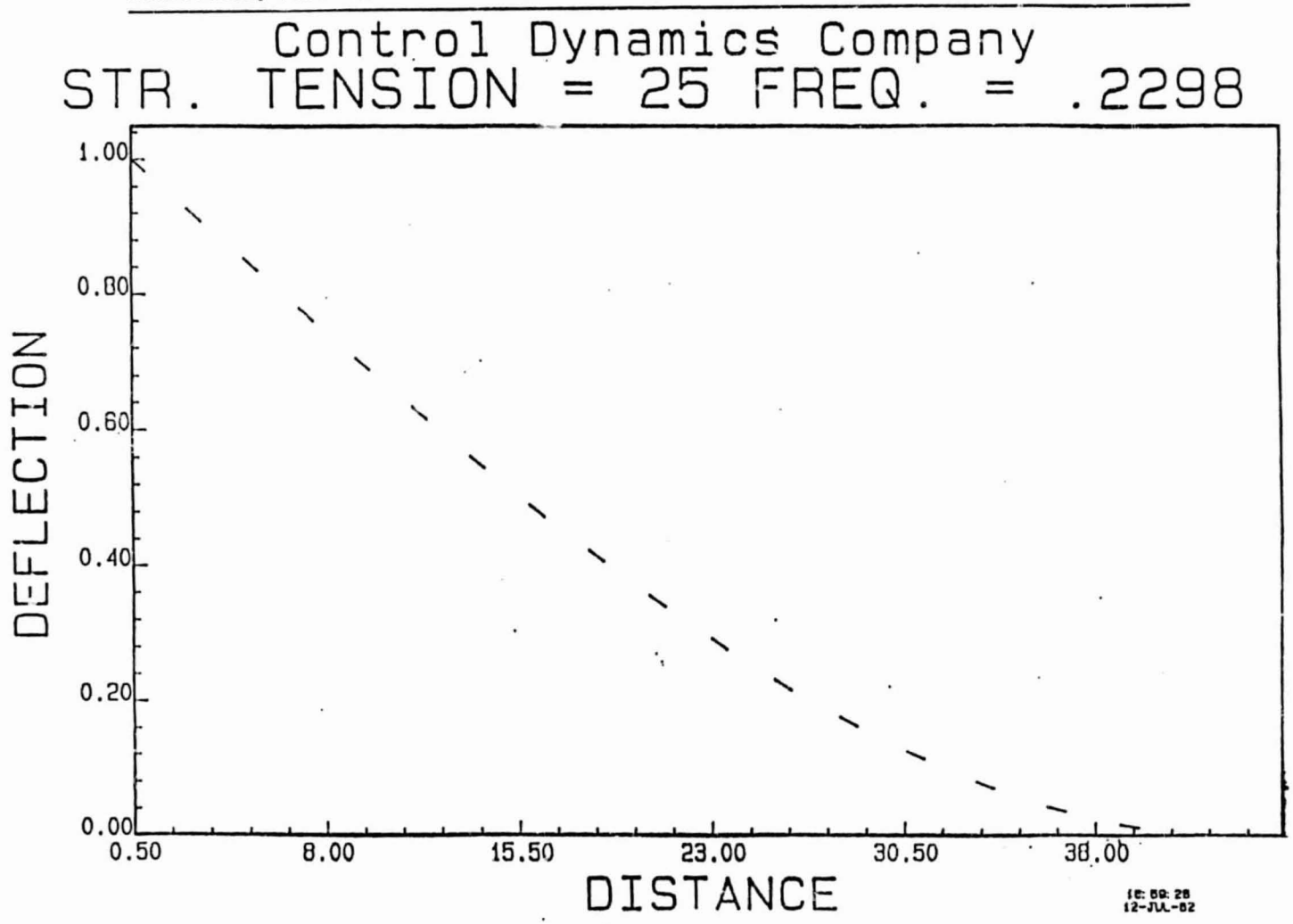
Control Dynamics Company
STR. TENSION = 25 FREQ. = .2298
DEFLECTION
1.00
0.80
0.60
0.40
0.20
0.00
0.50
8.00
15.50
23.00
30.50
38.00
DISTANCE
12-JUL-82

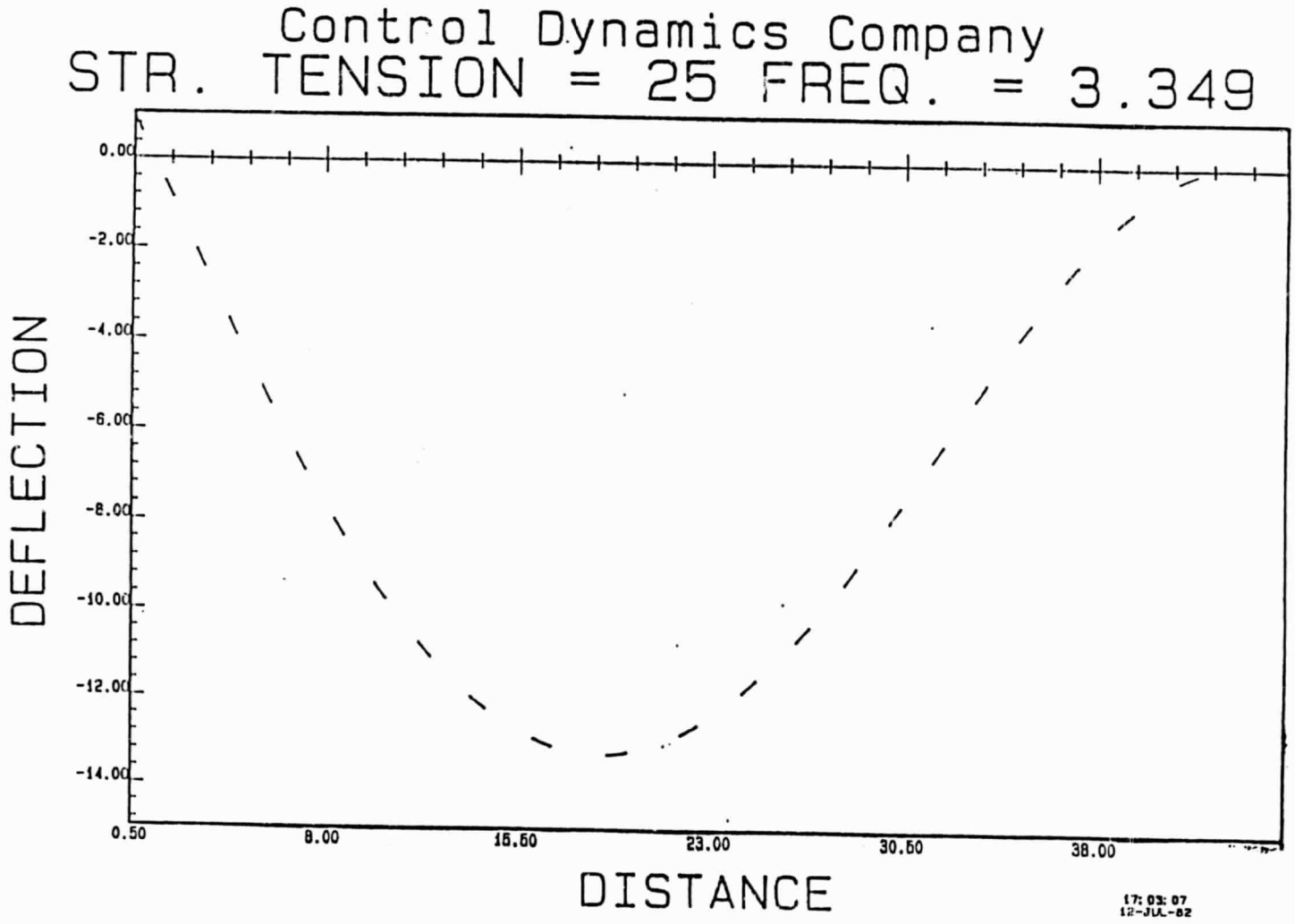
Control Dynamics Company
STR. TENSION = 25 FREQ. = 3.349
DEFLECTION
0.00
-2.00
-4.00
-6.00
-8.00
-10.00
-12.00
-14.00
0.50
8.00
15.50
23.00
30.50
38.00
DISTANCE
17:03:07
12-JUL-82

CONTROL DYNAMICS
HUNTSVILLE, ALABAMA

GTV-LSS CONTROL

GEORGE B. DOANE III
OCTOBER 18, 1982

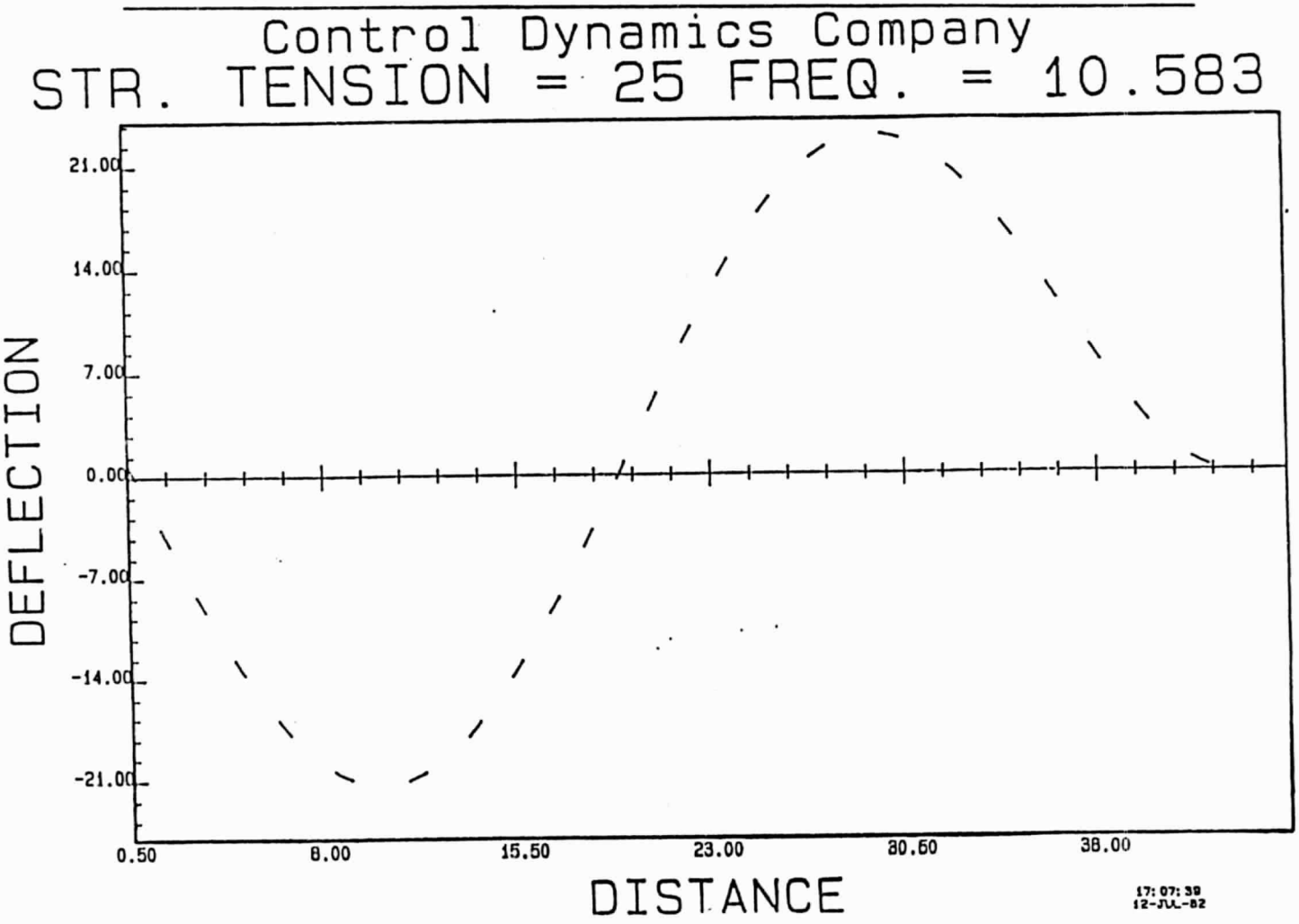

CONTROL DYNAMICS
HUNTSVILLE, ALABAMA

GTV-LSS CONTROL

GEORGE B. DOANE III
OCTOBER 18, 1982

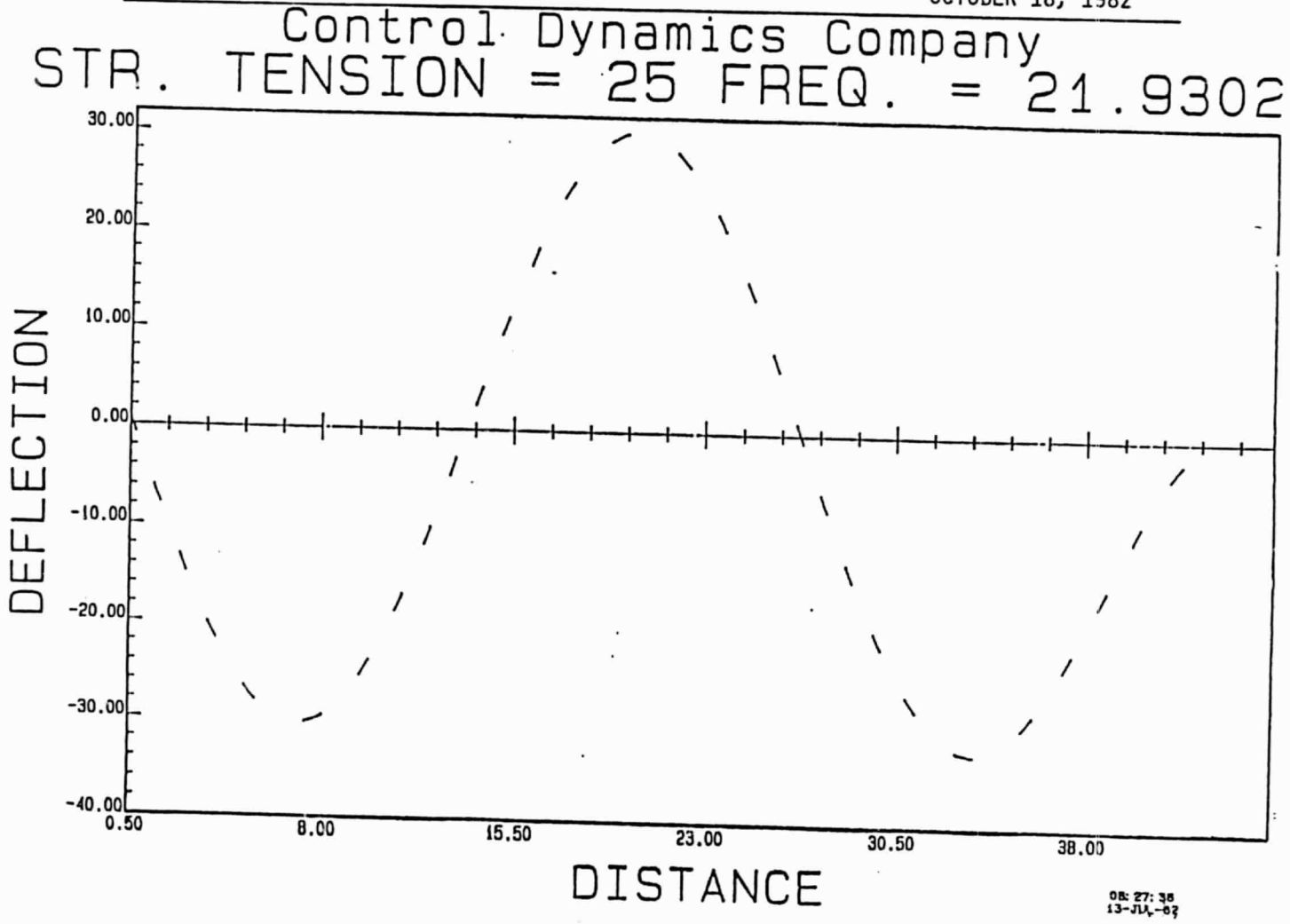

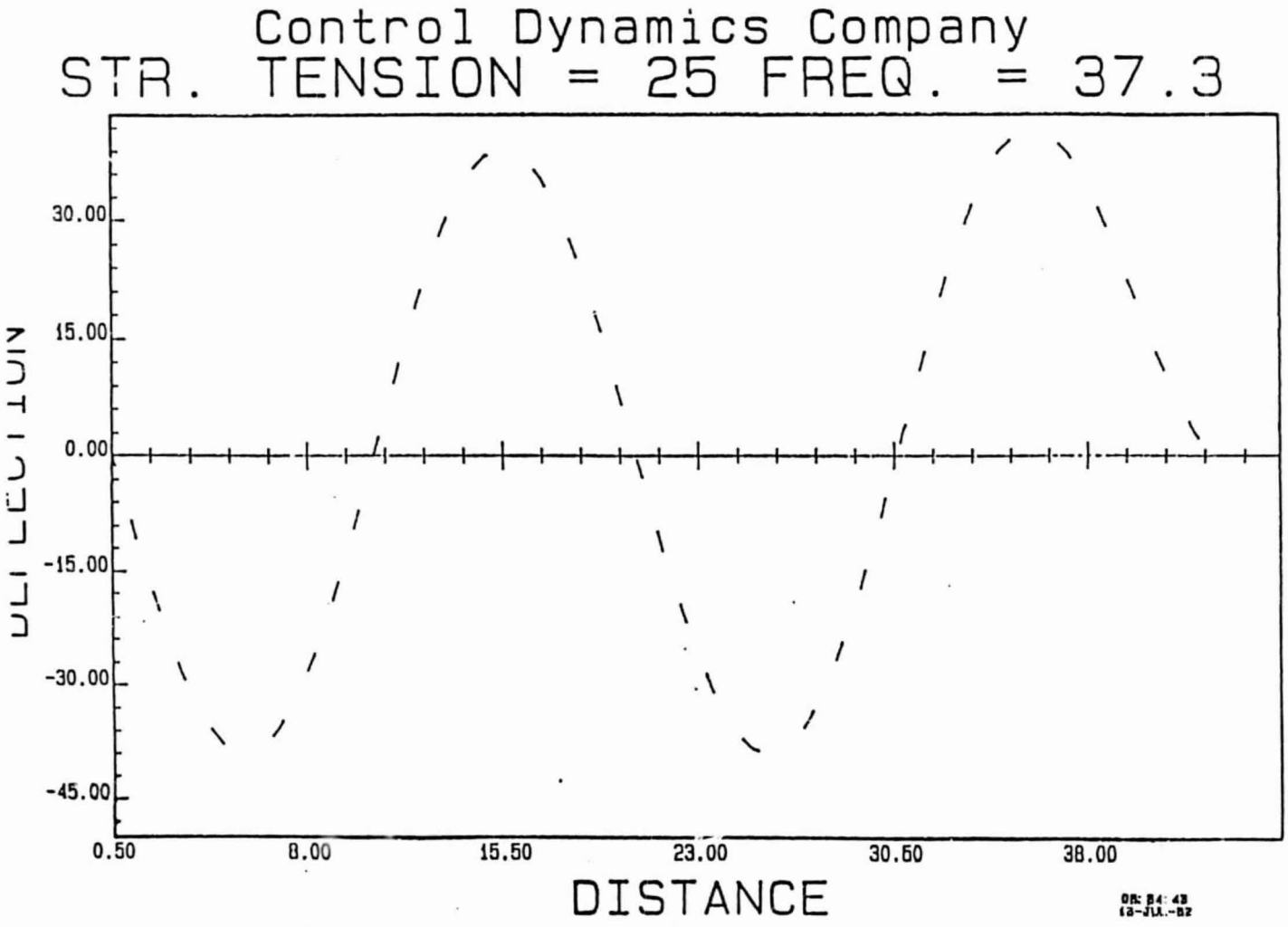
Control Dynamics Company
STR. TENSION = 25 FREQ. = 37.3
30.00
15.00
0.00
-15.00
-30.00
-45.00
0.50
8.00
15.50
23.00
30.50
38.00
DISTANCE

SIMULATION/IMU ALGORITHM DEVELOPMENT

- SIMULATION DEVELOPMENT
- MODAL ANALYSIS MODEL
- IMU REFERENCE ALGORITHMS
- PREPARATORY MEASUREMENTS AND TESTS
- TEST SCENARIOS

SIMULATION DEVELOPMENT

GENERATE NORMAL MODES FOR COMPOSITE STRUCTURE

Φ_{ij}, w_j, ζ_j FOR EACH MODE EMPLOYED

$$\ddot{\xi}_j + 2\zeta_j\omega_j\xi_j + \omega^2{}_j\xi_j = \sum_i(\Phi_{ij} \cdot \underline{F}_i + \underline{\Psi}_{ij} \cdot \underline{T}_i)$$

$\underline{F}_i$ = DISTURBANCE FORCES

$\underline{T}_i$ = CONTROL AND DISTURBANCE TORQUES

MODAL ANALYSIS MODEL

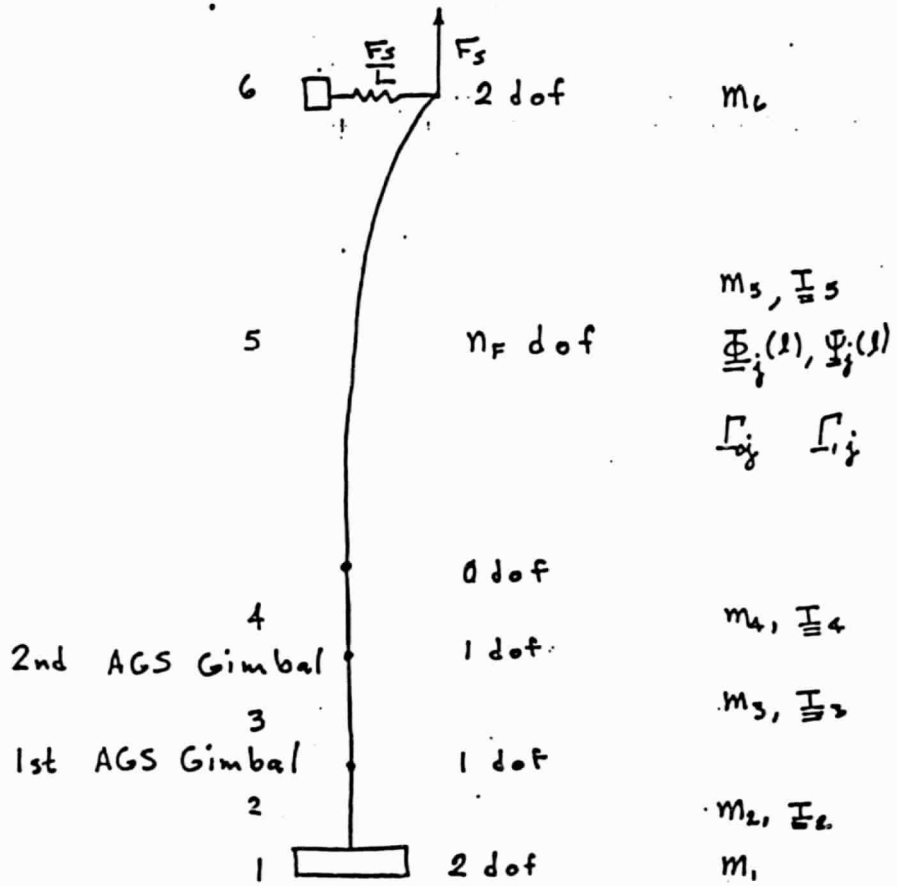

COORDINATE REFERENCE DEFINITIONS

E frame: Laboratory earth fixed

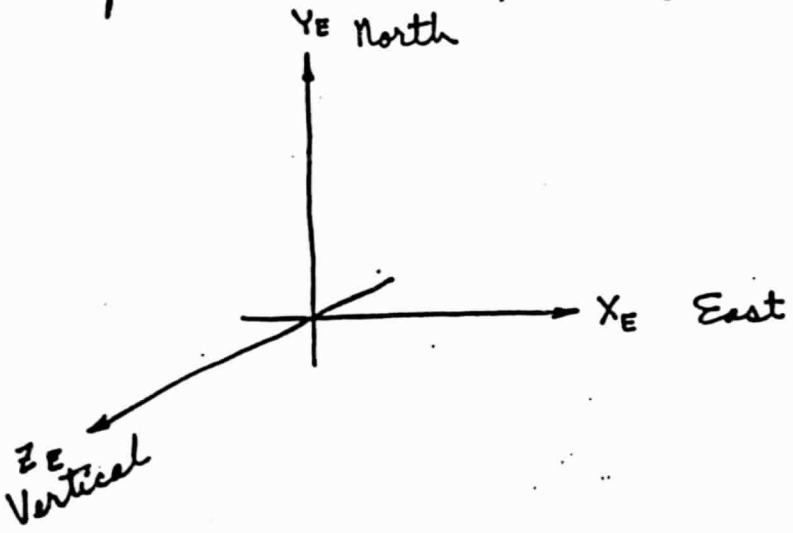

$$\underline{\omega}_E = \begin{bmatrix} 0 \\ 5.937 \\ 4.235 \end{bmatrix} \times 10^{-5} \frac{\text{rad}}{\text{sec}}$$

$$|\underline{\omega}_E| = 15 \frac{\text{sec}}{\text{sec}}$$

$$\underline{g}_E = \begin{bmatrix} 0 \\ 0 \\ 9.81 \end{bmatrix} \frac{\text{m}}{\text{sec}^2}$$

B_I FRAME: BODY FIXED FRAME, ITH INSTRUMENT PACKAGE

I = 1, 2, 3

ALIGNED WITH E INITIALLY.

STRUCTURE MODEL

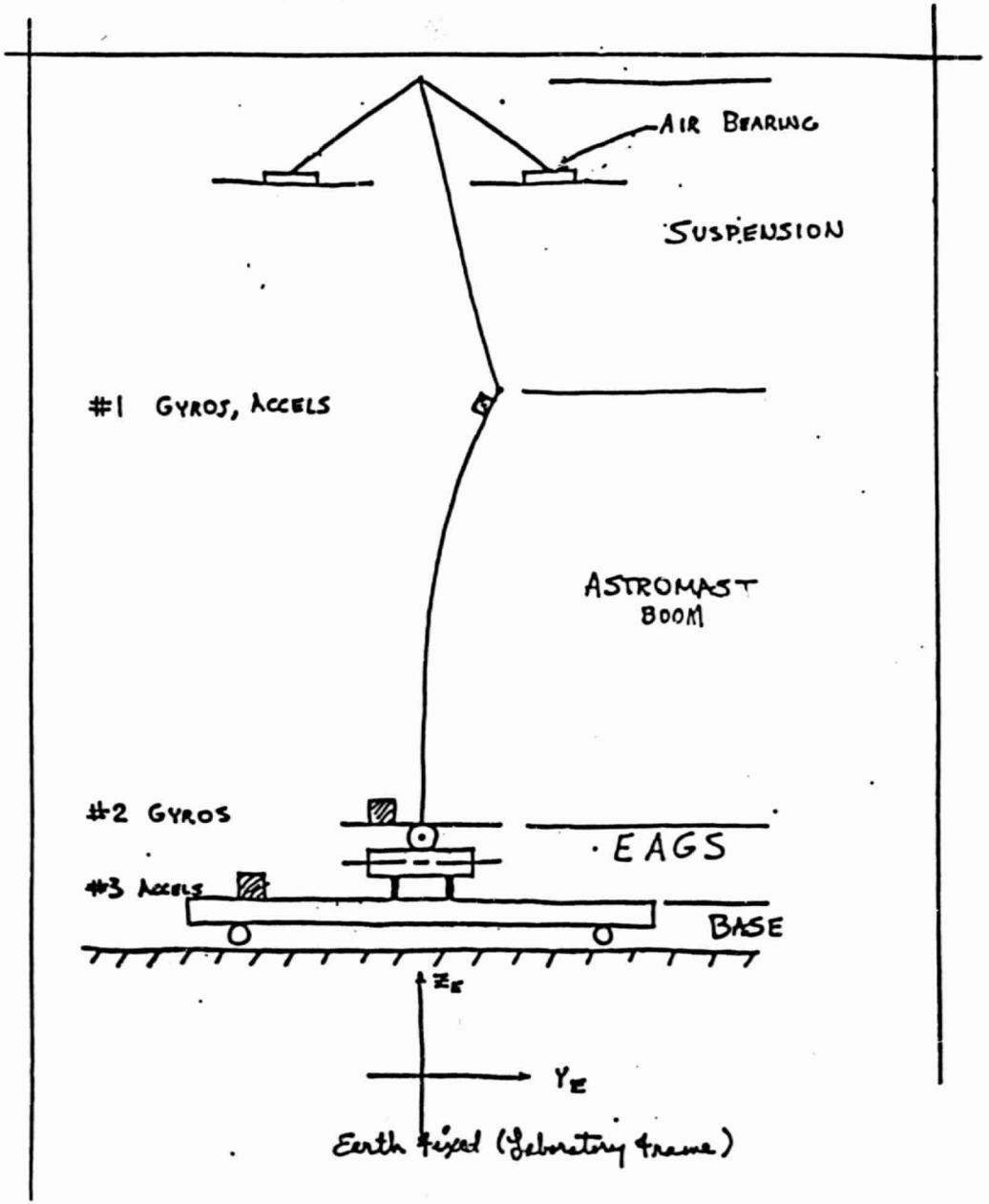

GYRO ALGORITHM (GYROPACKAGE)

ASSUME 4 GYRO OUTPUT CHANNELS (NEED ONLY 3)

CONVERT INPUT PULSE COUNTS TO ANGULAR CHANGE

$$\Delta\theta_1 = F_1(N_1)$$
$$\Delta\theta_2 = F_2(N_2)$$
$$\Delta\theta_3 = F_3(N_3)$$
$$\Delta\theta_4 = F_4(N_4)$$

THIS MAY BE A TABLE LOOK UP PROCESS

$$\omega_1 = S_1\Delta\theta_1/\Delta t + B_1$$
$$\omega_2 = S_2\Delta\theta_2/\Delta t + B_2$$
$$\omega_3 = S_3\Delta\theta_3/\Delta t + B_3$$
$$\omega_4 = S_4\Delta\theta_4/\Delta t + B_4$$

S_1 SCALE FACTOR ADJUSTMENT

B_1 BIAS ADJUSTMENT

$$\omega_{BX} = A_{x1}\omega_1 + A_{x2}\omega_2 + A_{x3}\omega_3 + A_{x4}\omega_4$$
$$\omega_{BY} = A_{y1}\omega_1 + A_{y2}\omega_2 + A_{y3}\omega_3 + A_{y4}\omega_4$$
$$\omega_{BZ} = A_{z1}\omega_1 + A_{z2}\omega_2 + A_{z3}\omega_3 + A_{z4}\omega_4$$

A_{ij} PSEUDO INVERSE OF GYRO MOUNT MATRIX

GYRO ALGORITHM (GYROPACKAGE) (CONTINUED)

$$\Delta Q_1 = (\omega_{BZ} + \omega_{EZ})Q_2 - (\omega_{BY} + \omega_{EY})Q_3 + (\omega_{BX} - \omega_{EX})Q_4\Delta t$$
$$\Delta Q_2 = -(\omega_{BZ} + \omega_{EZ})Q_1 + (\omega_{BX} + \omega_{EX})Q_3 + (\omega_{BY} - \omega_{EY})Q_4\Delta t$$
$$\Delta Q_3 = +(\omega_{BY} + \omega_{EY})Q_1 - (\omega_{BX} + \omega_{EX})Q_2 + (\omega_{BZ} - \omega_{EZ})Q_4\Delta t$$
$$\Delta Q_4 = -(\omega_{BX} - \omega_{EX})Q_1 - (\omega_{BY} - \omega_{EY})Q_2 - (\omega_{BZ} - \omega_{EZ})Q_4\Delta t$$

$$Q_1 = Q_1 + \Delta Q_1$$
$$Q_2 = Q_2 + \Delta Q_2$$
$$Q_3 = Q_3 + \Delta Q_3$$
$$Q_4 = Q_4 + \Delta Q_4$$

INITIALIZE THESE TO

$$Q_1 = 0$$
$$Q_2 = 0$$
$$Q_3 = 0$$
$$Q_4 = 1$$

GYRO ALGORITHM (GYROPACKAGE) (CONTINUED)

$$F = \frac{3}{2} - \frac{1}{2}\left(Q_1^2 + Q_2^2 + Q_3^2 + Q_4^2\right)$$

$$\left.\begin{aligned} Q_1 &= Q_1 F \\ Q_2 &= Q_2 F \\ Q_3 &= Q_3 F \\ Q_4 &= Q_4 F \end{aligned}\right\}$$

TRANSFER $Q_1 \ldots Q_4$ TO FACILITY COMPUTER
ALSO ω_{BX}, ω_{BY}, ω_{BZ}

GYRO ALGORITHM (GYROPACKAGE) (CONTINUED)

$$BE_{11} = Q_1^2 - Q_2^2 - Q_3^2 + Q_4^2$$

$$BE_{12} = 2Q_1Q_2 + 2Q_3Q_4$$

$$BE_{13} = 2Q_1Q_3 - 2Q_2Q_4$$

$$BE_{21} = 2Q_1Q_2 - 2Q_3Q_4$$

$$BE_{22} = -Q_1^2 + Q_2^2 - Q_3^2 + Q_4^2$$

$$BE_{23} = 2Q_2Q_3 + 2Q_1Q_4$$

$$BE_{31} = 2Q_3Q_1 + 2Q_2Q_4$$

$$BE_{32} = 2Q_2Q_3 - 2Q_1Q_4$$

$$BE_{33} = -Q_1^2 - Q_2^2 + Q_3^2 + Q_4^2$$

TRANSFORMATION EARTH FIXED (LABORATORY) FRAME TO BODY FIXED FRAME.

ACCELOROMETER ALGORITHM

$$\left.\begin{aligned} \Delta V_1 &= F_1(N_1) \\ \Delta V_2 &= F_2(N_2) \\ \Delta V_3 &= F_3(N_3) \end{aligned}\right\}$$

PULSES TO ΔV CONVERSION

$$\left.\begin{aligned} a_1 &= SA_1 \cdot \Delta V_1/\Delta t + BA_1 \\ a_2 &= SA_2 \cdot \Delta V_2/\Delta t + BA_2 \\ a_3 &= SA_3 \cdot \Delta V_3/\Delta t + BA_3 \end{aligned}\right\}$$

SCALE FACTOR AND BIAS ADJUSTMENTS

$$\begin{aligned} a_{BX} &= AB_{x1} \cdot a_1 + AB_{x2} \cdot a_2 + AB_{x3} \cdot a_3 \\ a_{BY} &= AB_{y1} \cdot a_1 + AB_{y2} \cdot a_2 + AB_{y3} \cdot a_3 \\ a_{BZ} &= AB_{z1} \cdot a_1 + AB_{z2} \cdot a_2 + AB_{z3} \cdot a_3 \end{aligned}$$

ACCELOROMETER ALGORITHM (CONTINUED)

$$a^E_{BX} = BE_{11} \cdot a_{BX} + BE_{21} \cdot a_{BY} + BE_{31} \cdot a_{BZ}$$

$$a^E_{BY} = BE_{12} \cdot a_{BX} + BE_{22} \cdot a_{BY} + BE_{32} \cdot a_{BZ}$$

$$a^E_{BZ} = BE_{13} \cdot a_{BX} + BE_{23} \cdot a_{BY} + BE_{33} \cdot a_{BZ}$$

TRANSFORM TO E FRAME. NOT NECESSARY FOR BASE AGS ACCELOROMETER

$$\ddot{X}_E = a_B{}^E{}_X - g_{EX} + 2\omega_{EY}\dot{Z}_E - 2\omega_{EZ}\dot{Y}_E + \omega_{EY}(\omega_{EX}Y_E - \omega_{EY}X_E) + \omega_{EZ}(\omega_{EX}Z_E - \omega_{EZ}X_E)$$

$$\ddot{Y}_E = a_B{}^E{}_Y - g_{EY} + 2\omega_{EZ}\dot{X}_E - 2\omega_{EX}\dot{Z}_E + \omega_{EZ}(\omega_{EY}Z_E - \omega_{EZ}Y_E) + \omega_{EX}(\omega_{EY}X_E - \omega_{EX}Y_E)$$

$$\ddot{Z}_E = a_B{}^E{}_Z - g_{EZ} + 2\omega_{EZ}\dot{X}_E - 2\omega_{EX}\dot{Z}_E + \omega_{EX}(\omega_{EZ}X_E - \omega_{EX}Z_E) + \omega_{EY}(\omega_{EZ}X_E - \omega_{EX}Z_E)$$

ACCELORGMETER ALGORITHM (CONTINUED)

$$X_E = X_E + \dot{X}_E \cdot \Delta t + \frac{1}{2} \ddot{X}_E \cdot \Delta t^2$$

$$Y_E = Y_E + \dot{Y}_E \cdot \Delta t + \frac{1}{2} \ddot{Y}_E \cdot \Delta t^2$$

$$Z_E = Z_E + \dot{Z}_E \cdot \Delta t + \frac{1}{2} \ddot{Z}_E \cdot \Delta t^2$$

SET X_E, Y_E, Z_E
AND $\dot{X}_E$, $\dot{Y}_E$, $\dot{Z}_E$
EACH TO 0.0 INITIALLY

$$\dot{X}_E = \dot{X}_E + \ddot{X}_E \cdot \Delta t$$

$$\dot{Y}_E = \dot{Y}_E + \ddot{Y}_E \cdot \Delta t$$

$$\dot{Z}_E = \dot{Z}_E + \ddot{Z}_E \cdot \Delta t$$

TRANSFER $\ddot{X}_E$, $\ddot{Y}_E$, $\ddot{Z}_E$, $\dot{X}_E$, $\dot{Y}_E$, $\dot{Z}_E$, X_E, Y_E, Z_E TO
FACILITY COMPUTER

IMU ALGORITHMS FLOW CHART

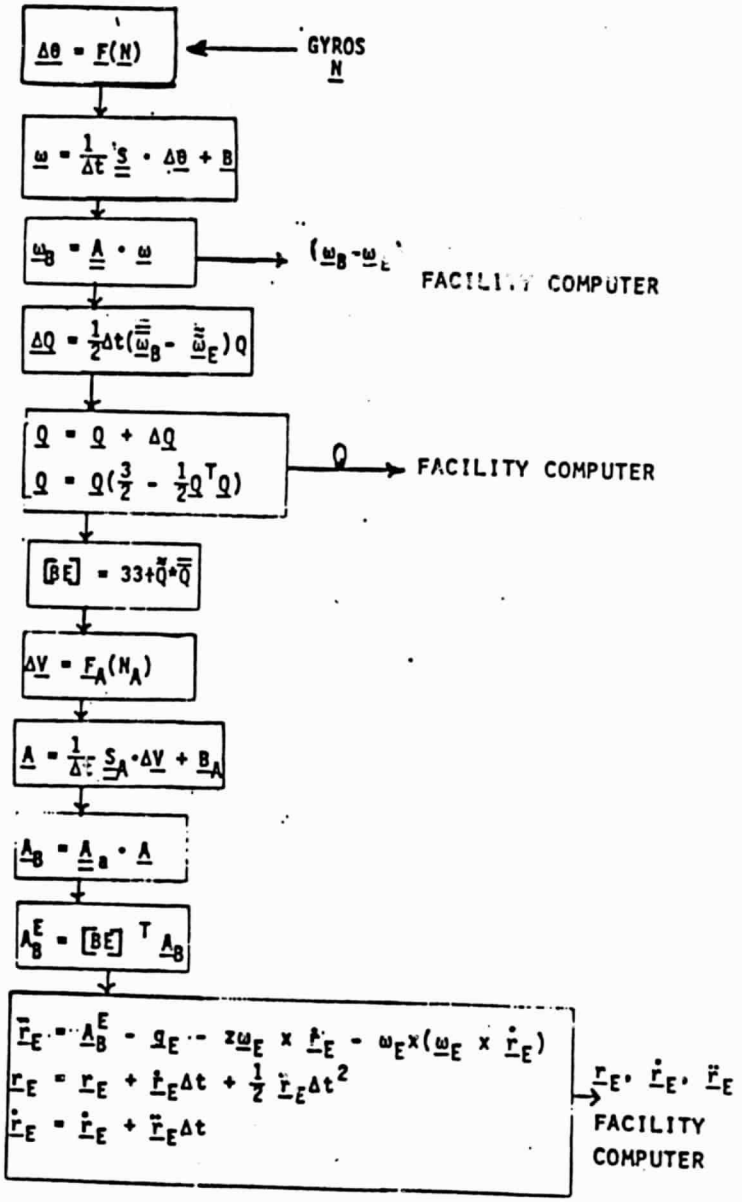

PREPARATORY MEASUREMENTS AND TESTS

INITIAL PLACEMENT OF SENSOR PACKAGES

- VERIFICATION OF SENSOR MOUNTING MATRICES
- ALIGNMENT DETERMINATION

PRELIMINARY TESTS

- DETERMINE ENVIRONMENTAL NOISE LEVELS
- PERFORM END-TO-END TEST OF DATA GATHERING SYSTEM INCLUDING FACILITY AND COSMIC COMPUTERS
- MEASURE $\underline{w}_E$ AND $\underline{G}_E$ (MAY REQUIRE FILTERING)

TEST SCENARIO

ESTABLISH TEST GOALS, DISTURBANCE PROFILE, EXPECTED RESPONSE

- PULSE TRAINS, SINUSOIDS

PERFORM SYSTEM HEALTH CHECKS

REMEASURE W_E, G_E (STRUCTURE CAGED)

INTRODUCE DISTURBANCE PROFILE (STRUCTURE UNCAGED)

OBSERVE RESPONSE

PROCESS & STORE DATA COMPILE REPORT

SUMMARY

ANALYTICAL WORK PROCEEDING WELL

NEED INPUTS FROM TEST AND HARDWARE DESIGNS

MASS AND FLEXIBILITY DATA

TRIPOD
BASE AND BASE TO AGS MOUNTING

LOOKING FORWARD TO CONTINUING WORK INTO LAB PHASE

November 10, 1982

National Aeronautics and Space Administration
Marshall Space Flight Center, AL 35812

Attention: Ms. Marena McClure
AP25-O

Subject: Thirteenth Month Progress Report for "Definition of Ground Test for Verification of Large Space Structure Control", Contract No. NAS8-34700

Control Dynamics Company is pleased to submit the enclosed Progress Report for the period of October 1, 1982 through October 31, 1982. Distribution in accordance with the contract specified standard distribution list is shown below.

Sherman M. Seltzer, President

SMS/tll

cc:

ED12/Dr. Waites	5 copies
EM12-11/Jordan	1 copy
AS 24D	3 copies
AT01	1 copy
AP25-O	1 copy

D3

N85 13841

APPENDIX B. ATTACHMENT FROM MR # 13 PLANAR MODEL

SIMPLIFIED PLANAR MODEL OF GROUND TEST VERIFICATION STRUCTURE

Figure 1 depicts the planar version of the LSS-GTV structure for which a model has been developed. The model is 12th order including 6 structural modes. One mode results from the base translation, one from the gimbal rotation, three from the flex characteristics of the Astromast Boom and gyro package, and one from the tether and tripod. The model includes one input, one disturbance and one output which are a control torque at the gimbal, a translational force at the base, and the rotation rate of the Astromast tip, respectively.

The Gimbalflex program has been amended to output the system model in the following form

$$\ddot{\underline{\eta}} + 2\zeta\Omega\dot{\underline{\eta}} + \Omega^2\underline{\eta} = d\underline{V_1} + c\underline{V_2} \ , \tag{1}$$

$$\Theta = \underline{V_3}\eta \ . \tag{2}$$

The values $\underline{\eta}$ are the modal coordinates, d is the scalar disturbance input, c is the control input, and Θ is the tip rate sensor output. The values of omega, V_1, V_2, and V_3 along with the transition matrix from physical to modal coordinates ($\underline{\xi} = T\underline{\eta}$, where $\underline{\xi}$ are the physical coordinates) are attached.

The model can then be cast into state variable form as

$$\begin{bmatrix} \dot{\underline{\eta}}_1 \\ \dot{\underline{\eta}}_2 \end{bmatrix} = \begin{bmatrix} [0]_6 & I_6 \\ -\Omega^2 & -2\zeta\Omega \end{bmatrix} \begin{bmatrix} \underline{\eta}_1 \\ \underline{\eta}_2 \end{bmatrix} + \begin{bmatrix} 0_6 & 0_6 \\ \underline{V_1} & \underline{V_2} \end{bmatrix} \begin{bmatrix} d \\ c \end{bmatrix} \tag{3}$$

$$\Theta = \begin{bmatrix} 0_6^T & \underline{V_3}^T \end{bmatrix} \begin{bmatrix} \underline{\eta}_1 \\ \underline{\eta}_2 \end{bmatrix} \tag{4}$$

where $\underline{\eta}_1 = \eta$ and $\underline{\eta}_2 = \dot{\eta}$. The term $[0]_6$ is a 6×6 zero matrix, I_6 is a 6×6 identity matrix, and 0_6 is a 6th order vector of zeros. By row and column interchanges, the system can be cast into block diagonal form so that the discretization process outlined in ED12-81-2 may be applied. Ongoing work includes production of coding to automate this process.

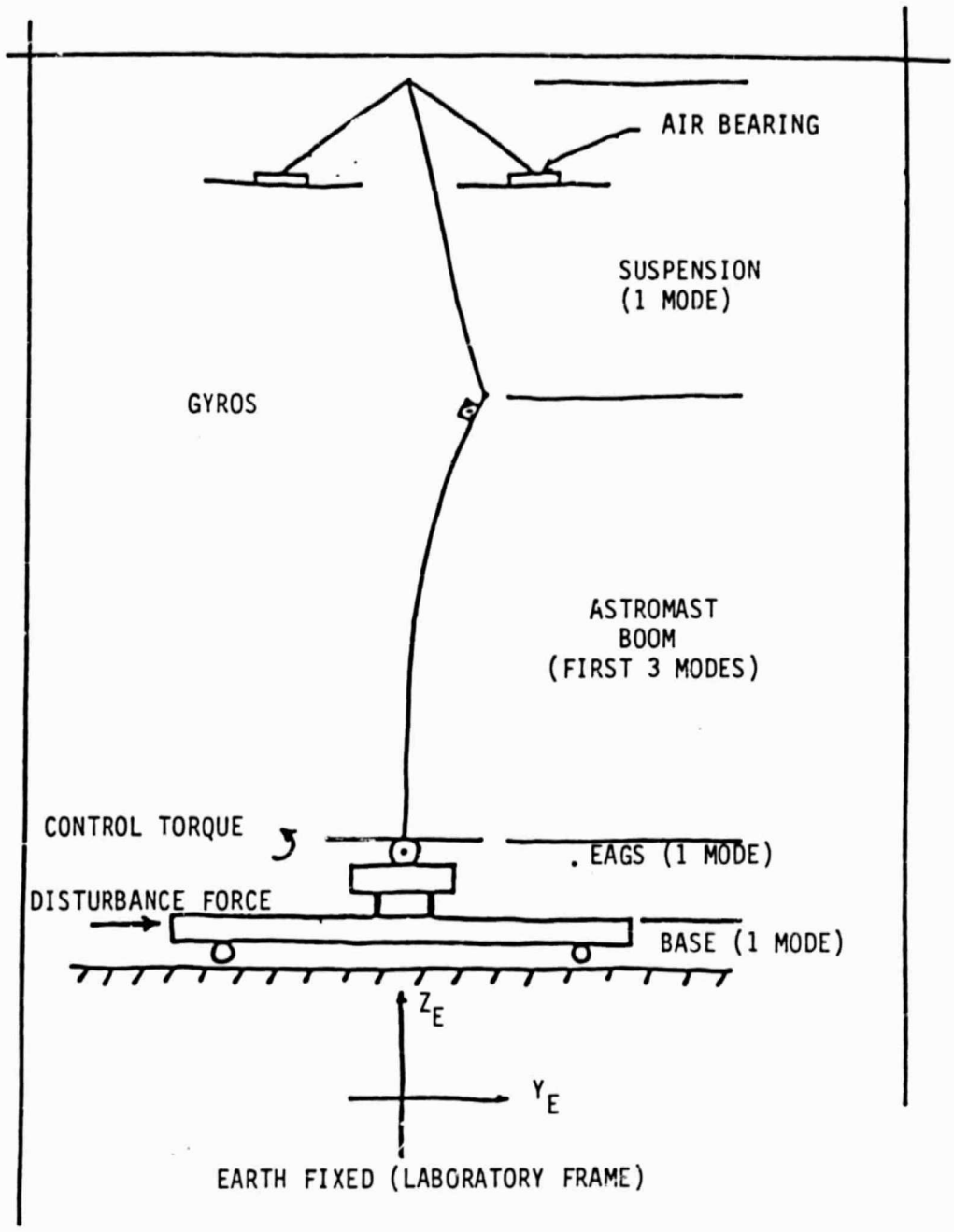

FIGURE 1. Planar Version of the LSS-GTV Structure.

APPENDIX C.

ATTACHMENT FROM MR # 14 ELIMINATION OF UNCONTROLLABLE RIGID BODY MODE

ELIMINATION OF THE UNCONTROLLABLE RIGID BODY MODE FROM THE PLANAR SYSTEM MODEL

The Gimbalflex program outputs the system model in the form

$$\underline{\ddot{\eta}} + 2\zeta\Omega\underline{\dot{\eta}} + \Omega^2\underline{\eta} = \underline{V_1}d + \underline{V_2}c \tag{1}$$

and

$$\theta = \underline{V_3}^T\underline{\eta} \tag{2}$$

(See Progress Report 13.) The matrix, Ω, and vectors $\underline{V_1}$, $\underline{V_2}$, and $\underline{V_3}$, as given in the previous report, appear in Table 1 for convenience. The fifth and sixth diagonal elements of Ω reveal two very low frequency modes, relative to the others present; one at .0136 rad/sec and another at .0141 rad/sec. These are actually rigid body modes, however, for numerical reasons in computing, they do not appear as exactly zero frequency.

Examination of Figure 1 reveals that there are two rigid body modes modeled. One is due to the pure translation of the whole experiment assembly and is uncontrollable because the only control input is a torque at the gimbal. The other rigid body mode is due to the pointing of the gimbal and is the one we wish to control. The problem arises from the Vector $\underline{V_2}$ which relates the control input to the modal coordinates. Since its fifth and sixth elements are both nonzero, neither rigid body mode can be thrown away as is. The two rigid body modes must be transformed so that one is unaffected by the control input and one is left controllable. The uncontrollable mode can then be eliminated from the model for design purposes.

Consider a subspace of the modal coordinates containing only the rigid body modes ($\Omega_{ii} = 0$) and let it be denoted by the subscript "R". The system in this subspace is

$$\ddot{\underline{\eta}}_R = \underline{V_{1R}}d + \underline{V_{2R}}c \tag{3}$$

and

$$\theta_R = \underline{V_{3R}}^T\underline{\eta}_R. \tag{4}$$

Now the desired transformation is

$$\overline{\underline{\eta}}_R = Q\underline{\eta}_R. \tag{5}$$

Premultiplying (3) by Q and then substituting according to (5) gives

$$\ddot{\underline{\eta}}_R = Q\underline{V}_{1R}d + Q\underline{V}_{2R}c \ . \tag{6}$$

For the case where there is exactly one controllable and one uncontrollable mode and a scalar input, the requirement for Q is simply that $Q\underline{V}_{2R}$ have one zero element. Since there is some arbitrariness within this bound on the elements of Q, let us require that Q be orthonormal so that we have the property $Q^{-1} = Q^T$ and the inverse is guaranteed to exist.

To this end, let

$$Q = \begin{vmatrix} q_{11} & q_{12} \\ q_{21} & q_{22} \end{vmatrix} \tag{7}$$

and

$$V_{2R} = \begin{vmatrix} b_1 \\ b_2 \end{vmatrix} \tag{8}$$

It is now obvious that

$$Q = \frac{1}{(b_1^{\,2} + b_2^{\,2})^{1/2}} \begin{vmatrix} b_2 & -b_1 \\ b_1 & b_2 \end{vmatrix} \tag{9}$$

satisfies the requirements made.

The output equation (4) may now be written in terms of the new modal coordinates, $\underline{\eta}_R$, and the transformation, Q, as

$$\Theta = \underline{V}_{3R}^T Q^{-1} \underline{\eta}_R . \tag{10}$$

Because of the special properties assumed for Q, this may be rewritten as

$$\Theta = (Q\underline{V}_{3R})^T \underline{\eta}_R \tag{11}$$

Now equations (6), (9), and (11) together describe the new rigid body subspace for the modal coordinate system so that one rigid body mode is not affected by the control input and one is controllable.

Such a transformation was applied to the two rigid body modes of the original

planar system model and the results are shown in Table 2. Note that the order of the new coordinates was changed so that the rigid body mode appears as Ω_{11} which has been set to exactly zero. Some error is incurred in setting this value to zero; however, work is underway to alleviate the problem of nonzero "rigid body" modes being produced by the Gimbalflex program.

Ongoing work includes generalization of the process described here to any number of rigid body modes and control inputs and automation of the process.

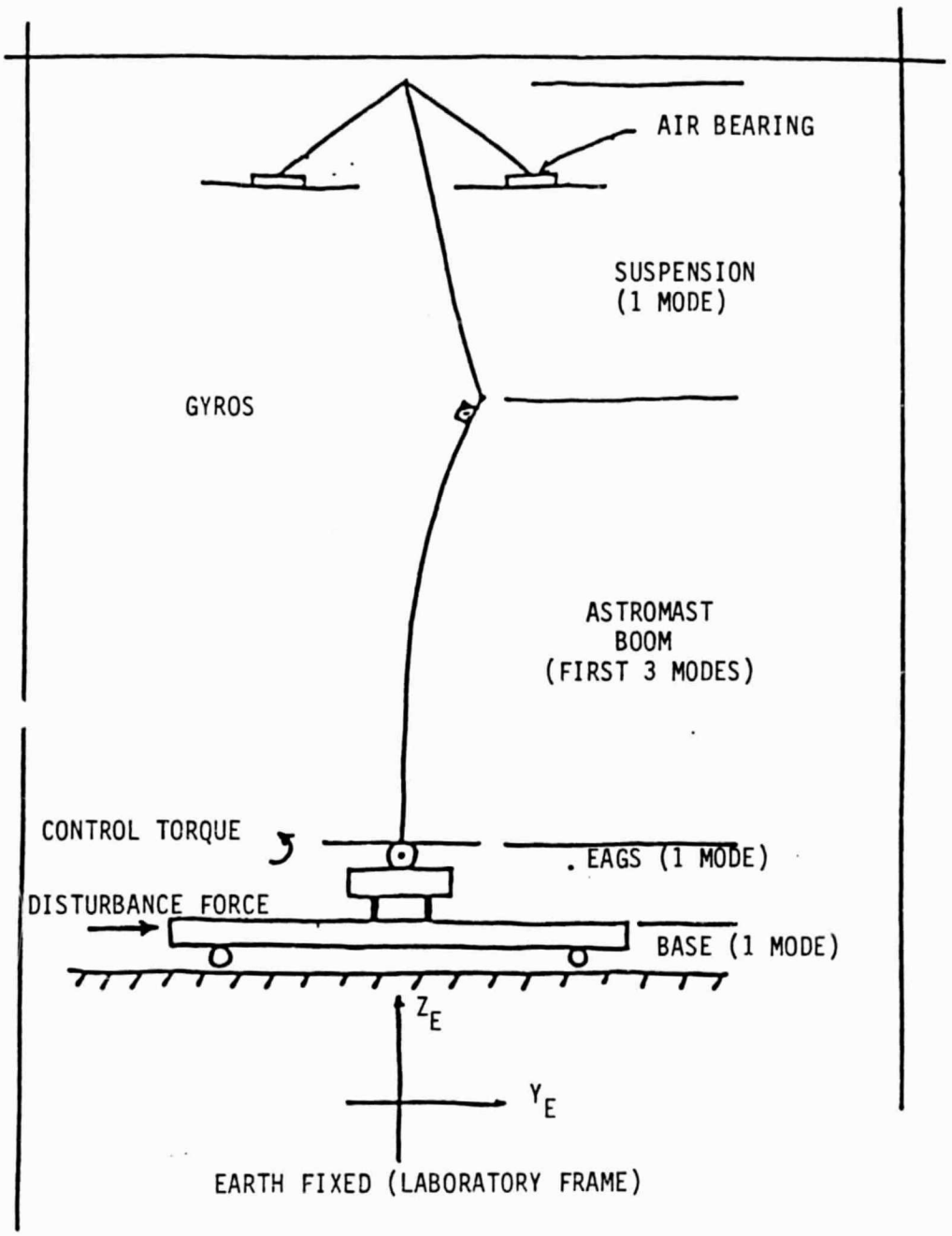

FIGURE 1. Planar Version of the LSS-GTV Structure.

OMEGA

0.226562E+02	0.000000E+00	0.000000E+00	0.000000E+00	0.000000E+00	0.000000E+00
0.000000E+00	0.682493E+02	0.000000E+00	0.000000E+00	0.000000E+00	0.000000E+00
0.000000E+00	0.000000E+00	0.204687E+01	0.000000E+00	0.000000E+00	0.000000E+00
0.000000E+00	0.000000E+00	0.000000E+00	0.588515E+01	0.000000E+00	0.000000E+00
0.000000E+00	0.000000E+00	0.000000E+00	0.000000E+00	0.136280E-01	0.000000E+00
0.000000E+00	0.000000E+00	0.000000E+00	0.000000E+00	0.000000E+00	0.140858E-01

V1 VECTOR

-0.247507E+00
-0.695723E-01
-0.137923E+00
-0.699262E+00
0.945106E-01
-0.897639E+00

V2 VECTOR

0.161269E-01
0.525093E-02
0.763951E-02
0.401554E-01
-0.614603E-02
0.177831E-02

V3 VECTOR

0.102167E+00
-0.177320E+00
0.591773E-02
-0.279082E-01
-0.615234E-02
0.177607E-02

TABLE 1. ORIGINAL PLANAR SYSTEM MODEL

OMEGA

0.000000E+00	0.000000E+00	0.000000E+00	0.000000E+00	0.000000E+00
0.000000E+00	0.682493E+02	0.000000E+00	0.000000E+00	0.000000E+00
0.000000E+00	0.000000E+00	0.204687E+01	0.000000E+00	0.000000E+00
0.000000E+00	0.000000E+00	0.000000E+00	0.588515E+01	0.000000E+00
0.000000E+00	0.000000E+00	0.000000E+00	0.000000E+00	0.226562E+02

V1 VECTOR

-0.340200E+00
-0.695723E-01
-0.137923E+00
-0.699262E+00
-0.247507E+00

V2 VECTOR

0.639800E-02
0.525093E-02
0.763951E-02
0.401554E-01
0.161269E-01

V3 VECTOR

0.640300E-02
-0.177320E+00
0.591773E-02
-0.279082E-01
0.102167E+00

TABLE 2. PLANAR SYSTEM MODEL WITH UNCONTROLLABLE RIGID BODY MODE ELIMINATED

D5

APPENDIX D.

ATTACHMENT FROM MR #16, HP 9845C SPEED TEST RESULTS AND HARDWARE/SOFTWARE STUDY OF COMPUTATIONAL SPEED PROBLEM

SPEED TEST ON HP 9845C

The speed tests are summarized by Table 1 with the following definitions.

n: system order

m: number of outputs from digital controller

r: number of inputs to digital controller

The digital controller is implemented using matrix arithmetic and the following recurrence relation.

$$x(i+1) = Ax(i) + Bu(i)$$

$$y(i) = Cx(i)$$

i: iteration number

A: nxn system matrix

B: nxr input matrix

C: mxn output matrix

x: nx1 state vector

u: rx1 input vector

y: mx1 output vector

TEST CASE*	ms/iteration
Digital Controller (n=4, m=3, r=6)	14.5
Digital Controller (n=9, M=3, r=6)	
vectors filled with zeroes-	46.0
with write of values to floppy	47.0
Digital Controller (n=6, m=3, r=6)	
vectors filled with zeroes	27.7
no zeroes in vectors	34.0
*all cases tested fo. 1000 iterations	

Table 1. Summary of digital controller implementation speed test on HP 9845C.

As is obvious from Table 1, only the lowest order digital controller implementation could be carried out within the required 20ms sample period. For this reason the HP 9845C desktop computer was deemed unfit for this particular task.

Hardware/Software Study of Computational Speed Problem

A study was made to determine the availability and approximate cost of computers and/or hardware accessories necessary to meet the 20ms sample period speed requirements. Additional requirements were that the control algorithym could be programmed in a high level language (FORTRAN OR BASIC) and that the machine have sufficient storage to store the data from a complete experiment.

The results of the study are sumarized in Table 2 and informative comments with respect to the individual machines follow.

COMPUTER	RAM	MASS STORAGE	TERMINAL	HARD COPY	INTERFACE	SOFTWARE		DELIVERY	TOTAL PRICE
						OPERATING SYSTEM	LANGUAGE		
HP9020S $49,945	1Mb	5.25" floppy 10 Mb internal fixed disk	Internal Monochrome (no color)	Internal Thermal Printer	GP-IO (16-bit parallel)	BASIC language System w/3D Graphics HP-UX (single user) w/Graphics/ 9000AGP & Graphics/9000 DEL	BASIC FORTRAN 77 HP-PASCAL	24 wks.	$50,645
HP9020B $28,250	512kb	5.25" floppy (std.) 10 Mb internal fixed disk $4,540	Internal Monochrome (no color)	Internal Thermal Printer $4,895	GP-IO $700	BASIC language system $4,035	BASIC	11 wks.	$42,420
HP9700 $21,660	256kb	16.5 Mb fixed disk	Hewlett Packard 26224 (no color) $2,210	Dot Matrix Impact Printer $1,000*	GP-IO $700*	RTE A.1	FORTRAN $2,250	10 wks.	$39,150
HP9845 w/Array Processor $14,500	187kb	Dual 5.25" floppy disks	Internal (full color)	Internal Thermal	GP-IO (2) $524 ea. $1,050	BASIC	BASIC	?	$15,550
Seattle Computer Co.'s Gazelle $8,435	128kb	8" floppy 15 Mb fixed	Televideo 950 $1,050	Dot Matrix Impact Printer $1000*	Interfacer 2: 3 16 bit parallel & 1 serial	MS-DOS	FORTRAN	less than 1 week	$10,774

TABLE 2. Summary of hardware/software requirements to meet computational speed requirements for GIV experiment digital controller. (*Estimated cost)

INFORMATIVE COMMENTS

1) The HP9020S is the single user, one package, desktop version of Hewlett Packard's new 32 bit processor machine. It includes hardware math and uses an 18MHz clock. Everything needed, hardware & software, with the exception of the GP-IO, is included with the "S" package as shown in the table.

2) The HP9020B is the same machine (package and processor) as the HP9020S with no standard peripherals or software. Shown in the table are the minimal add-ons required so that the system may meet the task requirements.

3) The HPA700 (from the 1000 series) is a mini-computer geared toward multi-user environments and expandability. It is the lowest priced mini available from HP which takes advantage of hardware mathematics and should meet the speed requirements easily.

4) The HP9845C system would be built around the existing 9845C in the test lab. The necessary purchase is essentially the array processor unit built by ANALOGIC. The array processor would speed up array manipulations only and would sup · no increase in speed for control algorithms which did not take advantage of matrix arithmetic. There is much concern and uncertainty over the fact that in this system, the 9845 must communicate with both the COSMEC I and the array processor. This is seen as a possible deterrent to the increased speed gained by use of the array processor.

5) Seattle Computer Company's Gazelle is an 8086 based micro system which takes advantage of the 8087 coprocessor. No benchmarks regarding speed are available from the company, however, considering the timing specs given by Intel for the 8086-8087 combination, the machine should be well within the speed requirements for the task. A dealer handling the Gazelle is located in Atlanta, and an inspection of the machine and possibly a test run are suggested.

APPENDIX E.

SECTION 1. METHOD OF DETERMINING MODE SHAPES AND NATURAL FREQUENCIES OF THE NASA UNMODIFIED TEST STRUCTURE

SECTION 2. CONTINUOUS BEAM CLOSED FROM SOLUTION TO THE NASA-LSS ASTROMAST TORSIONAL VIBRATION

Appendix E
Section 1
Method of Determining Mode Shapes and Natural Frequencies of the NASA Unmodified Test Structure

Abstract

This paper illustrates the methods used to determine the lower natural frequencies and their corresponding mode shapes of the NASA-LSS Astromast (Unmodified Test Structure), and the mass integrals associated with the mode shapes. The test structure is modeled as a cantilever beam with 91 lumped masses and without the tip mass on the free end of the beam. This uncouples the torsion and bending modes and allows for them to be determined separately. We limited the frequency range to have an upper bound of 100. rad/sec (15.92 Hz.). In this range from 0.-100. rad/sec, we found three bending frequencies and one torsion frequency.

Introduction

One of the simpler approaches available for determining eigenvalues and eigenvectors is used in the development of this structural model. But use of a simplified method requires simplifying the assumptions being made. The first assumption is to treat the beam as cantilevered. This is a fairly safe assumption when considering the weight of the mast as compared to the weight of the LSS/GTV experiment equipment. The lumped mass approach is a second assumption which has been shown many times in the past to be reliable, especially when the distance between masses is relatively small as in this case. The ASTROMAST is modeled with no tip mass as this is how it is first tested in shaker tests. The tip mass is included in another program which incorporates the frequencies of the beam itself and uses modal synthesis to determine frequencies of the entire test structure. Without the tip mass/instrument package

connected to the free end of the beam, torsional and bending modes are uncoupled. This is due to there being no offset on the end which would couple the two modes.

Problem Description and Method of Solution

The problem in this case is to determine the natural frequencies, mode shapes, and mass integrals of the LSS Astromast. The beam is divided into 91 equal sections, as in the actual mast itself, with mass equally distributed across the beam at each node and having essentially massless connectors between the nodes. Transfer matrices can now be generated to relate conditions from one point to another anywhere on the beam. The matrices for the bending and torsion cases are shown in Attachment 1. The procedure for determining eigenvalues in translation is shown below. The torsional method is similar but much easier due to the smaller size of the transfer matrix.

Starting with the tip (free end), the point and field matrices can be multiplied back to the base to yield the following equation:

$$\begin{bmatrix} y \\ \Theta \\ M \\ V \end{bmatrix}_T = \begin{bmatrix} & U1 & \\ & & \end{bmatrix} \begin{bmatrix} y \\ \theta \\ M \\ V \end{bmatrix}_B$$

Utilizing the fact that the moment and shear are zero at the tip and deflection and slope are zero at the base, a subsequent matrix can be formed relating known tip conditions to unknown base conditions:

$$\begin{bmatrix} 0 \\ 0 \end{bmatrix}_T = \begin{bmatrix} U22 \end{bmatrix} \begin{bmatrix} M \\ V \end{bmatrix}_B$$

Therefore, to have a nontrivial solution of the above equation; the determinant of matrix U22 must equal zero. Since U22 is a function of the system's natural frequency, when the determinant is zero an eigenvalue has been located.

Once an eigenvalue is defined, the mode shapes can be calculated. Going back to the above equation, set M=1.0 and then solve for V. This procedure generates a consistent set of base conditions for the structure. The transfer matrices can now be used again once the base conditions are established:

$$\begin{bmatrix} y \\ \Theta \\ M \\ V \end{bmatrix}_1 = \begin{bmatrix} \\ T1 \\ \\ \end{bmatrix} \begin{bmatrix} 0 \\ 0 \\ 1. \\ V \end{bmatrix}_B$$

This equation solves for conditions at lump number 1 relative to the base. Then conditions at 2 can be solved based on conditions at 1, and this process is continued until the tip conditions are reached. The intermediate values are written to plot files where they can later be retrieved and plotted as eigenvectors. In the same routine the mass integrals can also be calculated using the eigenvector data and the following formulas for translation:

$$\Gamma_0 = \text{Sum } (mi*yi)$$

$$\Gamma_1 = \text{Sum } (mi*li*yi*)$$

$$M = \text{Sum } (mi*(yi**2)).$$

Basically, the same process is used for the torsional modes as that used for the bending modes. The tip and base conditions are now related by the following formula:

$$\begin{bmatrix} \phi \\ 0 \end{bmatrix}_T = \begin{bmatrix} \\ U1 \\ \\ \end{bmatrix} \begin{bmatrix} 0 \\ T \end{bmatrix}_B$$

Only one term, which is a function of natural frequency, is now set to zero instead of a determinant of a matrix. The base torque is now set equal to 1.0 and the values for twist and torque are determined from the individual transfer matrices just as in the bending case. The formulas used for the rotation mass integrals are as follows:

$$\Gamma_0 = 0.$$

$$\Gamma_1 = \text{Sum } (Ii*\phi i)$$

$$M = \text{Sum } (Ii*(\phi i**2)).$$

Results

Using the methods described previously and a range of 0.-100. rad/sec, three bending modes and one torsional mode were located. The three bending modes occurred at

3.882 rad/sec (00.62 Hz),
24.609 rad/sec (3.92 Hz),
70.238 rad/sec (11.18 Hz);

and the torsional mode occurred at

43.208 rad/sec (6.88 Hz).

The plots for these mode shapes can be seen in Attachment 2. (Dr. George Doane's closed system analysis (Section 2) backed up the torsional frequency and an independent program written by Dr. Eugene Worley backed up the bending mode values.)

The mass integrals calculated are as follows for each frequency:

	3.882	24.609	70.238	43.208
Γ_0	1.725E-04	1.597E-05	2.767E-06	0.000
Γ_1	6.481E-02	2.128E-03	8.731E-05	5.265E-01
M	3.779E-06	9.151E-08	1.069E-08	1.338E-06

The bending mass integrals agreed very closely with Dr. Worley's calculated values.

Conclusions

Therefore, the methods and assumptions used in this paper are deemed feasible and very reliable and are recommended to be used in similar projects in the future.

Attachment 1. UNCOUPLED TRANSFER MATRICES

Translation:

Point

$$\begin{bmatrix} 1 & 0 & 0 & 0 \\ 0 & 1 & 0 & 0 \\ 0 & 0 & 1 & 0 \\ m\omega^2 & 0 & 0 & 1 \end{bmatrix}$$

Field

$$\begin{bmatrix} 1 & 5.625 & A_{y\Theta} & A_{yy} \\ 0 & 1 & A_{\Theta\Theta} & A_{\Theta Y} \\ 0 & 0 & 1 & 5.625 \\ 0 & 0 & 0 & 1 \end{bmatrix} \begin{bmatrix} y \\ \Theta \\ M \\ V \end{bmatrix}$$

Rotation:

Point

$$\begin{bmatrix} 1 & 0 \\ -J\omega^2 & 1 \end{bmatrix}$$

Field

$$\begin{bmatrix} 1 & ATOR \\ 0 & 1 \end{bmatrix} \begin{bmatrix} \phi \\ T \end{bmatrix}$$

$$KTR = \begin{bmatrix} 1.80464 \cdot 10^3 & -5.07554 \cdot 10^3 \\ -5.07554 \cdot 10^3 & 3.97252 \cdot 10^5 \end{bmatrix}$$

$A = KTR^{-1}$
$A(1,1) = A_{yy}$
$A(1,2) = A(2,1) = A_{y\Theta} = A_{\Theta y}$
$A(2,2) = A_{\Theta\Theta}$

$ATOR = 5.58 \cdot 10^{-5}$

Beam length = 512 inches
Section length - 5.625 inches
D = 4.457 inches
Mass of beam = 0.012940 snails
Mass of one lumped mass = (0.012940)/(91) = MI snails
Inertia of one lumped mass = JI = MI $\cdot$ D^2 snails-inches^2

ATTACHMENT 2. MODE SHAPES

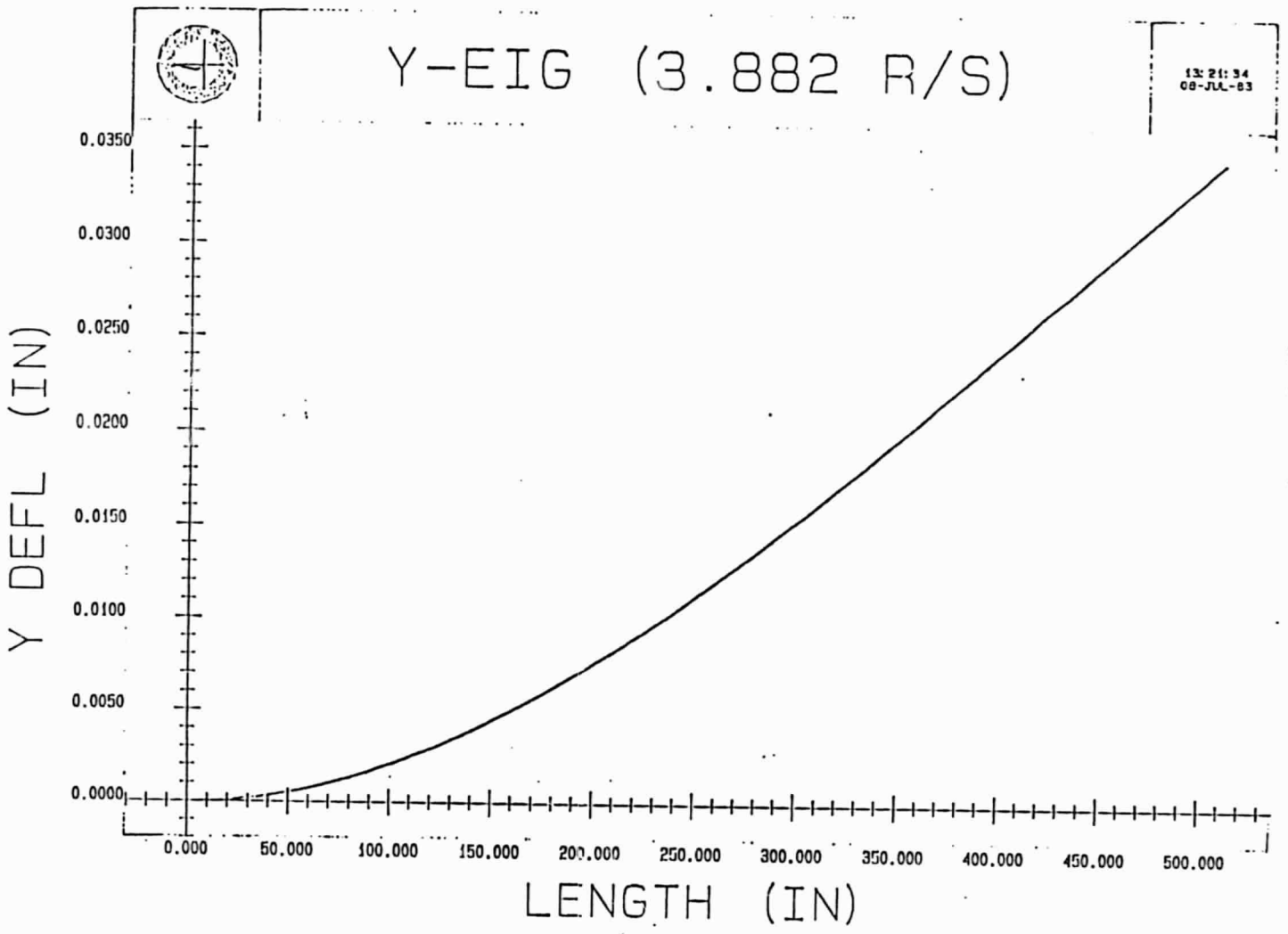

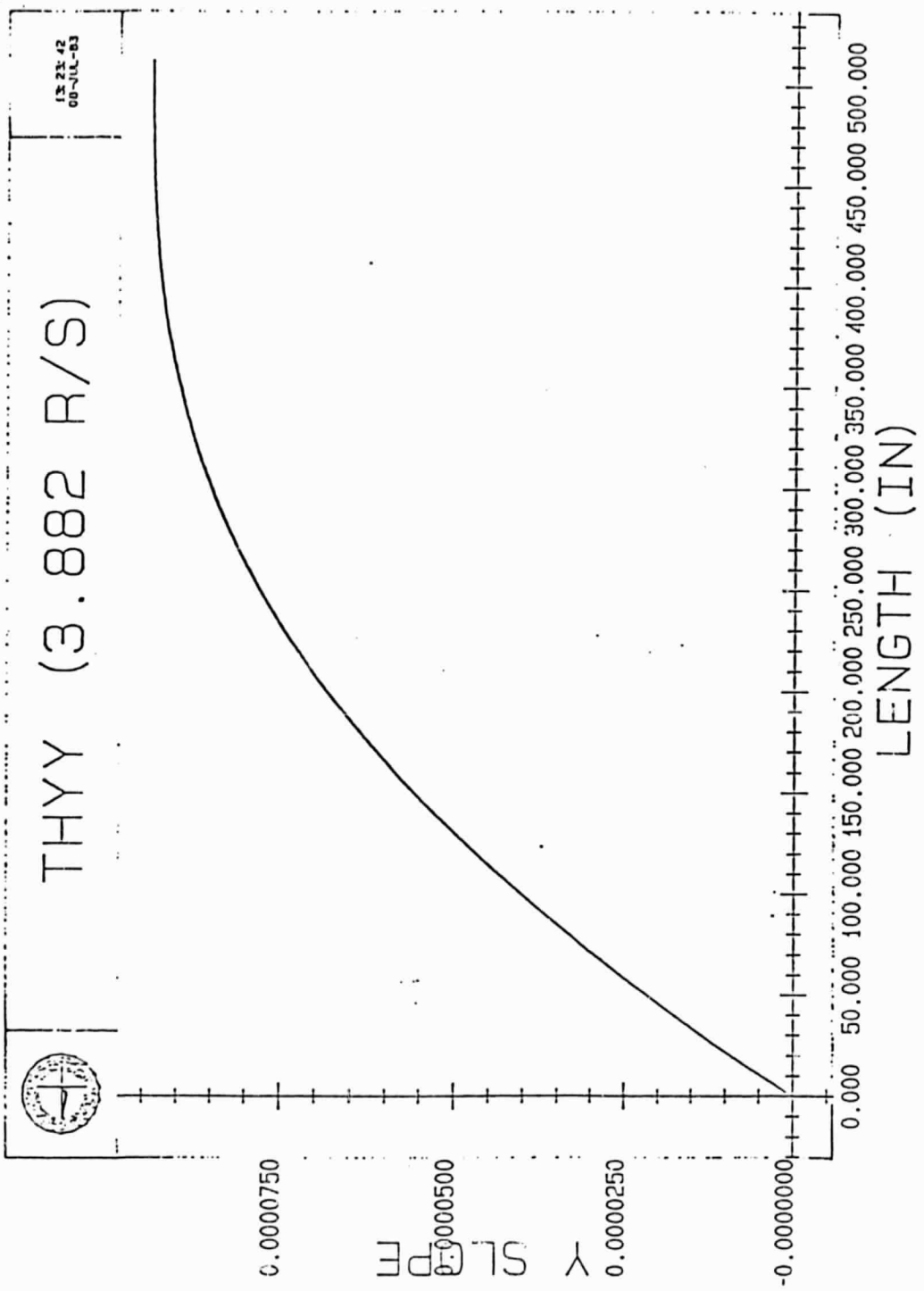

NM	LENGTH	Y-DEFL	SLOPE	MOMENT
0.0000D+00	0.0000D+00	0.0000D+00	0.0000D+00	0.1000D+01
0.1000D+01	0.5625D+01	0.5807D-05	0.2591D-05	0.9850D+00
0.2000D+01	0.1125D+02	0.2608D-04	0.5144D-05	0.9699D+00
0.3000D+01	0.1688D+02	0.6060D-04	0.7657D-05	0.9549D+00
0.4000D+01	0.2250D+02	0.1091D-03	0.1013D-04	0.9399D+00
0.5000D+01	0.2812D+02	0.1713D-03	0.1256D-04	0.9248D+00
0.6000D+01	0.3375D+02	0.2474D-03	0.1496D-04	0.9098D+00
0.7000D+01	0.3938D+02	0.3367D-03	0.1732D-04	0.8948D+00
0.8000D+01	0.4500D+02	0.4392D-03	0.1963D-04	0.8797D+00
0.9000D+01	0.5063D+02	0.5545D-03	0.2191D-04	0.8647D+00
0.1000D+02	0.5625D+02	0.6826D-03	0.2415D-04	0.8497D+00
0.1100D+02	0.6188D+02	0.8231D-03	0.2635D-04	0.8347D+00
0.1200D+02	0.6750D+02	0.9759D-03	0.2851D-04	0.8197D+00
0.1300D+02	0.7313D+02	0.1141D-02	0.3063D-04	0.8047D+00
0.1400D+02	0.7875D+02	0.1317D-02	0.3271D-04	0.7897D+00
0.1500D+02	0.8437D+02	0.1506D-02	0.3475D-04	0.7748D+00
0.1600D+02	0.9000D+02	0.1705D-02	0.3676D-04	0.7599D+00
0.1700D+02	0.9563D+02	0.1916D-02	0.3872D-04	0.7449D+00
0.1800D+02	0.1013D+03	0.2138D-02	0.4065D-04	0.7301D+00
0.1900D+02	0.1069D+03	0.2370D-02	0.4253D-04	0.7152D+00
0.2000D+02	0.1125D+03	0.2613D-02	0.4438D-04	0.7004D+00
0.2100D+02	0.1181D+03	0.2867D-02	0.4619D-04	0.6855D+00
0.2200D+02	0.1238D+03	0.3130D-02	0.4796D-04	0.6708D+00
0.2300D+02	0.1294D+03	0.3403D-02	0.4969D-04	0.6560D+00
0.2400D+02	0.1350D+03	0.3686D-02	0.5139D-04	0.6413D+00
0.2500D+02	0.1406D+03	0.3978D-02	0.5304D-04	0.6267D+00
0.2600D+02	0.1463D+03	0.4280D-02	0.5466D-04	0.6121D+00
0.2700D+02	0.1519D+03	0.4590D-02	0.5624D-04	0.5976D+00
0.2800D+02	0.1575D+03	0.4910D-02	0.5778D-04	0.5831D+00
0.2900D+02	0.1631D+03	0.5237D-02	0.5928D-04	0.5686D+00
0.3000D+02	0.1688D+03	0.5574D-02	0.6075D-04	0.5543D+00
0.3100D+02	0.1744D+03	0.5918D-02	0.6218D-04	0.5399D+00
0.3200D+02	0.1800D+03	0.6270D-02	0.6357D-04	0.5257D+00
0.3300D+02	0.1856D+03	0.6630D-02	0.6492D-04	0.5116D+00
0.3400D+02	0.1913D+03	0.6998D-02	0.6624D-04	0.4975D+00
0.3500D+02	0.1969D+03	0.7372D-02	0.6752D-04	0.4835D+00
0.3600D+02	0.2025D+03	0.7754D-02	0.6877D-04	0.4696D+00
0.3700D+02	0.2081D+03	0.8143D-02	0.6998D-04	0.4558D+00
0.3800D+02	0.2138D+03	0.8539D-02	0.7115D-04	0.4421D+00
0.3900D+02	0.2194D+03	0.8941D-02	0.7228D-04	0.4285D+00
0.4000D+02	0.2250D+03	0.9349D-02	0.7339D-04	0.4150D+00
0.4100D+02	0.2306D+03	0.9764D-02	0.7446D-04	0.4016D+00
0.4200D+02	0.2363D+03	0.1018D-01	0.7548D-04	0.3883D+00
0.4300D+02	0.2419D+03	0.1061D-01	0.7648D-04	0.3751D+00
0.4400D+02	0.2475D+03	0.1104D-01	0.7744D-04	0.3621D+00
0.4500D+02	0.2531D+03	0.1148D-01	0.7837D-04	0.3492D+00
0.4600D+02	0.2588D+03	0.1192D-01	0.7927D-04	0.3365D+00
0.4700D+02	0.2644D+03	0.1237D-01	0.8013D-04	0.3239D+00
0.4800D+02	0.2700D+03	0.1282D-01	0.8096D-04	0.3114D+00
0.4900D+02	0.2756D+03	0.1328D-01	0.8175D-04	0.2991D+00
0.5000D+02	0.2812D+03	0.1374D-01	0.8252D-04	0.2870D+00
0.5100D+02	0.2869D+03	0.1420D-01	0.8325D-04	0.2750D+00
0.5200D+02	0.2925D+03	0.1467D-01	0.8396D-04	0.2632D+00
0.5300D+02	0.2981D+03	0.1514D-01	0.8463D-04	0.2516D+00
0.5400D+02	0.3038D+03	0.1562D-01	0.8527D-04	0.2401D+00
0.5500D+02	0.3094D+03	0.1610D-01	0.8589D-04	0.2289D+00

,00D+02	0.3150D+03	0.1658D-01	0.8647D-04	0.2178D+00
700D+02	0.3206D+03	0.1707D-01	0.8702D-04	0.2069D+00
800D+02	0.3263D+03	0.1756D-01	0.8755D-04	0.1963D+00
900D+02	0.3319D+03	0.1805D-01	0.8803D-04	0.1858D+00
000D+02	0.3375D+03	0.1855D-01	0.8852D-04	0.1756D+00
.100D+02	0.3431D+03	0.1905D-01	0.8896D-04	0.1656D+00
,200D+02	0.3488D+03	0.1955D-01	0.8938D-04	0.1558D+00
5300D+02	0.3544D+03	0.2005D-01	0.8978D-04	0.1463D+00
5400D+02	0.3600D+03	0.2056D-01	0.9015D-04	0.1370D+00
6500D+02	0.3656D+03	0.2106D-01	0.9049D-04	0.1280D+00
6600D+02	0.3713D+03	0.2157D-01	0.9082D-04	0.1192D+00
6700D+02	0.3769D+03	0.2208D-01	0.9112D-04	0.1106D+00
.6800D+02	0.3825D+03	0.2260D-01	0.9139D-04	0.1024D+00
.6900D+02	0.3881D+03	0.2311D-01	0.9165D-04	0.9435D-01
.7000D+02	0.3938D+03	0.2363D-01	0.9189D-04	0.8664D-01
.7100D+02	0.3994D+03	0.2414D-01	0.9210D-04	0.7920D-01
.7200D+02	0.4050D+03	0.2466D-01	0.9230D-04	0.7206D-01
,.7300D+02	0.4106D+03	0.2518D-01	0.9248D-04	0.6521D-01
).7400D+02	0.4163D+03	0.2570D-01	0.9264D-04	0.5867D-01
).7500D+02	0.4219D+03	0.2622D-01	0.9279D-04	0.5244D-01
0.7600D+02	0.4275D+03	0.2674D-01	0.9292D-04	0.4652D-01
0.7700D+02	0.4331D+03	0.2726D-01	0.9303D-04	0.4093D-01
0.7800D+02	0.4388D+03	0.2779D-01	0.9313D-04	0.3566D-01
0.7900D+02	0.4444D+03	0.2831D-01	0.9322D-04	0.3073D-01
0.8000D+02	0.4500D+03	0.2884D-01	0.9329D-04	0.2615D-01
0.8100D+02	0.4556D+03	0.2936D-01	0.9335D-04	0.2190D-01
0.8200D+02	0.4613D+03	0.2988D-01	0.9341D-04	0.1802D-01
0.8300D+02	0.4669D+03	0.3041D-01	0.9345D-04	0.1449D-01
0.8400D+02	0.4725D+03	0.3094D-01	0.9348D-04	0.1133D-01
0.8500D+02	0.4781D+03	0.3146D-01	0.9351D-04	0.8541D-02
0.8600D+02	0.4838D+03	0.3199D-01	0.9353D-04	0.6132D-02
0.8700D+02	0.4894D+03	0.3251D-01	0.9354D-04	0.4109D-02
0.8800D+02	0.4950D+03	0.3304D-01	0.9355D-04	0.2478D-02
0.8900D+02	0.5006D+03	0.3356D-01	0.9355D-04	0.1245D-02
0.9000D+02	0.5063D+03	0.3409D-01	0.9356D-04	0.4173D-03
0.9100D+02	0.5120D+03	0.3462D-01	0.9356D-04	0.1506D-13

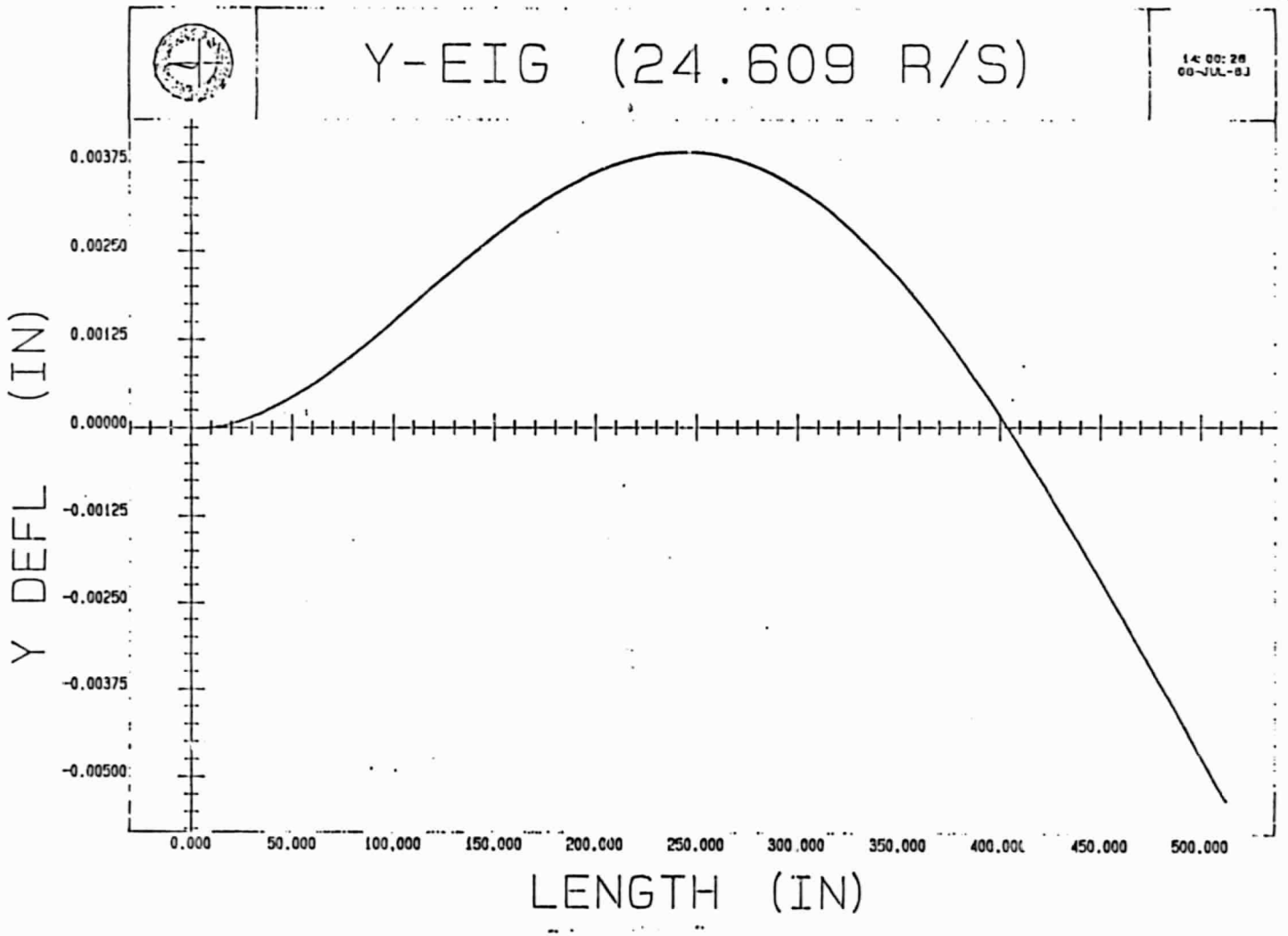

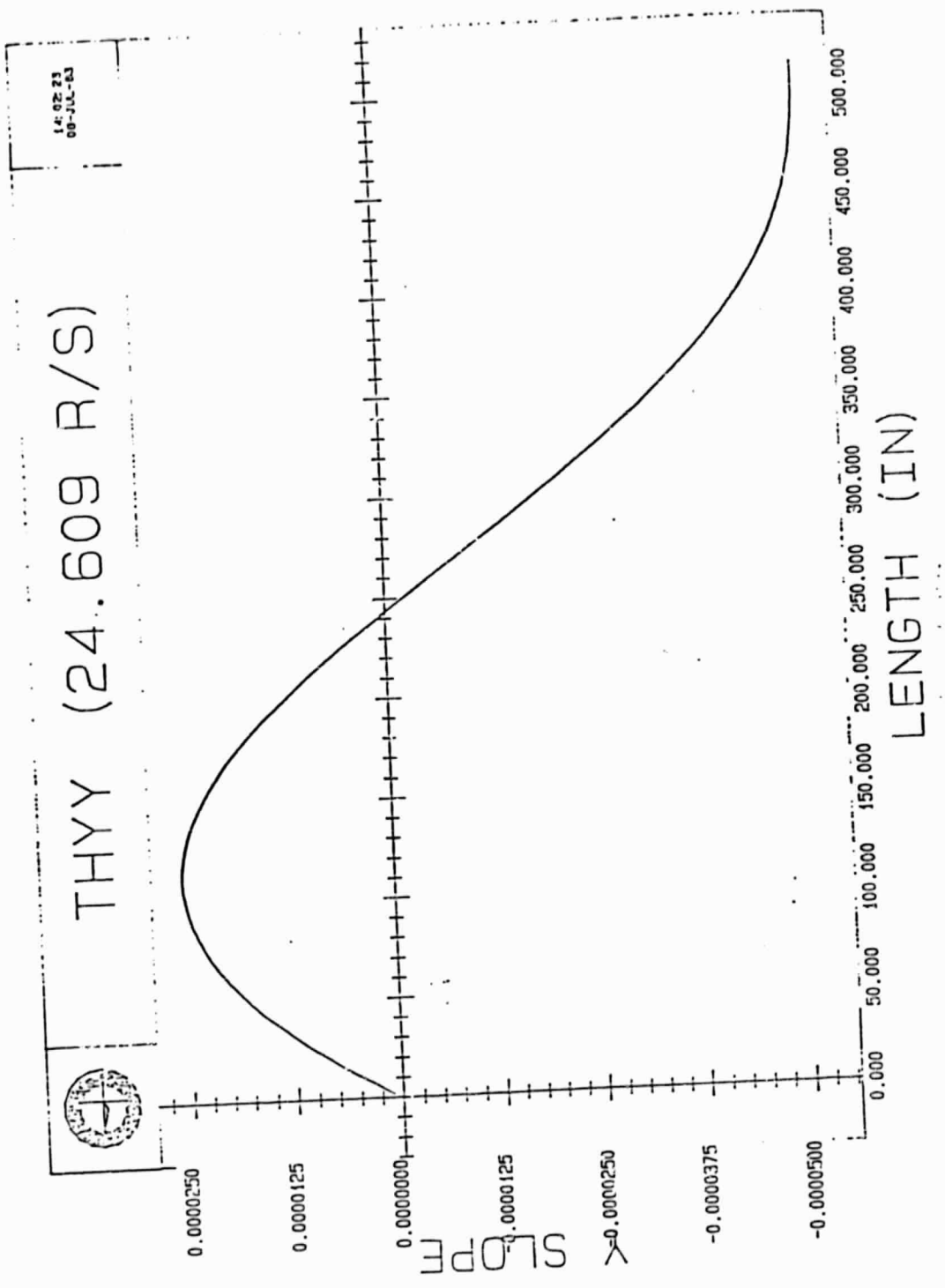

FREQ. = 24.609 RAD/SEC

NM	LENGTH	Y DEFL.	SLOPE	MOMENT
0.0000D+00	0.0000D+00	0.0000D+00	0.0000D+00	0.1000D+01
0.1000D+01	0.5625D+01	0.2046D-05	0.2543D-05	0.9482D+00
0.2000D+01	0.1125D+02	0.1802D-04	0.4952D-05	0.8963D+00
0.3000D+01	0.1688D+02	0.4716D-04	0.7224D-05	0.8445D+00
0.4000D+01	0.2250D+02	0.8870D-04	0.9362D-05	0.7927D+00
0.5000D+01	0.2812D+02	0.1419D-03	0.1136D-04	0.7409D+00
0.6000D+01	0.3375D+02	0.2060D-03	0.1323D-04	0.6892D+00
0.7000D+01	0.3938D+02	0.2802D-03	0.1496D-04	0.6376D+00
0.8000D+01	0.4500D+02	0.3638D-03	0.1656D-04	0.5862D+00
0.9000D+01	0.5063D+02	0.4560D-03	0.1802D-04	0.5349D+00
0.1000D+02	0.5625D+02	0.5561D-03	0.1935D-04	0.4838D+00
0.1100D+02	0.6188D+02	0.6633D-03	0.2055D-04	0.4330D+00
0.1200D+02	0.6750D+02	0.7769D-03	0.2162D-04	0.3825D+00
0.1300D+02	0.7313D+02	0.8962D-03	0.2255D-04	0.3324D+00
0.1400D+02	0.7875D+02	0.1020D-02	0.2335D-04	0.2828D+00
0.1500D+02	0.8437D+02	0.1149D-02	0.2403D-04	0.2336D+00
0.1600D+02	0.9000D+02	0.1281D-02	0.2457D-04	0.1850D+00
0.1700D+02	0.9563D+02	0.1415D-02	0.2499D-04	0.1370D+00
0.1800D+02	0.1013D+03	0.1552D-02	0.2529D-04	0.8969D-01
0.1900D+02	0.1069D+03	0.1690D-02	0.2546D-04	0.4314D-01
0.2000D+02	0.1125D+03	0.1829D-02	0.2552D-04-0.2601D-02	
0.2100D+02	0.1181D+03	0.1968D-02	0.2545D-04-0.4745D-01	
0.2200D+02	0.1238D+03	0.2106D-02	0.2527D-04-0.9135D-01	
0.2300D+02	0.1294D+03	0.2244D-02	0.2497D-04-0.1342D+00	
0.2400D+02	0.1350D+03	0.2379D-02	0.2457D-04-0.1760D+00	
0.2500D+02	0.1406D+03	0.2512D-02	0.2406D-04-0.2166D+00	
0.2600D+02	0.1463D+03	0.2641D-02	0.2344D-04-0.2561D+00	
0.2700D+02	0.1519D+03	0.2767D-02	0.2272D-04-0.2942D+00	
0.2800D+02	0.1575D+03	0.2889D-02	0.2191D-04-0.3310D+00	
0.2900D+02	0.1631D+03	0.3006D-02	0.2099D-04-0.3664D+00	
0.3000D+02	0.1688D+03	0.3118D-02	0.1999D-04-0.4004D+00	
0.3100D+02	0.1744D+03	0.3225D-02	0.1891D-04-0.4328D+00	
0.3200D+02	0.1800D+03	0.3325D-02	0.1774D-04-0.4637D+00	
0.3300D+02	0.1856D+03	0.3418D-02	0.1649D-04-0.4929D+00	
0.3400D+02	0.1913D+03	0.3504D-02	0.1516D-04-0.5205D+00	
0.3500D+02	0.1969D+03	0.3583D-02	0.1377D-04-0.5464D+00	
0.3600D+02	0.2025D+03	0.3654D-02	0.1231D-04-0.5706D+00	
0.3700D+02	0.2081D+03	0.3717D-02	0.1079D-04-0.5930D+00	
0.3800D+02	0.2138D+03	0.3771D-02	0.9218D-05-0.6136D+00	
0.3900D+02	0.2194D+03	0.3816D-02	0.7591D-05-0.6324D+00	
0.4000D+02	0.2250D+03	0.3853D-02	0.5918D-05-0.6493D+00	
0.4100D+02	0.2306D+03	0.3880D-02	0.4203D-05-0.6644D+00	
0.4200D+02	0.2363D+03	0.3897D-02	0.2451D-05-0.6776D+00	
0.4300D+02	0.2419D+03	0.3905D-02	0.6669D-06-0.6888D+00	
0.4400D+02	0.2475D+03	0.3903D-02-0.1144D-05-0.6982D+00		
0.4500D+02	0.2531D+03	0.3890D-02-0.2977D-05-0.7058D+00		
0.4600D+02	0.2588D+03	0.3868D-02-0.4827D-05-0.7114D+00		
0.4700D+02	0.2644D+03	0.3835D-02-0.6690D-05-0.7151D+00		
0.4800D+02	0.2700D+03	0.3792D-02-0.8559D-05-0.7170D+00		
0.4900D+02	0.2756D+03	0.3738D-02-0.1043D-04-0.7171D+00		
0.5000D+02	0.2812D+03	0.3675D-02-0.1230D-04-0.7153D+00		
0.5100D+02	0.2869D+03	0.3601D-02-0.1417D-04-0.7118D+00		
0.5200D+02	0.2925D+03	0.3516D-02-0.1602D-04-0.7065D+00		
0.5300D+02	0.2981D+03	0.3422D-02-0.1785D-04-0.6995D+00		
0.5400D+02	0.3038D+03	0.3317D-02-0.1967D-04-0.6909D+00		
0.5500D+02	0.3094D+03	0.3202D-02-0.2146D-04-0.6807D+00		

0.5600D+02 0.3150D+03 0.3078D-02-0.2322D-04-0.6689D+00
0.5700D+02 0.3206D+03 0.2944D-02-0.2495D-04-0.6556D+00
0.5800D+02 0.3263D+03 0.2800D-02-0.2664D-04-0.6409D+00
0.5900D+02 0.3319D+03 0.2647D-02-0.2829D-04-0.6248D+00
0.6000D+02 0.3375D+03 0.2485D-02-0.2990D-04-0.6074D+00
0.6100D+02 0.3431D+03 0.2314D-02-0.3147D-04-0.5889D+00
0.6200D+02 0.3488D+03 0.2135D-02-0.3298D-04-0.5692D+00
0.6300D+02 0.3544D+03 0.1948D-02-0.3444D-04-0.5483D+00
0.6400D+02 0.3600D+03 0.1752D-02-0.3584D-04-0.5268D+00
0.6500D+02 0.3656D+03 0.1549D-02-0.3719D-04-0.5043D+00
0.6600D+02 0.3713D+03 0.1338D-02-0.3847D-04-0.4811D+00
0.6700D+02 0.3769D+03 0.1121D-02-0.3970D-04-0.4572D+00
0.6800D+02 0.3825D+03 0.8967D-03-0.4086D-04-0.4327D+00
0.6900D+02 0.3881D+03 0.6662D-03-0.4196D-04-0.4079D+00
0.7000D+02 0.3938D+03 0.4297D-03-0.4299D-04-0.3827D+00
0.7100D+02 0.3994D+03 0.1877D-03-0.4396D-04-0.3573D+00
0.7200D+02 0.4050D+03-0.5955D-04-0.4486D-04-0.3317D+00
0.7300D+02 0.4106D+03-0.3117D-03-0.4569D-04-0.3063D+00
0.7400D+02 0.4163D+03-0.5684D-03-0.4645D-04-0.2810D+00
0.7500D+02 0.4219D+03-0.8292D-03-0.4716D-04-0.2559D+00
0.7600D+02 0.4275D+03-0.1094D-02-0.4779D-04-0.2313D+00
0.7700D+02 0.4331D+03-0.1362D-02-0.4836D-04-0.2072D+00
0.7800D+02 0.4388D+03-0.1633D-02-0.4887D-04-0.1837D+00
0.7900D+02 0.4444D+03-0.1907D-02-0.4932D-04-0.1610D+00
0.8000D+02 0.4500D+03-0.2183D-02-0.4972D-04-0.1393D+00
0.8100D+02 0.4556D+03-0.2462D-02-0.5003D-04-0.1186D+00
0.8200D+02 0.4613D+03-0.2742D-02-0.5034D-04-0.9912D-01
0.8300D+02 0.4669D+03-0.3024D-02-0.5057D-04-0.8096D-01
0.8400D+02 0.4725D+03-0.3309D-02-0.5076D-04-0.6426D-01
0.8500D+02 0.4781D+03-0.3592D-02-0.5091D-04-0.4917D-01
0.8600D+02 0.4838D+03-0.3878D-02-0.5102D-04-0.3582D-01
0.8700D+02 0.4894D+03-0.4164D-02-0.5110D-04-0.2434D-01
0.8800D+02 0.4950D+03-0.4450D-02-0.5115D-04-0.1488D-01
0.8900D+02 0.5006D+03-0.4737D-02-0.5118D-04-0.7581D-02
0.9000D+02 0.5063D+03-0.5025D-02-0.5119D-04-0.2573D-02
0.9100D+02 0.5120D+03-0.5313D-02-0.5120D-04 0.5038D-14

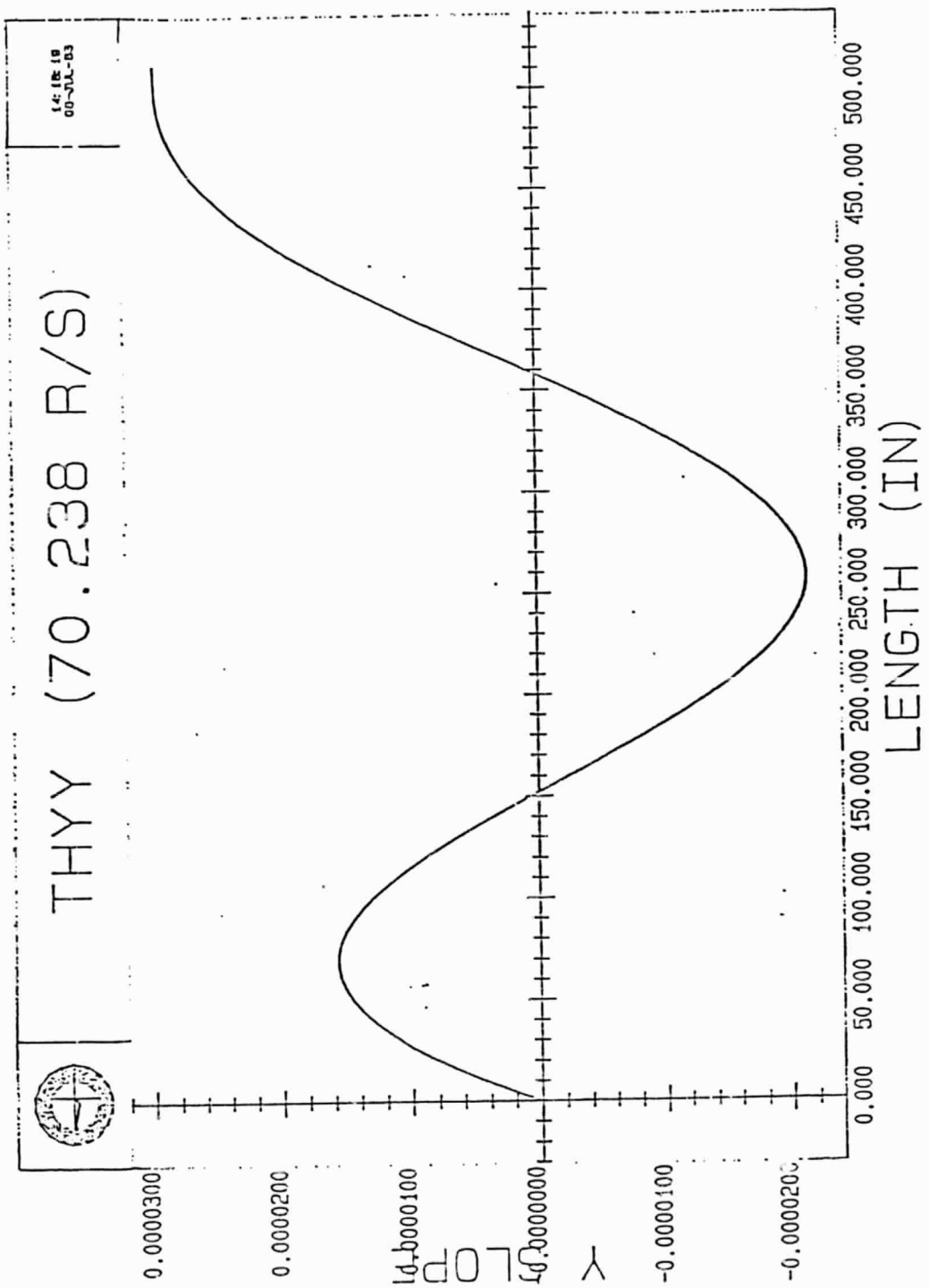

FREQ. = 70.236

NM	LENGTH	Y DEFL.	SLOPE	MOMENT
0.0000D+00	0.0000D+00	0.0000D+00	0.0000D+00	0.1000D+01
0.1000D+01	0.5625D+01	-0.1228D-05	0.2502D-03	0.9161D+00
0.2000D+01	0.1125D+02	0.1100D-04	0.4784D-05	0.8322D+00
0.3000D+01	0.1688D+02	0.3545D-04	0.6848D-03	0.7484D+00
0.4000D+01	0.2250D+02	0.7092D-04	0.8693D-05	0.6647D+00
0.5000D+01	0.2812D+02	0.1162D-03	0.1032D-04	0.5812D+00
0.6000D+01	0.3375D+02	0.1700D-03	0.1173D-04	0.4983D+00
0.7000D+01	0.3938D+02	0.2312D-03	0.1292D-04	0.4160D+00
0.8000D+01	0.4500D+02	0.2987D-03	0.1390D-04	0.3346D+00
0.9000D+01	0.5063D+02	0.3711D-03	0.1467D-04	0.2544D+00
0.1000D+02	0.5625D+02	0.4475D-03	0.1523D-04	0.1756D+00
0.1100D+02	0.6188D+02	0.5266D-03	0.1559D-04	0.9867D-01
0.1200D+02	0.6750D+02	0.6073D-03	0.1575D-04	0.2377D-01
0.1300D+02	0.7313D+02	0.6887D-03	0.1572D-04	-0.4873D-01
0.1400D+02	0.7875D+02	0.7696D-03	0.1550D-04	-0.1185D+00
0.1500D+02	0.8437D+02	0.8491D-03	0.1510D-04	-0.1853D+00
0.1600D+02	0.9000D+02	0.9262D-03	0.1454D-04	-0.2487D+00
0.1700D+02	0.9563D+02	0.1000D-02	0.1381D-04	-0.3084D+00
0.1800D+02	0.1013D+03	0.1070D-02	0.1293D-04	-0.3642D+00
0.1900D+02	0.1069D+03	0.1135D-02	0.1191D-04	-0.4158D+00
0.2000D+02	0.1125D+03	0.1194D-02	0.1077D-04	-0.4629D+00
0.2100D+02	0.1181D+03	0.1247D-02	0.9502D-05	-0.5053D+00
0.2200D+02	0.1238D+03	0.1292D-02	0.8133D-05	-0.5427D+00
0.2300D+02	0.1294D+03	0.1331D-02	0.6674D-05	-0.5751D+00
0.2400D+02	0.1350D+03	0.1361D-02	0.5137D-05	-0.6022D+00
0.2500D+02	0.1406D+03	0.1384D-02	0.3536D-05	-0.6240D+00
0.2600D+02	0.1463D+03	0.1397D-02	0.1886D-05	-0.6402D+00
0.2700D+02	0.1519D+03	0.1402D-02	0.1999D-06	-0.6510D+00
0.2800D+02	0.1575D+03	0.1398D-02	-0.1507D-05	-0.6562D+00
0.2900D+02	0.1631D+03	0.1385D-02	-0.3220D-05	-0.6560D+00
0.3000D+02	0.1688D+03	0.1362D-02	-0.4925D-05	-0.6502D+00
0.3100D+02	0.1744D+03	0.1331D-02	-0.6608D-05	-0.6391D+00
0.3200D+02	0.1800D+03	0.1291D-02	-0.8256D-05	-0.6227D+00
0.3300D+02	0.1856D+03	0.1242D-02	-0.9854D-05	-0.6013D+00
0.3400D+02	0.1913D+03	0.1185D-02	-0.1139D-04	-0.5749D+00
0.3500D+02	0.1969D+03	0.1120D-02	-0.1285D-04	-0.5439D+00
0.3600D+02	0.2025D+03	0.1047D-02	-0.1422D-04	-0.5084D+00
0.3700D+02	0.2081D+03	0.9674D-03	-0.1550D-04	-0.4688D+00
0.3800D+02	0.2138D+03	0.8812D-03	-0.1667D-04	-0.4254D+00
0.3900D+02	0.2194D+03	0.7891D-03	-0.1772D-04	-0.3785D+00
0.4000D+02	0.2250D+03	0.6918D-03	-0.1864D-04	-0.3285D+00
0.4100D+02	0.2306D+03	0.5899D-03	-0.1943D-04	-0.2758D+00
0.4200D+02	0.2363D+03	0.4842D-03	-0.2008D-04	-0.2207D+00
0.4300D+02	0.2419D+03	0.3755D-03	-0.2058D-04	-0.1637D+00
0.4400D+02	0.2475D+03	0.2645D-03	-0.2093D-04	-0.1053D+00
0.4500D+02	0.2531D+03	0.1521D-03	-0.2113D-04	-0.4579D-01
0.4600D+02	0.2588D+03	0.3906D-04	-0.2117D-04	0.1430D-01
0.4700D+02	0.2644D+03	-0.7375D-04	-0.2103D-04	0.7453D-01
0.4800D+02	0.2700D+03	-0.1855D-03	-0.2078D-04	0.1345D+00
0.4900D+02	0.2756D+03	-0.2953D-03	-0.2035D-04	0.1937D+00
0.5000D+02	0.2812D+03	-0.4025D-03	-0.1977D-04	0.2518D+00
0.5100D+02	0.2869D+03	-0.5060D-03	-0.1904D-04	0.3083D+00
0.5200D+02	0.2925D+03	-0.6053D-03	-0.1816D-04	0.3627D+00
0.5300D+02	0.2981D+03	-0.6995D-03	-0.1713D-04	0.4148D+00
0.5400D+02	0.3038D+03	-0.7878D-03	-0.1600D-04	0.4642D+00
0.5500D+02	0.3094D+03	-0.8697D-03	-0.1478D-04	0.5104D+00

0.5600D+02 0.3150D+03-0.9444D-03-0.1334D-01 0.5532D+00
0.5700D+02 0.3206D+03-0.1011D-02-0.1184D-01 0.5922D+00
0.5800D+02 0.3263D+03-0.1070D-02-0.1025D-01 0.6273D+00
0.5900D+02 0.3319D+03-0.1120D-02-0.8572D-05 0.6581D+00
0.6000D+02 0.3375D+03-0.1161D-02-0.6819D-05 0.6846D+00
0.6100D+02 0.3431D+03-0.1192D-02-0.5003D-05 0.7064D+00
0.6200D+02 0.3488D+03-0.1213D-02-0.3137D-05 0.7236D+00
0.6300D+02 0.3544D+03-0.1224D-02-0.1231D-05 0.7359D+00
0.6400D+02 0.3600D+03-0.1225D-02 0.7003D-06 0.7434D+00
0.6500D+02 0.3656D+03-0.1213D-02 0.2645D-05 0.7461D+00
0.6600D+02 0.3713D+03-0.1195D-02 0.4591D-05 0.7440D+00
0.6700D+02 0.3769D+03-0.1164D-02 0.6524D-05 0.7372D+00
0.6800D+02 0.3825D+03-0.1123D-02 0.8434D-05 0.7258D+00
0.6900D+02 0.3881D+03-0.1072D-02 0.1031D-04 0.7100D+00
0.7000D+02 0.3938D+03-0.1011D-02 0.1214D-04 0.6899D+00
0.7100D+02 0.3994D+03-0.9402D-03 0.1391D-04 0.6658D+00
0.7200D+02 0.4050D+03-0.8600D-03 0.1561D-04 0.6381D+00
0.7300D+02 0.4106D+03-0.7707D-03 0.1723D-04 0.6069D+00
0.7400D+02 0.4163D+03-0.6728D-03 0.1877D-04 0.5727D+00
0.7500D+02 0.4219D+03-0.5667D-03 0.2022D-04 0.5358D+00
0.7600D+02 0.4275D+03-0.4530D-03 0.2157D-04 0.4967D+00
0.7700D+02 0.4331D+03-0.3322D-03 0.2281D-04 0.4558D+00
0.7800D+02 0.4388D+03-0.2049D-03 0.2395D-04 0.4136D+00
0.7900D+02 0.4444D+03-0.7152D-04 0.2497D-04 0.3706D+00
0.8000D+02 0.4500D+03 0.6724D-04 0.2588D-04 0.3273D+00
0.8100D+02 0.4556D+03 0.2108D-03 0.2668D-04 0.2843D+00
0.8200D+02 0.4613D+03 0.3587D-03 0.2737D-04 0.2421D+00
0.8300D+02 0.4669D+03 0.5103D-03 0.2795D-04 0.2013D+00
0.8400D+02 0.4725D+03 0.6650D-03 0.2842D-04 0.1626D+00
0.8500D+02 0.4781D+03 0.8224D-03 0.2880D-04 0.1264D+00
0.8600D+02 0.4838D+03 0.9819D-03 0.2909D-04 0.9354D-01
0.8700D+02 0.4894D+03 0.1143D-02 0.2929D-04 0.6452D-01
0.8800D+02 0.4950D+03 0.1306D-02 0.2943D-04 0.4001D-01
0.8900D+02 0.5006D+03 0.1470D-02 0.2951D-04 0.2066D-01
0.9000D+02 0.5063D+03 0.1635D-02 0.2955D-04 0.7104D-02
0.9100D+02 0.5120D+03 0.1800D-02 0.2956D-04 0.1479D-13

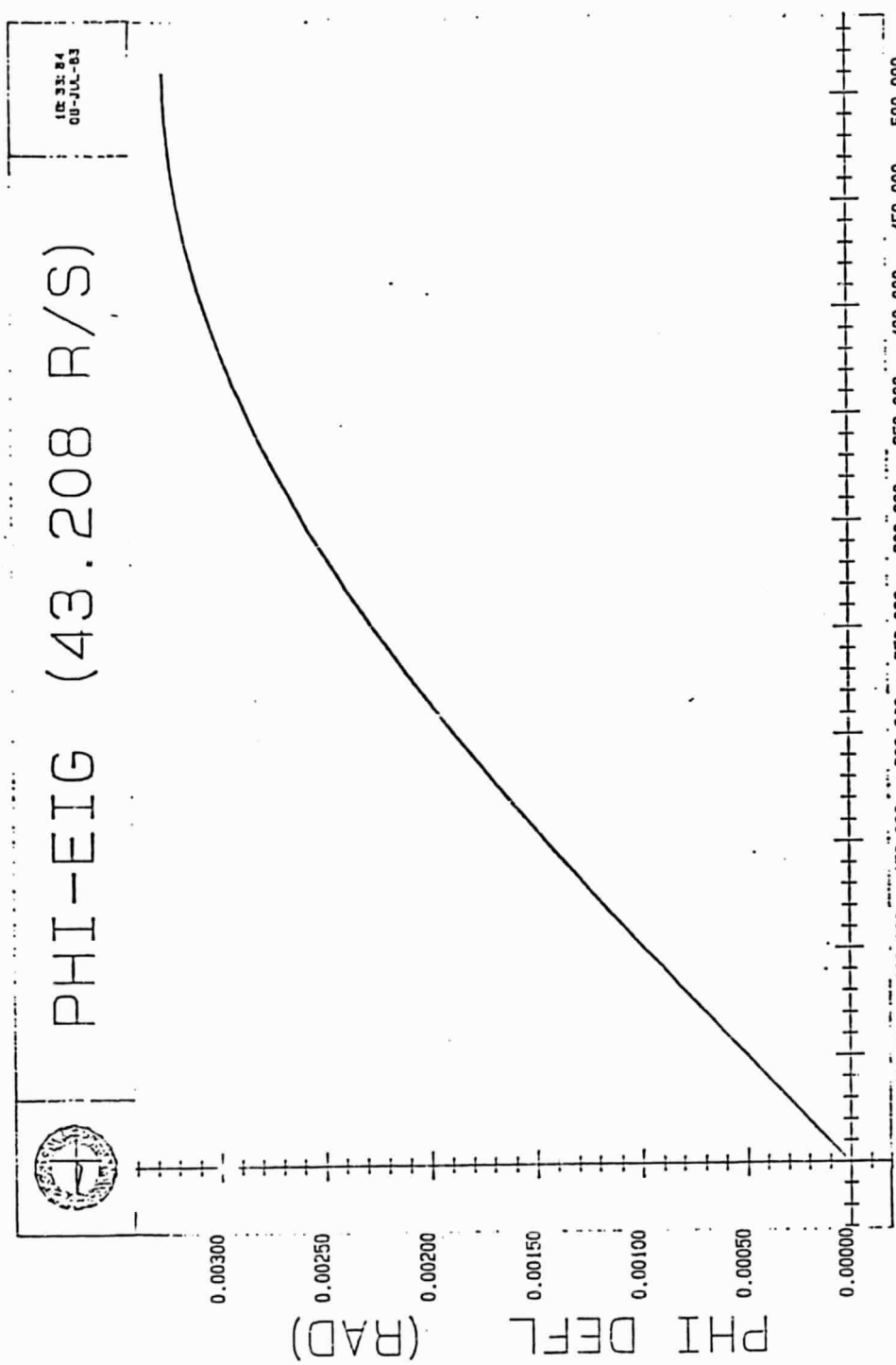

FREQ. =43.208 RAD/SEC

NM	LENGTH	PHI DEFL.	TORQUE
0.0000D+00	0.0000D+00	0.0000D+00	0.1000D+01
0.1000D+01	0.5625D+01	0.5580D-04	0.9997D+00
0.2000D+01	0.1125D+02	0.1116D-03	0.9991D+00
0.3000D+01	0.1688D+02	0.1673D-03	0.9982D+00
0.4000D+01	0.2250D+02	0.2230D-03	0.9971D+00
0.5000D+01	0.2812D+02	0.2787D-03	0.9956D+00
0.6000D+01	0.3375D+02	0.3342D-03	0.9938D+00
0.7000D+01	0.3938D+02	0.3897D-03	0.9918D+00
0.8000D+01	0.4500D+02	0.4450D-03	0.9894D+00
0.9000D+01	0.5063D+02	0.5002D-03	0.9868D+00
0.1000D+02	0.5625D+02	0.5553D-03	0.9838D+00
0.1100D+02	0.6188D+02	0.6102D-03	0.9806D+00
0.1200D+02	0.6750D+02	0.6649D-03	0.9771D+00
0.1300D+02	0.7313D+02	0.7194D-03	0.9733D+00
0.1400D+02	0.7875D+02	0.7737D-03	0.9692D+00
0.1500D+02	0.8437D+02	0.8278D-03	0.9648D+00
0.1600D+02	0.9000D+02	0.8817D-03	0.9602D+00
0.1700D+02	0.9563D+02	0.9352D-03	0.9552D+00
0.1800D+02	0.1013D+03	0.9885D-03	0.9500D+00
0.1900D+02	0.1069D+03	0.1042D-02	0.9445D+00
0.2000D+02	0.1125D+03	0.1094D-02	0.9387D+00
0.2100D+02	0.1181D+03	0.1147D-02	0.9327D+00
0.2200D+02	0.1238D+03	0.1199D-02	0.9264D+00
0.2300D+02	0.1294D+03	0.1250D-02	0.9198D+00
0.2400D+02	0.1350D+03	0.1302D-02	0.9129D+00
0.2500D+02	0.1406D+03	0.1353D-02	0.9057D+00
0.2600D+02	0.1463D+03	0.1403D-02	0.8983D+00
0.2700D+02	0.1519D+03	0.1453D-02	0.8906D+00
0.2800D+02	0.1575D+03	0.1503D-02	0.8827D+00
0.2900D+02	0.1631D+03	0.1552D-02	0.8745D+00
0.3000D+02	0.1688D+03	0.1601D-02	0.8661D+00
0.3100D+02	0.1744D+03	0.1649D-02	0.8573D+00
0.3200D+02	0.1800D+03	0.1697D-02	0.8484D+00
0.3300D+02	0.1856D+03	0.1745D-02	0.8392D+00
0.3400D+02	0.1913D+03	0.1791D-02	0.8297D+00
0.3500D+02	0.1969D+03	0.1838D-02	0.8200D+00
0.3600D+02	0.2025D+03	0.1883D-02	0.8101D+00
0.3700D+02	0.2081D+03	0.1929D-02	0.7999D+00
0.3800D+02	0.2138D+03	0.1973D-02	0.7894D+00
0.3900D+02	0.2194D+03	0.2017D-02	0.7788D+00
0.4000D+02	0.2250D+03	0.2061D-02	0.7679D+00
0.4100D+02	0.2306D+03	0.2104D-02	0.7569D+00
0.4200D+02	0.2363D+03	0.2146D-02	0.7455D+00
0.4300D+02	0.2419D+03	0.2187D-02	0.7339D+00
0.4400D+02	0.2475D+03	0.2228D-02	0.7221D+00
0.4500D+02	0.2531D+03	0.2269D-02	0.7102D+00
0.4600D+02	0.2588D+03	0.2308D-02	0.6980D+00
0.4700D+02	0.2644D+03	0.2347D-02	0.6856D+00
0.4800D+02	0.2700D+03	0.2386D-02	0.6730D+00
0.4900D+02	0.2756D+03	0.2423D-02	0.6602D+00
0.5000D+02	0.2812D+03	0.2460D-02	0.6472D+00
0.5100D+02	0.2869D+03	0.2496D-02	0.6340D+00
0.5200D+02	0.2925D+03	0.2531D-02	0.6206D+00
0.5300D+02	0.2981D+03	0.2566D-02	0.6071D+00
0.5400D+02	0.3038D+03	0.2600D-02	0.5933D+00
0.5500D+02	0.3094D+03	0.2633D-02	0.5794D+00

0.5600D+02	0.3150D+03	0.2665D-02	0.5654D+00
0.5700D+02	0.3206D+03	0.2697D-02	0.5511D+00
0.5800D+02	0.3263D+03	0.2728D-02	0.5367D+00
0.5900D+02	0.3319D+03	0.2758D-02	0.5222D+00
0.6000D+02	0.3375D+03	0.2787D-02	0.5074D+00
0.6100D+02	0.3431D+03	0.2815D-02	0.4926D+00
0.6200D+02	0.3488D+03	0.2843D-02	0.4776D+00
0.6300D+02	0.3544D+03	0.2869D-02	0.4624D+00
0.6400D+02	0.3600D+03	0.2895D-02	0.4471D+00
0.6500D+02	0.3656D+03	0.2920D-02	0.4317D+00
0.6600D+02	0.3713D+03	0.2944D-02	0.4161D+00
0.6700D+02	0.3769D+03	0.2967D-02	0.4005D+00
0.6800D+02	0.3825D+03	0.2990D-02	0.3847D+00
0.6900D+02	0.3881D+03	0.3011D-02	0.3688D+00
0.7000D+02	0.3938D+03	0.3032D-02	0.3528D+00
0.7100D+02	0.3994D+03	0.3051D-02	0.3366D+00
0.7200D+02	0.4050D+03	0.3070D-02	0.3204D+00
0.7300D+02	0.4106D+03	0.3088D-02	0.3041D+00
0.7400D+02	0.4163D+03	0.3105D-02	0.2877D+00
0.7500D+02	0.4219D+03	0.3121D-02	0.2712D+00
0.7600D+02	0.4275D+03	0.3136D-02	0.2547D+00
0.7700D+02	0.4331D+03	0.3150D-02	0.2380D+00
0.7800D+02	0.4388D+03	0.3164D-02	0.2213D+00
0.7900D+02	0.4444D+03	0.3176D-02	0.2046D+00
0.8000D+02	0.4500D+03	0.3187D-02	0.1877D+00
0.8100D+02	0.4556D+03	0.3198D-02	0.1708D+00
0.8200D+02	0.4613D+03	0.3207D-02	0.1539D+00
0.8300D+02	0.4669D+03	0.3216D-02	0.1369D+00
0.8400D+02	0.4725D+03	0.3224D-02	0.1199D+00
0.8500D+02	0.4781D+03	0.3230D-02	0.1028D+00
0.8600D+02	0.4838D+03	0.3236D-02	0.8573D-01
0.8700D+02	0.4894D+03	0.3241D-02	0.6862D-01
0.8800D+02	0.4950D+03	0.3245D-02	0.5148D-01
0.8900D+02	0.5006D+03	0.3248D-02	0.3433D-01
0.9000D+02	0.5063D+03	0.3249D-02	0.1717D-01
0.9100D+02	0.5120D+03	0.3250D-02	0.1266D-15

Definition of Terms

NM	number of point mass along ASTROMAST
LENGTH	location along ASTROMAST of the corresponding NM (inches)
Y-DEFL	deflection of ASTROMAST at corresponding NM (inches)
SLOPE	slope at corresponding NM (in/in)
MOMENT	moment at corresponding NM (in-lb)
PHI DEFLECTION	angular rotation at corresponding NM (radians)
TORQUE	torque at corresponding NM (in-lb)

Appendix E
Section 2

A Continuous Beam Closed Form Solution to the NASA-LSS Astromast Torsional Vibration

As one of the solutions to find the torsional vibration frequencies of the NASA-LSS beams the following continuous beam solution is offered.

It is necessary to develop the equations of the continuous beam in order to understand the calculation of the numerical values required. Consider a beam

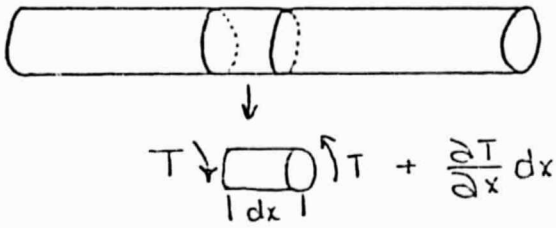

After Thompson, let x be measured along the length of the rod. The angle of twist in any length dx of the rod due to a torque T is

$$d\theta = \frac{T}{C}\, dx$$

where

$d\theta$ = angle twist across the segment dx
T = torque applied to segment
C = constant of proportionality

Rearranging yields

$$\frac{\partial \theta}{\partial x} = \frac{T}{C}$$

and

$$\frac{\partial^2 \theta}{\partial x^2} = \frac{1}{C}\,\frac{\partial T}{\partial x}$$

Thus the change in torque across the segment is given by

$$\frac{\partial T}{\partial x} dx = C \frac{\partial^2 \theta}{\partial x^2} dx$$

This torque increment is balanced by the inertial reaction term associated with the segment.

$$C \frac{\partial^2 \theta}{\partial x^2} dx = J \frac{\partial^2 \theta}{\partial t^2} dx$$

where J is the polar mass moment of inertia about the longitudinal axis of the rod, per unit length of the segment.

Thus both C and J are per unit length values and the dx's may be divided out. Thus

$$\frac{\partial^2 \theta}{\partial t^2} = \frac{C}{J} \frac{\partial^2 \theta}{\partial x^2} \triangleq k^2 \frac{\partial^2 \theta}{\partial x^2}$$

To calculate C let

$$d\theta = \frac{T}{C} dx \quad ; \quad T = C \frac{d\theta}{dx}$$

now for a segment dx = 5.625",

$$T = \frac{C}{5.625} d\theta.$$

From Dr. Glaese's model, <u>across a segment</u> the relationship

$$T = 1.79196 \times 10^4 \theta$$

obtains:

$$\frac{c}{5.625} = 1.79178 \times 10^4$$

$$c = 100796.88$$

To determine J, recall that the total moment of inertia associated with the segment is given by

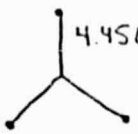

$$\text{mass} = \frac{5.0}{(91)(32.2)(12)} = 1.422 \times 10^{-4} \text{ snails}$$

J segment = $1.422 \times 10^{-4} \times (4.46)^2 = 2.829 \times 10^{-3}$ snail-inches^2
therefore the J per unit length is

$$J = \frac{2.829 \times 10^{-3}}{5.625} = 5.03 \times 10^{-4} \text{ j}$$

now

$$k^2 = \frac{c}{J} = \frac{10.079888 \times 10^4}{5.03 \times 10^{-4}} = 2.004 \times 10^8$$

$$k_1 = 1.4155 \times 10^4$$

Thompson states that the solution to

$$\frac{\partial^2 \theta}{\partial t^2} = k^2 \frac{\partial^2 \theta}{\partial x^2}$$

to be

$$\theta(x,t) = \left(A \sin\left(\frac{\omega x}{k}\right) + B \cos\left(\frac{\omega x}{k}\right)\right)\left(C \sin \omega t + D \cos \omega t\right).$$

The boundary conditions for a uniform rod in torsional oscillation with one end fixed and the other end free are

(1) when $x=0$, $\theta=0$

(2) when $x=\ell$, torque $=0$; or

$$\frac{\partial\theta}{\partial x}=0$$

Because the time origin is arbitrary the general solution may be taken to be

$$\theta=\left(A\sin\left(\frac{\omega x}{k}\right)+B\cos\left(\frac{\omega x}{k}\right)\right)\sin\omega t$$

Clearly (1) results in B=0; (2) in requiring

$$\cos\left(\frac{\omega\ell}{k}\right)=0.$$

This is satisfied when

$$\frac{\omega_n\ell}{k}=\frac{\pi}{2},\frac{3\pi}{2},\frac{5\pi}{2},\ldots,\left(n+\tfrac{1}{2}\right)\pi\ ;\quad n=0,1,2,\ldots$$

Hence

$$\frac{\ell}{k}=\frac{512}{1.4155\times10^{4}}$$

$$\omega_n=\frac{14155\pi}{512}\left(n+\tfrac{1}{2}\right)=86.85\left(n+\tfrac{1}{2}\right).$$

Construct the table:

n	ω_n	f_n
0	43.42	6.92
1	130.28	20.74
2	217.13	34.58

OMIT

APPENDIX F. ATTACHMENT FROM MR # 22 RESULTS OF MODAL SYNTHESIS MODEL

ATTACHMENT A.

Results of Modal Synthesis Model

Definition of nomenclature:

beam tip:	translates in X and Y directions
	rotates about X, Y, and Z axes
beam base:	translates in X and Y directions
	rotates about X, Y, and Z axes
elevation gimbal:	rotates about X-axis
azimuth gimbal:	rotates about Y-axis
roll gimbal:	rotates about Z-axis
base:	translates in X and Y directions

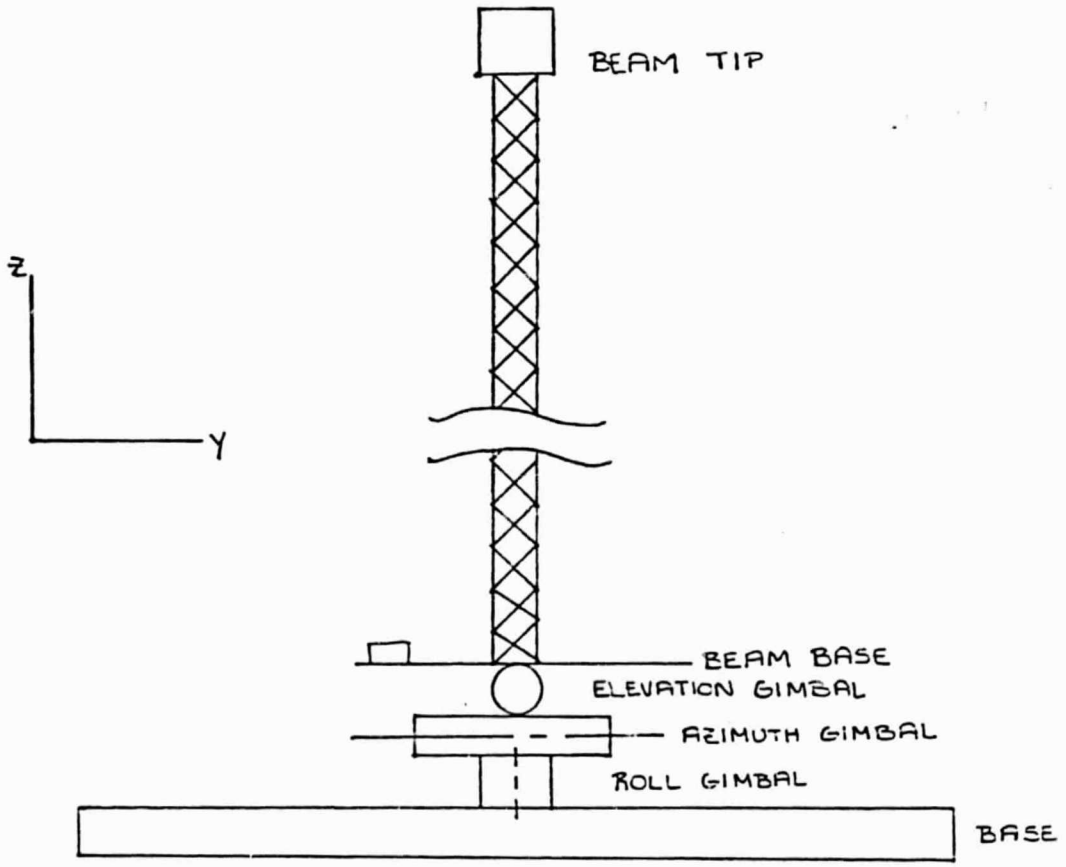

MODAL FREQUENCY 0.0000000	RAD/SEC		
BASE TRANSLATION	0.7208357	0.0000000	0.000000(
ROLL GIMBAL ROTATION	0.0000000		
AZIMUTH GIMBAL ROTATION	0.0000000		
ELEVATION GIMBAL ROTATION	0.0000000		
BEAM BASE TRANSLATION	0.7208357	0.0000000	0.000000(
BEAM BASE ROTATION	0.0000000	0.0000000	0.000000(
TIP INSTRUMENT PACKAGE TRANSLATION	0.7208357	0.0000000	0.000000(
TIP INSTRUMENT PACKAGE ROTATION	0.0000000	0.0000000	0.000000(
MODAL FREQUENCY 0.0000000	RAD/SEC		
BASE TRANSLATION	0.0000000	0.7208357	0.000000(
ROLL GIMBAL ROTATION	0.0000000		
AZIMUTH GIMBAL ROTATION	0.0000000		
ELEVATION GIMBAL ROTATION	0.0000000		
BEAM BASE TRANSLATION	0.0000000	0.7208357	0.000000(
BEAM BASE ROTATION	0.0000000	0.0000000	0.000000(
TIP INSTRUMENT PACKAGE TRANSLATION	0.0000000	0.7208357	0.000000:
TIP INSTRUMENT PACKAGE ROTATION	0.0000000	0.0000000	0.000000(
MODAL FREQUENCY 0.0000000	RAD/SEC		
BASE TRANSLATION	0.0101980	-0.0012932	0.000000(
ROLL GIMBAL ROTATION	0.1187835		
AZIMUTH GIMBAL ROTATION	0.0000000		
ELEVATION GIMBAL ROTATION	0.0000000		
BEAM BASE TRANSLATION	0.0101980	-0.0012932	0.000000(
BEAM BASE ROTATION	0.0000000	0.0000000	0.118783:
TIP INSTRUMENT PACKAGE TRANSLATION	-0.2215391	0.0280927	0.000000(
TIP INSTRUMENT PACKAGE ROTATION	0.0000000	0.0000000	0.118783:
MODAL FREQUENCY 0.0000000	RAD/SEC		
BASE TRANSLATION	-0.2426753	-0.0000825	0.000000(
ROLL GIMBAL ROTATION	0.0075818		
AZIMUTH GIMBAL ROTATION	0.0063638		
ELEVATION GIMBAL ROTATION	0.0000000		
BEAM BASE TRANSLATION	-0.0791644	-0.0000825	0.000000(
BEAM BASE ROTATION	0.0000000	0.0063638	0.007581(
TIP INSTRUMENT PACKAGE TRANSLATION	3.2468774	0.0017931	-0.001574:
TIP INSTRUMENT PACKAGE ROTATION	0.0000000	0.0063638	0.007581:
MODAL FREQUENCY 0.0000000	RAD/SEC		
BASE TRANSLATION	-0.0000439	0.2133059	0.000000(
ROLL GIMBAL ROTATION	0.0009661		
AZIMUTH GIMBAL ROTATION	0.0000033		
ELEVATION GIMBAL ROTATION	0.0064128		
BEAM BASE TRANSLATION	0.0000413	0.1025569	0.000000(
BEAM BASE ROTATION	0.0064128	0.0000033	0.000966
TIP INSTRUMENT PACKAGE TRANSLATION	-0.0001019	-3.2637730	0.012510(
TIP INSTRUMENT PACKAGE ROTATION	0.0064128	0.0000033	0.000966
MODAL FREQUENCY 5.913205	RAD/SEC		
BASE TRANSLATION	0.6340323	0.0000961	0.000000(
ROLL GIMBAL ROTATION	0.0017399		
AZIMUTH GIMBAL ROTATION	-0.0497098		
ELEVATION GIMBAL ROTATION	0.0000120		

BEAM BASE TRANSLATION	-0.6432107	-0.0001104	0.000000
BEAM BASE ROTATION	0.0000120	-0.0497098	0.001739
TIP INSTRUMENT PACKAGE TRANSLATION	0.5985857	-0.0000565	-0.008594
TIP INSTRUMENT PACKAGE ROTATION	-0.0000228	0.0345617	-0.016302

MODAL FREQUENCY 7.293426 RAD/SEC

BASE TRANSLATION	-0.0003125	0.4891170	0.000000
ROLL GIMBAL ROTATION	-0.0001548		
AZIMUTH GIMBAL ROTATION	0.0000250		
ELEVATION GIMBAL ROTATION	0.0602246		
BEAM BASE TRANSLATION	0.0003297	-0.5509624	0.000000
BEAM BASE ROTATION	0.0602246	0.0000250	-0.000154
TIP INSTRUMENT PACKAGE TRANSLATION	-0.0003538	0.5674684	-0.088492
TIP INSTRUMENT PACKAGE ROTATION	-0.0453606	-0.0000090	0.000052

MODAL FREQUENCY 11.29450 RAD/SEC

BASE TRANSLATION	-0.0302741	-0.0009661	0.000000
ROLL GIMBAL ROTATION	0.0184101		
AZIMUTH GIMBAL ROTATION	0.0024533		
ELEVATION GIMBAL ROTATION	-0.0000814		
BEAM BASE TRANSLATION	0.0327604	0.0004400	0.000000
BEAM BASE ROTATION	-0.0000814	0.0024533	0.018410
TIP INSTRUMENT PACKAGE TRANSLATION	0.0370206	-0.0081332	0.000938
TIP INSTRUMENT PACKAGE ROTATION	-0.0000700	-0.0043433	-0.715111

MODAL FREQUENCY 20.44361 RAD/SEC

BASE TRANSLATION	-0.4059115	-0.0021554	0.000000
ROLL GIMBAL ROTATION	-0.0001958		
AZIMUTH GIMBAL ROTATION	0.0339763		
ELEVATION GIMBAL ROTATION	-0.0002847		
BEAM BASE TRANSLATION	0.4670748	0.0027617	0.000000
BEAM BASE ROTATION	-0.0002847	0.0339763	-0.000195
TIP INSTRUMENT PACKAGE TRANSLATION	0.3724887	0.0012984	-0.023614
TIP INSTRUMENT PACKAGE ROTATION	-0.0003839	0.0924256	0.030584

MODAL FREQUENCY 23.29484 RAD/SEC

BASE TRANSLATION	0.0019001	-0.4684157	0.000000
ROLL GIMBAL ROTATION	0.0001902		
AZIMUTH GIMBAL ROTATION	-0.0001598		
ELEVATION GIMBAL ROTATION	-0.0616555		
BEAM BASE TRANSLATION	-0.0022019	0.5963746	0.000000
BEAM BASE ROTATION	-0.0616555	-0.0001598	0.000190
TIP INSTRUMENT PACKAGE TRANSLATION	-0.0018192	0.3291788	-0.179170
TIP INSTRUMENT PACKAGE ROTATION	-0.0919095	-0.0005578	-0.009847

MODAL FREQUENCY 57.86488 RAD/SEC

BASE TRANSLATION	-0.1169710	-0.0530800	0.000000
ROLL GIMBAL ROTATION	0.0000152		
AZIMUTH GIMBAL ROTATION	0.0105723		
ELEVATION GIMBAL ROTATION	-0.0074173		
BEAM BASE TRANSLATION	0.1546738	0.0750166	0.000000
BEAM BASE ROTATION	-0.0074173	0.0105723	0.000015
TIP INSTRUMENT PACKAGE TRANSLATION	-0.1921388	-0.0510709	0.102847
TIP INSTRUMENT PACKAGE ROTATION	0.0371458	-0.1227977	-0.002712

MODAL FREQUENCY 58.02358 RAD/SEC

BASE TRANSLATION	0.0377891	-0.1626017	0.000000

ROLL GIMBAL ROTATION	0.0000524		
AZIMUTH GIMBAL ROTATION	-0.0034170		
ELEVATION GIMBAL ROTATION	-0.0227311		
BEAM BASE TRANSLATION	-0.0500081	0.2299638	0.000000
BEAM BASE ROTATION	-0.0227311	-0.0034170	0.000052
TIP INSTRUMENT PACKAGE TRANSLATION	0.0637058	-0.1613539	0.215034
TIP INSTRUMENT PACKAGE ROTATION	0.1153053	0.0100853	-0.001361

TRANSLATIONS (INCHES)

ROTATIONS (RADIANS)

APPENDIX G. AIAA PAPER

DEFINITION OF GROUND TEST FOR LARGE SPACE STRUCTURE (LSS) CONTROL VERIFICATION

I. INTRODUCTION

As the United States moves into the Shuttle era of space technology, there are numerous proposals from the scientific, civilian and Defense Communities which envision the use of Large Space Structures (LSS). By definition, a LSS is very flexible, probably lightly damped, and exhibits multiple vibrational modes of very low frequency.

Many of the missions alluded to above require high performance from the LSS. This high performance takes the form of such things as extremely accurate pointing of lenses and the attainment of vibration free observation image planes.

To meet the rigorous control requirements of LSS, a new or extended body of control theory has been developed. To test these various schemes, MSFC (Marshall Space Flight Center) is establishing a LSS laboratory in which experimentation with large beams, LSS components, or even perhaps a given full-size LSS may be performed.

This paper delineates the program currently underway to develop the laboratory facility and concurrently to develop and install the first experiment in the laboratory.

II. LSS Ground Verification Experiment

The Ground Test Verification (GTV) experiment is described by the drawing of Figure 1. The first test article will be the ASTROMAST beam as shown. The ASTROMAST is extremely lightweight (about 5 pounds) and approximately 45 feet in length and is constructed almost entirely of S-GLASS. It is of the type to be flown in SAFE I.

The test article will be mounted on the faceplate of the Advanced Gimbal System (AGS) engineering model which, along with an additional torque actuator in azimuth, provides the control inputs for the system. The azimuth gimbal also provides a means of rotating the entire experiment manually to produce different test scenarios. The ASTROMAST will be gravity unloaded by a constant tension cable whose upper end is free to translate.

The AGS will sit atop the base of the test structure which will be supported by air bearings or oil film bearings and will include actuators to provide translational disturbance inputs to the test fixture. These disturbances could represent astronaut pushoff or RCS (Reaction Control System) thruster firing.

Six separately packaged inertial measurement assemblies comprise the control system sensors. Two of the packages, containing three axis translational accelerometers, are identical. One will be mounted on the mast tip, and the other on the base of the test fixture. Three other packages contain ATM (Apollo Telescope Mount) rate gyros and will be installed on the AGS faceplate. The sixth package, the Kearfott Attitude Reference System (KARS), will be placed at the mast tip along with the accelerometer package.

The signals from these instruments will be read by the COSMEC I data gathering and control system, and processed according to the control strategy under scrutiny. The control actuator signals will then be transmitted to the AGS as inputs to the dynamical system.

The COSMEC I will be interfaced to a Hewlett Packard HP9845C desktop computer which will store data as it is collected during a test run, and then provide post experiment data reduction and display offline. The controller inputs and outputs (measurements and commands) will be recorded at each sample period or at some multiple of sample periods.

III. Project Management

The project management encompasses the technical and business management activities. These activities are required to plan, execute, control and report technical performance of the LSS ground verification experiment. Two more important and time consuming efforts, relative to the LSS ground experiment management, are developing and coordinating the schedules among the various participating MSFC elements and utilizing the resources in a cost-effective manner. To this end, the project management has been partitioned into three categories. They are planning and control, configuration management, and procurement management.

The planning and control element provides for the planning, authorizing, and controlling of the LSS ground test effort. This activity also provides for timely visibility into the performance, cost, and schedule and is keyed to the appropriate MSFC organizations and to the Work Breakdown Structure (WBS) and the WBS dictionary. Integrated project schedules for the overall LSS are included as a function of this element. The control function integrates cost, schedule, and performance and relates progress and variance from the initial planning.

The configuration management category provides for the definition and implementation of configuration management activities for both hardware and software required in the performance of the LSS experiment. In addition, it includes as-designed and as-built configuration (for all levels), change control, change tracking, and configuration accounting.

The procurement management element includes responsibility for providing the project performance surveillance, cost control, and status reporting on all elements. It also includes arranging for the acquisition of the test article and various components of the experiment.

The integration of these elements into a smooth operation is the main objective of the project management. Once the proper integration is established in the various MSFC participating elements, constant follow-up with participating elements helps ferret out any particular problem areas. This procedure provides an excellent method for interaction and for problem solving in the project management.

IV. Systems Engineering and Integration

The scenario for the first experiment in the LSS/GTV experiment facility involves the ASTROMAST as the test article atop the AGS and employs the COSMEC I system as the digital controller. From a systems point of view, the entire apparatus; including the base, AGS, ASTROMAST, tripod, and measurement devices; is considered the plant, or process, and the COSMEC I and its associated hardware and software are the controller.

Because the experiment employs a variety of types of measurement devices the COSMEC I system must deal with several different signal types as is expressed by the captions in Figure 1. To enhance the organization and speed of operation of the system, the measurement devices are monitored by hardware cards peripheral to the COSMEC I processor itself. Each device is sampled at a rate of 50 samples/second, thus ensuring adequate bandwidth of the digital controller. The digital controller is discussed in greater detail in the section dedicated to the COSMEC I subsystem.

Command outputs from the control algorithm implemented in the COSMEC I are converted to analog signals which drive the gimbal torquer amps. This conversion is handled by hardware cards analogous to those which monitor the measurement devices.

In addition to the candidate control algorithm, the COSMEC I carries out an inertial strapdown algorithm for the measurement devices which takes into account the effects of the acceleration due to gravity and the angular displacement due to earth rotation. This algorithm conditions the measurements so that they are true with respect to the laboratory reference frame.

A typical experiment would include disturbing the system via one of the actuators at the base and measuring the results with the system operating open loop, i.e., with the digital controller not included, then disturbing the system in a similar manner but with a candidate control algorithm in place. A comparison of the recorded results should give an indication of the success of the control algorithm. More importantly, a series of such tests could be used to determine the relative merit of different control schemes.

V. Design, Development, Fabrication, and Checkout of Subsystems

The subsystems which comprise the LSS/GTV experiment fixture as described are currently in various stages of development at NASA MSFC. Thorough verification of each of the subsystems in controlled test environments comprises a significant part of the preliminary system testing. The subsystems will not only be tested individually, but will be tested in an integrated laboratory environment where each of the subsystems will interact with the others in a manner much as if an actual test article were being used. Such testing is designed to ensure proper operation of the complete test fixture upon assembly.

A. AGS Gimbal Drive

The Advanced Gimbal System (AGS) is a precision, two axis gimbal system designed for high accuracy pointing applications. The AGS gimbals serve the elevation plane and a third gimbal has been added to the system in the azimuth. (See Figure 2.) The AGS essentially rides on the azimuth gimbal so that the AGS and its performance remain unaltered by the presence of the third gimbal. The AGS receives torque commands from the COSMEC I data and control system in the form of analog inputs over the range of -10 to +10 volts. This saturation represents the current limit of 27 amps which is built into the AGS servo amplifier as a protective measure. Because the AGS servo amplifier outputs a current which causes an applied torque proportional to the current, the control algorithms used in the COSMEC I must be designed to produce torque command signals.

The AGS gimbal torquers, with the power supply and servo amplifiers used in the ground test verification experiment, can generate 37.5 ft.-lbs. of torque

over an angular range of approximately ± 30 degrees. The azimuth torquer is capable of generating 13.8 ft.-lbs. over an angular range of about ± 5 degrees. It can, however, be set manually to allow the ± 5 degrees of rotation at any position about the 360 degrees of azimuth freedom. This allows the test article to be rotated to any position desired without remounting.

The power supply for the gimbal system (pitch, yaw, and roll) is a 100 amp d.c. supply with output voltage variable from zero to 35 volts. (The AGS requires 30 volts.) The line to the power supply is 208 volts, three phase, and in the worst case the input power to the supply should not exceed 2550 watts.

B. COSMEC I Data and Control System

1. System Aspects

The COSMEC I is an AIM 65 based micro system which is used to handle data from the control system sensors, output commands to the control system actuators, transmit data for storage to the HP 9845C desktop computer, and implement the control and inertial strapdown algorithms. The COSMEC I is a powerful eight bit micro system which uses special hardware and software to allow the handling of a variety of devices (sensors, actuators, etc.) in real time. This, along with the use of high speed hardware arithmetic processors to reduce computation time, makes the COSMEC I an excellent machine for use as a digital controller.

2. Hardware

The AIM 65, which is the heart of the COSMEC I, employs the Motorola MC6502 microprocessor operated at a two megahertz clock rate. (See Figure 3.) The

system includes 32 kbytes of random access memory (RAM), an alphanumeric keyboard, a single line display, a cassette tape machine for mass storage, and a small printer. The entire system is housed in a very portable package much resembling a suitcase.

The COSMEC I "reads" a variety of types of sensor output signals via interface cards which are an integral part of the COSMEC I system. (See Figure 4.) These cards allow the COSMEC I processor to interface in a similar manner (with regard to computation) with the ATM (Apollo Telescope Mount) rate gyros, the KARS (Kearfott Attitude Reference System), the accelerometer packages, and the AGS (Advanced Gimbal System), each of which has a different type output or input signal. The COSMEC I also features a real time clock which will prove useful in the recording of experimental data.

In order to carry out the large number of calculations required for implementation of the inertial strapdown algorithm and the control algorithm, the COSMEC I employs four hardware arithmetic processors connected on the system bus. Each of these processors can execute a 32 bit floating point multiply in 42 microseconds and they are operated so that they process in parallel, thus minimizing computation time. The dynamic range of the processors is $\pm 9.2 \times 10^{18}$ so there is little possibility of exceeding the computational range of the machine. Also, this eliminates the need for scaling of measurements in order to avoid machine overflow. Using the arithmetic processor units and assembly language programming, the inertial strapdown algorithm can be executed in approximately ten milliseconds and the first proposed control algorithm in about six milliseconds. This puts the total computation time at well under the allowed 20 milliseconds required to meet the 50 hertz sample rate.

3. Software

The software used in the COSMEC I system may be separated into four basic groups: 1) utility software for handling the various hardware cards which interface to instruments, 2) software to implement the control algorithm, 3) software to implement the inertial strapdown algorithm, and 4) initialization and startup software to ready the instruments and equipment for a test.

The hardware cards which interface the COSMEC I's processor to the measurement instruments and actuators are individual by their very nature, and some special software is required to handle each card. However, each card makes information available to the processor as digital words, which is the unifying feature of the system.

The digital controller software for the first ground test experiment will implement a linear discrete multivariable controller having multiple inputs and outputs. The controller will be in state variable form and will be programmed so that the system matrices are initial input data to the program and can be stored on tape and easily changed. The first controller software will be designed to implement a controller of up to ninth order having nine inputs and three outputs.

Because the inertial measurement instruments measure with respect to inertial reference space, there is a natural bias in the measurements due to the acceleration of gravity and earth's rotation. That is, in the earth based experiment the accelerometers measure about one g acceleration downward and the rate gyros measure about 15 deg/hr rotation while at rest with respect to the laboratory reference frame. The inertial strapdown algorithm provides a means of removing this bias from the measurement instruments.

In order to give the measurement instruments initial conditions and begin measurement for a test, initialization software is provided for the instrument strapdown algorithm. To begin a test, the structure will be stabilized with respect to the laboratory reference frame and the initialization routine will be executed. The strapdown algorithm will then be started and the apparatus will be ready to carry out a test.

C. Inertial Measurement Assemblies

Three different types of inertial measurement assemblies are planned for use on the Ground Test Verification structure in the first experiment. The Kearfott Attitude Reference System (KARS), the Apollo Telescope Mount (ATM) rate gyros, and two acccelerometer packages developed by NASA. Each of the instrument packages generates signals in a particular form different from the other instruments as was mentioned in the section dealing with the COSMEC I interface cards. These different signal types are pursued as each instrument package is discussed in detail in the following paragraphs.

1. Kearfott Attitude Reference System

The Kearfott Attitude Reference System (KARS) is an attitude measurement system designed for use in the U.S. Army remotely piloted vehicle. (See Figures 5 and 6.) It provides measurement resolution of 13.9×10^{-3} deg/sec in the pitch and yaw axes (axes transverse to the ASTROMAST) and 25.0×10^{-3} deg/sec in the roll axis (axis along the length of the ASTROMAST). The dynamic range of the rate gyro outputs of the KARS is 40 deg/sec in pitch and yaw and 70 deg/sec in roll. Because of its light weight (8.9 pounds), the KARS will be used as the mast tip rotation sensor in the first ground test experiment. Although the KARS

includes accelerometers and outputs measurements of linear acceleration, the measurements are not used in the ground test experiment because of inappropriate scaling of the instruments.

The output signals of the KARS are in the form of asynchronous digital pulses. One signal, the change in angular position in yaw for instance, requires two channels; one for pulses representing positive rotation and the other for pulses representing negative rotation. The COSMEC I system accumulates the pulses over a 20 millisecond period to produce measurements of the angular rate and position of the ASTROMAST tip.

The KARS outputs three digital health check signals. One signal represents a check of the motor voltage and the pickoff excitation voltage and the other two are over and under temperature signals. In the ground test experiment, these signals will be monitored at the system console.

2. ATM Rate Gyros

The Apollo Telescope Mount (ATM) rate gyro packages are designed to measure small angular rates very precisely. Each package measures angular rate in one axis (See Figure 7.) with resolution finer than 0.5×10^{-3} deg/sec and offers a dynamic range of ± 1.0 deg/sec. The ATM rate gyro packages will be mounted on the faceplate of the engineering AGS so that they will measure the rotation of the base of the test article. Because they will be rigidly mounted to the gimbal system, these sensor packages will most nearly measure the actuator inputs to the system.

The output signals of the ATM rate gyro packages are ± 45 volt analogs and are handled by the analog to digital converter card of the COSMEC I system where they are converted to 12 bit binary words.

The ATM rate gyro packages require a warmup period of about 20 minutes and then stabilize about 20 minutes after the warmup period ends, thus requiring on the order of 40 minutes to become ready for a test. Each package requires 1.5 amps during warmup and then 1.25 amps after stabilization; both at 28 Vdc.

3. Accelerometers

Two identical accelerometer packages (See Figure 8.) will be used on the ground test experiment fixture in the first test. One package will be placed on the mast tip along with the KARS and the other on the test fixture base as shown in Figure 1. The necessary electronics for each accelerometer package is included on board the instrument package itself as shown in Figure 9.

The accelerometers provide resolution finer than 0.0001 g and a dynamic range of ± 3 g with a bandwidth of 25 to 30 Hz. They require about 20 minutes for warmup, during which time each package requires 1.2 amps at 28Vdc. After warmup the power requirement reduces to about .9 amp per package.

The signals from the accelerometers are different from either those of the KARS or the ATM rate gyros. As in the case of the KARS, two channels are required for each of the degrees of freedom of the accelerometer package, i.e., six channels per accelerometer package. One channel of each pair carries a 2.4 kHz square wave synchronization signal and the other channel carries the acceleration information. Zero accleration is represented by a signal identical to

that of the synchronization channel, positive acceleration by an increase in frequency, and negative acceleration by a decrease in frequency as compared to the synchronization channel. As in the cases of the other instruments, these signals are monitored by a hardware card in the COSMEC I system.

D. Beam Containment Structure

The beam containment structure includes the tip support mechanism, the base, the disturbance actuators and signal sources, and power supply for the entire test fixture. This is essentially that equipment required of a laboratory to carry out dynamic testing of structures such as the ground test experiment. As depicted in Figure 1 the beam containment area can accommodate structures approaching 120 feet in height. Access is provided at various levels along the structure via catwalks. Also the control room for experimental operations is at a position about 50 feet above the base of the structure, thus making the experiment quite accessible with regard to viewing the experimental operations and so forth.

1. Tip Support Mechanism

The tip support mechanism is a tripod mounted on air bearings as shown in Figure 1 with a constant tension cable extending downward to connect to the tip instrument package. The cable connection point is incorporated into the tip instrument package mount assembly. The tip support mechanism is designed to support the weight of the tip instrument package and possibly some of the weight of the ASTROMAST beam without affecting the structural properties of the system by adding stiffness to the beam tip motion. The tripod is allowed about 18 inches of total translational freedom in each of its two translational axes.

This will prove to be quite adequate for the GTV experiment because the tip deflections are expected to be less then six inches and the distance between the mast tip and the tripod support floor is about 60 feet as compared to the relatively short tripod of three feet.

2. Base

The base for the GTV experiment will be supported by air bearings in a similar manner to the tip support tripod. It is designed to be restrained as little as possible in the two translational degrees of freedom but not allow any rotational freedom. Translation of the base provides the means of applying disturbances to the system. The disturbance actuators will be hydraulic and/or electromechanical in nature depending upon the frequency band of the applied disturbance signal. The disturbance system is designed to allow independent input signals to the two translational axes whether they be broadband random, sinusoidal, or a combination of both.

E. Facility Computer Interface and Utility Software

During testing, the COSMEC I data and control system will send data for storage to the HP 9845C desktop computer via a 16 bit parallel interface. Once a test run is completed, the HP 9845C will be available for display of data and possibly some data reduction. Also available is a Hewlett Packard 1000 series minicomputer to which the data stored on the HP 9845C can be transferred. The HP 1000 series mini system includes the necessary software for several sophisticated data reduction techniques. Using the combined power of the two machines, much will be possible in the way of data reduction and display for post analysis efforts.

VI. System Model and Expected Performance

For purposes of system studies and controller design, an analytical model of the Ground Test Experiment is necessary. This section describes the development of such a model and the following section compares it to the results of modal tests of the ASTROMAST beam carried out at NASA MSFC.

A. Introduction

Modeling of the Ground Test Verification (GTV) experiment was carried out in two distinct stages. The first stage involved modeling the ASTROMAST itself as it would be tested in the first open loop modal test, i.e., the beam alone in a cantilevered position. This produced modal frequencies, mode shapes, and mass integrals which were used in the second stage of the modeling process to develop, through modal synthesis, a model of the entire GTV experiment including the AGS and the beam containment structure.

B. ASTROMAST Beam Model

The ASTROMAST is a symmetric beam 512 inches in length and triangular of cross section. Three longerons form the corners of the beam and extend along its full length unbroken. The cross members which give the beam its shape divide the beam into 91 sections having equal length and mass and similar elastic properties. This sectioning was used advantageously in the modeling process.

As a first step, a single section of the beam (See Figure 10.) was modeled from its geometry and the elastic properties of S-GLASS. This provided the necessary information for a 91 element lumped mass model which was used to

determine the modal frequencies, mode shapes, and mass integrals of the beam in a cantilevered position. Because of the symmetry of the beam, bending in the two transverse planes must be uncoupled and identical, i.e., bending modes in one transverse plane must be exactly repeated in the orthogonal transverse plane, and torsion must also be uncoupled from these bending modes. This allowed a simplified analysis of the ASTROMAST beam via a model comprised of 91 infinitesimally thin discs of mass connected by massless beam segments. A two dimensional model was used to find the modal frequencies, mode shapes, and mass integrals of the ASTROMAST beam in bending. In this model each of the 91 lumps was allowed to translate in a direction transverse to the beam and to rotate about its own center of mass. (See Figure 11.) Also, shear and bending deformation were taken into account. Because the beam is very stiff longitudinally, deformation in this direction was considered negligible and, therefore, not modeled. The modal data resulting from the analysis of this model are shown in Table 1 along with the results of the torsional analysis.

Again, because of the symmetry of the beam, the torsional analysis could be carried out separately from the bending analysis. The beam in torsion is a one dimensional problem because the lumped masses are allowed only to rotate about the longitudinal axis. If the beam is assumed to be uniform, a closed form solution to the torsional bending problem can be found. This was done as a check of the numerical method; and indeed, the results of the two techniques compare favorably as shown in Table 2.

C. Complete System Model

Using the model of the ASTROMAST beam alone and a rigid body model of the AGS (Advanced Gimbal System), a complete system model was produced using modal

synthesis. The following are the major assumptions included in this model:

1) the tip support structure has neglible effects upon the structural behavior,
2) the AGS is rigid,
3) there is no stiffness associated with the translational motion of the base.

The first assumption is easily justified by the fact that the tether "string" which supports the tip will be approximately 60 feet long and very light as compared to the tip mass of about 32 pounds. Also, the tip deflections are expected to be at most a few inches in magnitude. The second assumption is justified when the stiffness of the AGS is compared to the relative flexibility of the ASTROMAST beam. As for the third assumption, the base of the experiment would be unrestrained if it were not driven by the disturbance actuators. Of course the actuators will not only provide a disturbance input as desired but may also passively restrain the base in some way. This will be incorporated into the model as more data become available concerning the disturbance actuators. The mathematical model of the GTV experiment structure incorporates five rigid body degrees of freedom. Two of these result from the translations of the base; the other three from the rotations of the gimbal system. In addition, the ASTROMAST is represented by its first seven flexible body modes to produce the system model summarized in Tables 3 and 4.

VII. Modal Test of ASTROMAST Beam

Modal tests have been conducted on the ASTROMAST beam at Marshall Space Flight Center. So that gravity would have as little effect as possible on the test results, the ASTROMAST was cantilevered in a hanging position for the modal test. In order to do this, a mounting bracket was fashioned as shown in Figure 12 so that the ASTROMAST could be mounted and then deployed downward under the influence of gravity. (See Figures 13 through 16.)

When fully deployed, the ASTROMAST exhibits a longitudinal twist of about 280 degrees as shown in the photograph of Figure 17. This twist contributes to coupling between the torsional and bending modes; and, although it was not included in the model described in Section VI, the model seems to describe the beam quite well as is discussed later in this section.

Testing using three different levels of input was found to produce the same experimental results with regard to the modal model. This shows that the ASTROMAST behaves in a linear manner over a typical range of input excitations, thus making it an excellent choice of test articles for the LSS/GTV experiment.

Typical modal damping for the ASTROMAST beam was found to be about 0.2 to 0.3 percent. This is in the range perdicted for the ACOSS model #2 typical LSS which was constructed (on paper) of graphite epoxy. The ASTROMAST is similar in that the S-GLASS members from which it is constructed are also a composite of fiber and resin and would be expected to have similar damping characteristics.

The lower modal frequencies of the cantilevered ASTROMAST beam as measured in the laboratory and as computed from the model described in Section VI are summarized in Table 5. The preliminary nature of the test data accounts for the

modes pedicted by the model which have not yet been identified and measured in the lab. However, it is clear that the model is in reasonable compliance with the actual structure. The modes determined experimentally thus far agree very well with the model as is revealed by the average percent error of about ten percent. Error in the model may be due to the unknown characteristics of the S-GLASS as a composite. Since the actual percentage of S-GLASS present in the beam members was unknown, they were assumed to be made entirely of S-GLASS. This error in the modulus of elasticity could account for some of the modeling error present.

VIII. System Assembly, Verification, and Use

The LSS/GTV experiment fixture will be assembled in the high bay area of building number 4419 at Marshall Space Flight Center. As mentioned earlier, each of the subsystems is being thoroughly tested independently in order to minimize the difficulties to be encountered upon assembly of the complete system.

After assembly of the entire test apparatus, proper communication between the subsystems will be verified and proper operation of the subsystems in the test scenario will be established. The health status of each of the instrument packages will be of major concern at this time. Once each of the subsystems has proven to be operating properly in the test environment, the system will be ready to be tested in the operational configuration, i.e., to carry out a test of the first candidate control algorithm.

Once the experiment fixture is shown to operate properly and consistently, it will be available for testing on a regular basis and will be operated by Test Lab personnel.

IX. Summary and Future LSS/GTV Development

MSFC is developing a LSS ground test facility to help verify LSS passive and active control theories. The facility is not parochial to the control area alone but has a wide purview of activities in which experimentation can be accomplished. These areas include but should not be limited to the following:

1. Subsystem and component testing,
2. Remote sensing and control,
3. Parameter estimation and model verification and,
4. Evolutionary modeling and control.

All of these areas are currently in the planning stages of the facility development and should be an integral part of the facility within the immediate future.

MODE	FREQUENCY (HZ)
FIRST BENDING MODE	0.618
SECOND BENDING MODE	3.917
THIRD BENDING MODE	11.179
FIRST TORSIONAL MODE	6.877
SECOND TORSIONAL MODE	20.628
THIRD TORSIONAL MODE	34.373

Table 1. Modal Frequencies of Cantilevered ASTROMAST Beam Model in Bending and Torsion.

MODE	CLOSED FORM FREQUENCY (HZ)	TORSIONAL BEAM FREQUENCY (HZ)
FIRST TORSIONAL MODE	6.92	6.88
SECOND TORSIONAL MODE	20.74	20.63
THIRD TORSIONAL MODE	34.58	34.37

Table 2. Torsional Mode Frequencies Resulting from Analytical Uniform Beam Closed Form Solution and 91 Element Lumped Mass Numerical Solution.

	MODE NUMBER 1			MODE NUMBER 2			MODE NUMBER 3		
	X	Y	Z	X	Y	Z	X	Y	Z
BASE TRANSLATION	0.7208357	0.0000000	0.0000000	0.0000000	0.7208357	0.0000000	0.0101980	-0.0012932	0.0000000
ROLL GIMBAL ROTATION	0.0000000			0.0000000			0.1187835		
AZIMUTH GIMBAL ROTATION	0.0000000			0.0000000			0.0000000		
ELEVATION GIMBAL ROTATION	0.0000000			0.0000000			0.0000000		
BEAM BASE TRANSLATION	0.7208357	0.0000000	0.0000000	0.0000000	0.7208357	0.0000000	0.0101980	-0.0012932	0.0000000
BEAM BASE ROTATION	0.0000000	0.0000000	0.0000000	0.0000000	0.0000000	0.0000000	0.0000000	0.0000000	0.1187835
TIP INSTRUMENT PACKAGE TRANSLATION	0.7208357	0.0000000	0.0000000	0.0000000	0.7208357	0.0000000	-0.2215391	0.0280927	0.0000000
TIP INSTRUMENT PACKAGE ROTATION	0.0000000	0.0000000	0.0000000	0.0000000	0.0000000	0.0000000	0.0000000	0.0000000	0.1187835

	MODE NUMBER 4			MODE NUMBER 5		
	X	Y	Z	X	Y	Z
BASE TRANSLATION	-0.2426753	-0.0000825	0.0000000	-0.0000439	0.2133059	0.0000000
ROLL GIMBAL ROTATION	0.0075818			0.0009661		
AZIMUTH GIMBAL ROTATION	0.0063638			0.0000033		
ELEVATION GIMBAL ROTATION	0.0000000			0.0064128		
BEAM BASE TRANSLATION	-0.0791644	-0.0000825	0.0000000	0.0000413	0.1025569	0.0000000
BEAM BASE ROTATION	0.0000000	0.0063638	0.0075818	0.0064128	0.0000033	0.0009661
TIP INSTRUMENT PACKAGE TRANSLATION	3.2468774	0.0017931	-0.0015743	-0.0001019	-3.2637730	0.0125100
TIP INSTRUMENT PACKAGE ROTATION	0.0000000	0.0063638	0.0075818	0.0064128	0.0000033	0.0009661

Table 3. LSS/GTV Experiment Structure Mathematical Model Rigid Body Modes.

FREQUENCY (HZ)	0.44			1.16			1.80			
	X	Y	Z	X	Y	Z	X	Y	Z	
BASE TRANSLATION	0.4340323	0.0000461	0.0000000	-0.0003125	0.4891170	0.0000000	-0.0302741	-0.0009661	0.0000000	
ROLL GIMBAL ROTATION	0.0017399			-0.0001548			0.0184101			
AZIMUTH GIMBAL ROTATION	-0.0497098			0.0000250			0.0024533			
ELEVATION GIMBAL ROTATION	0.0000120			0.0602246			-0.0000414			
BEAM BASE TRANSLATION	-0.4432107	-0.0001104	0.0000000	0.0003297	-0.5509624	0.0000000	0.0327604	0.0004400	0.0000000	
BEAM BASE ROTATION	0.0000120	-0.0497098	0.0017399	0.0602246	0.0000250	-0.0001548	-0.0000814	0.0024533	0.0184101	
TIP INSTRUMENT PACKAGE TRANSLATION	0.5985857	-0.0000565	-0.0085947	-0.0003538	0.5674684	-0.0884927	0.0370206	-0.0081332	0.0009380	
TIP INSTRUMENT PACKAGE ROTATION	-0.0000224	0.0345617	-0.0163021	-0.0453606	-0.0000090	0.0000523	-0.0000700	-0.0043433	-0.7151111	

FREQUENCY (HZ)	3.25			3.71			4.21			4.23		
	X	Y	Z	X	Y	Z	X	Y	Z	X	Y	Z
BASE TRANSLATION	-0.4059115	-0.0021554	0.0000000	0.0019001	-0.4884157	0.0000000	-0.1169710	-0.0530800	0.0000000	0.0377894	-0.1626017	0.0000000
ROLL GIMBAL ROTATION	-0.0001958			0.0001902			0.0000152			0.0000524		
AZIMUTH GIMBAL ROTATION	0.0339763			-0.0001598			0.0105723			-0.0034170		
ELEVATION GIMBAL ROTATION	-0.0002547			-0.0614555			-0.0074173			0.0377894	-0.1626017	0.0000000
BEAM BASE TRANSLATION	0.4670748	0.0027617	0.0000000	-0.0022049	0.5963746	0.0000000	0.1546736	0.0750166	0.0000000	-0.0500081	0.2299636	0.0000000
BEAM BASE ROTATION	-0.0002847	0.0339763	-0.0001958	-0.0616555	-0.0001598	0.0001902	-0.0074173	0.0105723	0.0000152	-0.0227311	-0.0034170	0.0000524
TIP INSTRUMENT PACKAGE TRANSLATION	0.3724687	0.0012984	-0.0236142	-0.0018192	0.3291788	-0.1791701	-0.1921388	-0.0510709	0.1028474	0.0637058	-0.1613539	0.2150347
TIP INSTRUMENT PACKAGE ROTATION	-0.0003839	0.0924256	0.0305842	-0.0919095	-0.0005578	-0.0098476	0.0371458	-0.1227977	-0.0027129	0.1153053	0.0100553	-0.0013618

Table 4. LSS/GTV Experiment Structure Mathematical Model Flexible Body Modes.

	Experimental (Hz)	Analytical (Hz)	% Difference
Bending*	0.56	0.62	11
	3.4	3.9	16
	----	11	--
Torsion	--	6.9	--
	21	21	0.0
	29	34	19

* Two modes at each frequency

Table 5. Summary of Modal Frequencies from Model and Test Results for the Cantilivered ASTROMAST Beam.

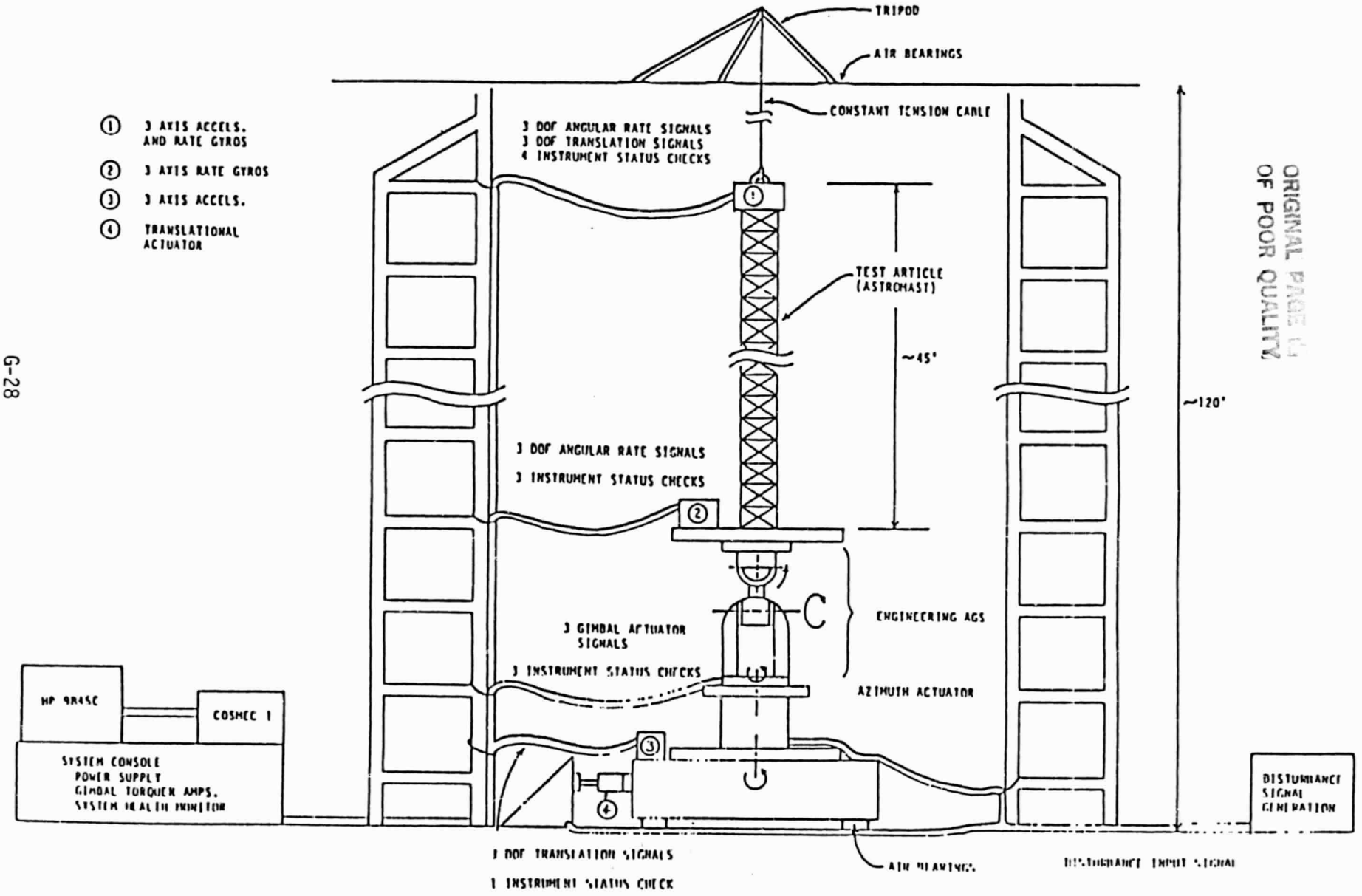

FIGURE 1.

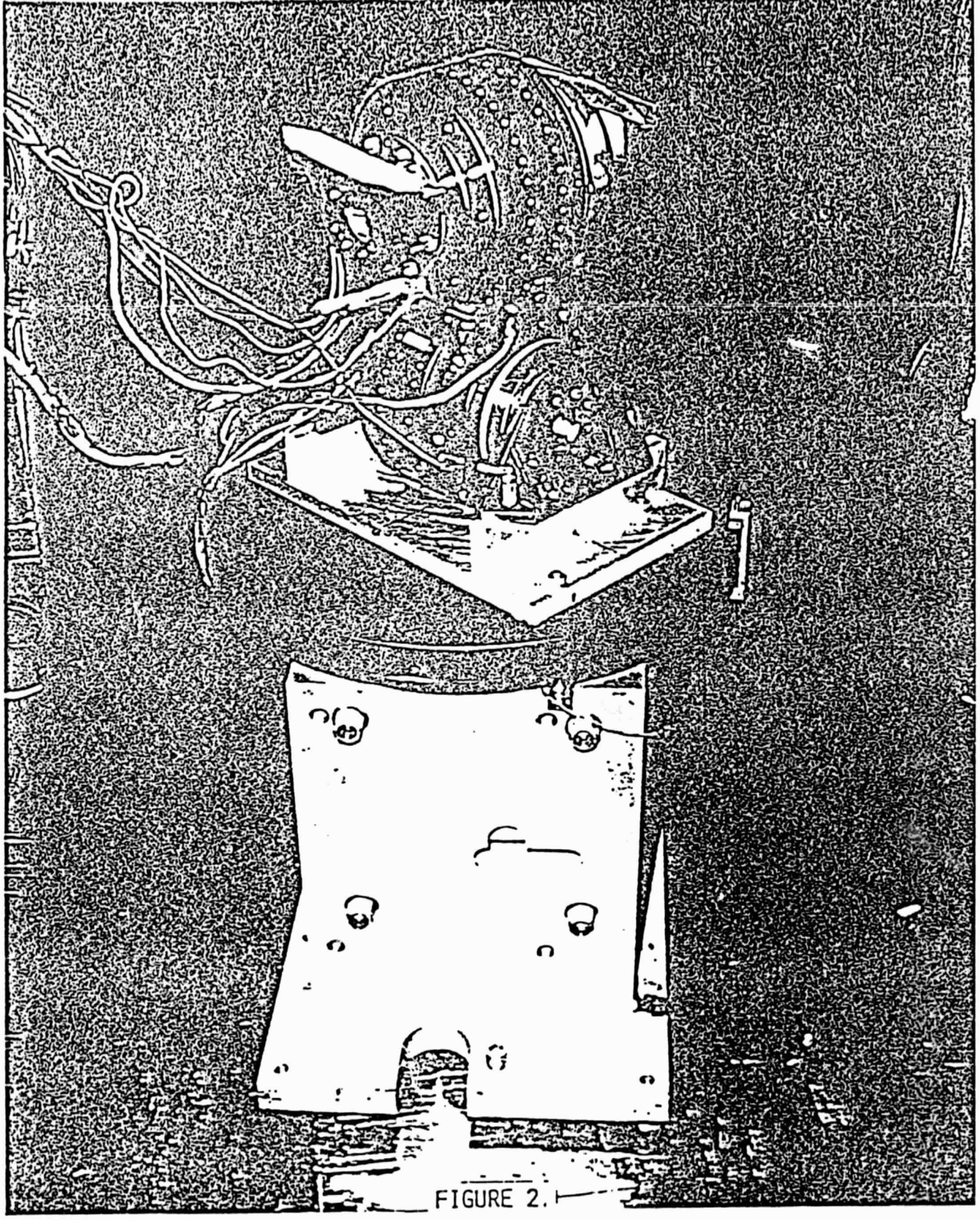

FIGURE 2.

FIGURE 3.

FIGURE 4.

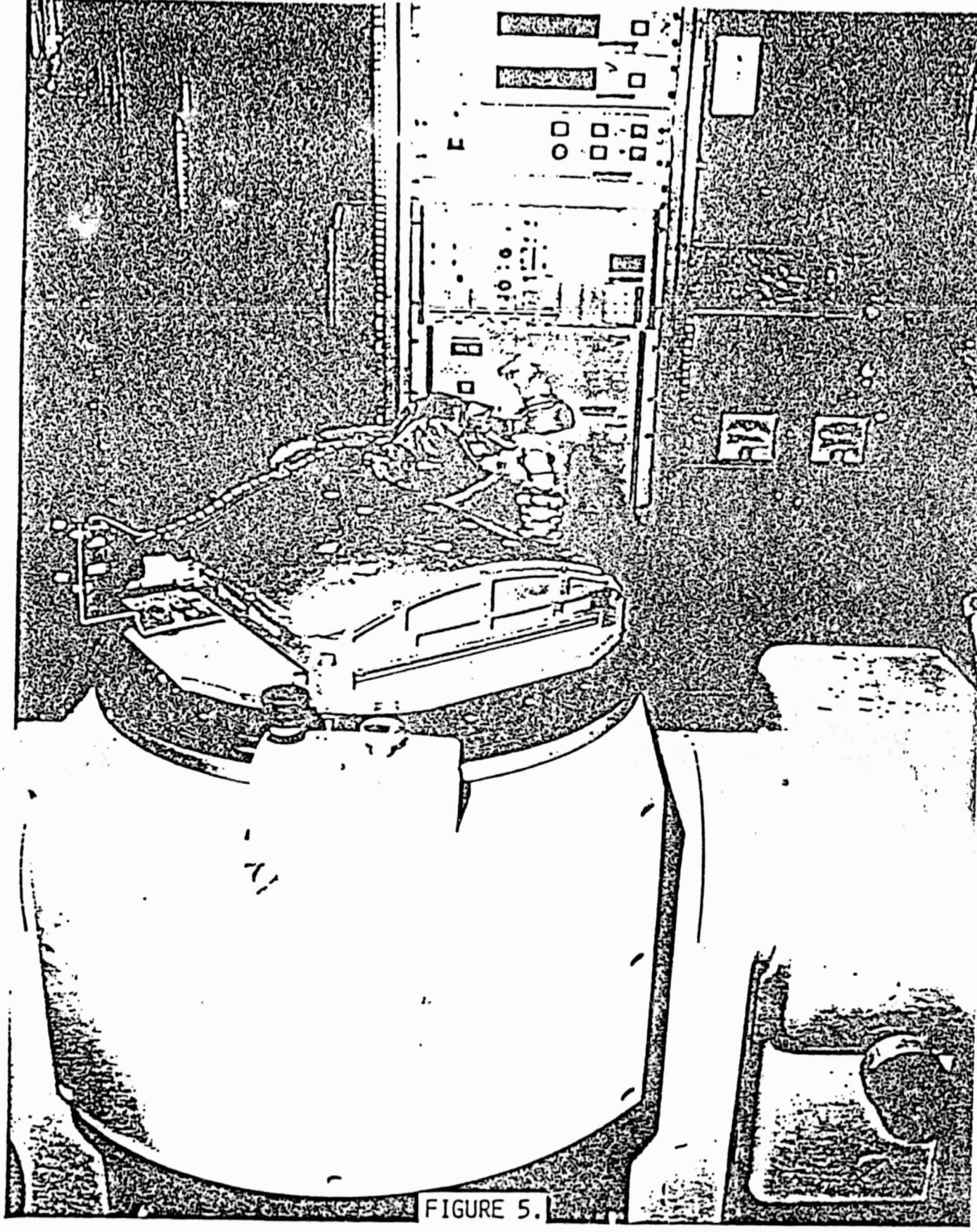

FIGURE 5.

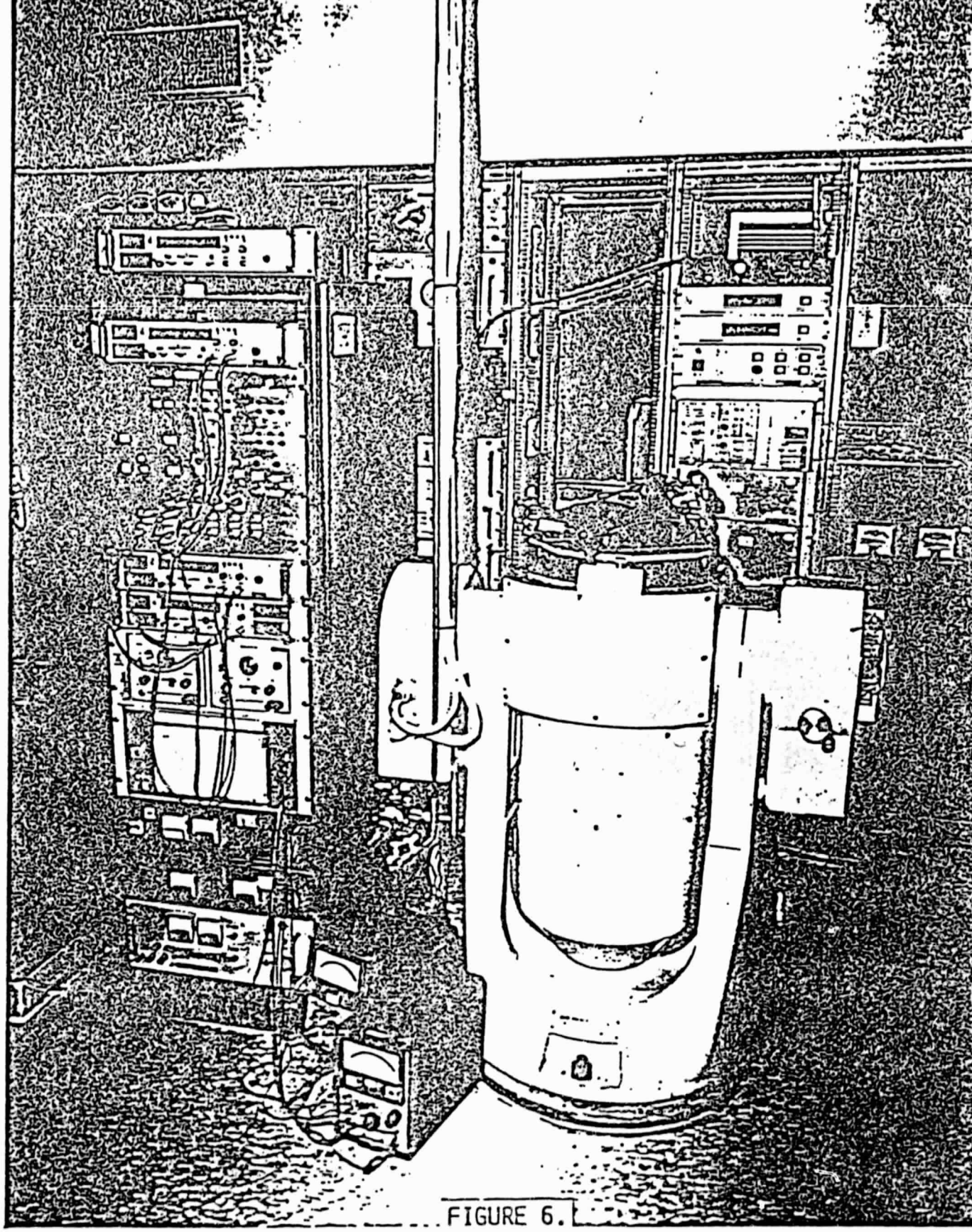

FIGURE 6.

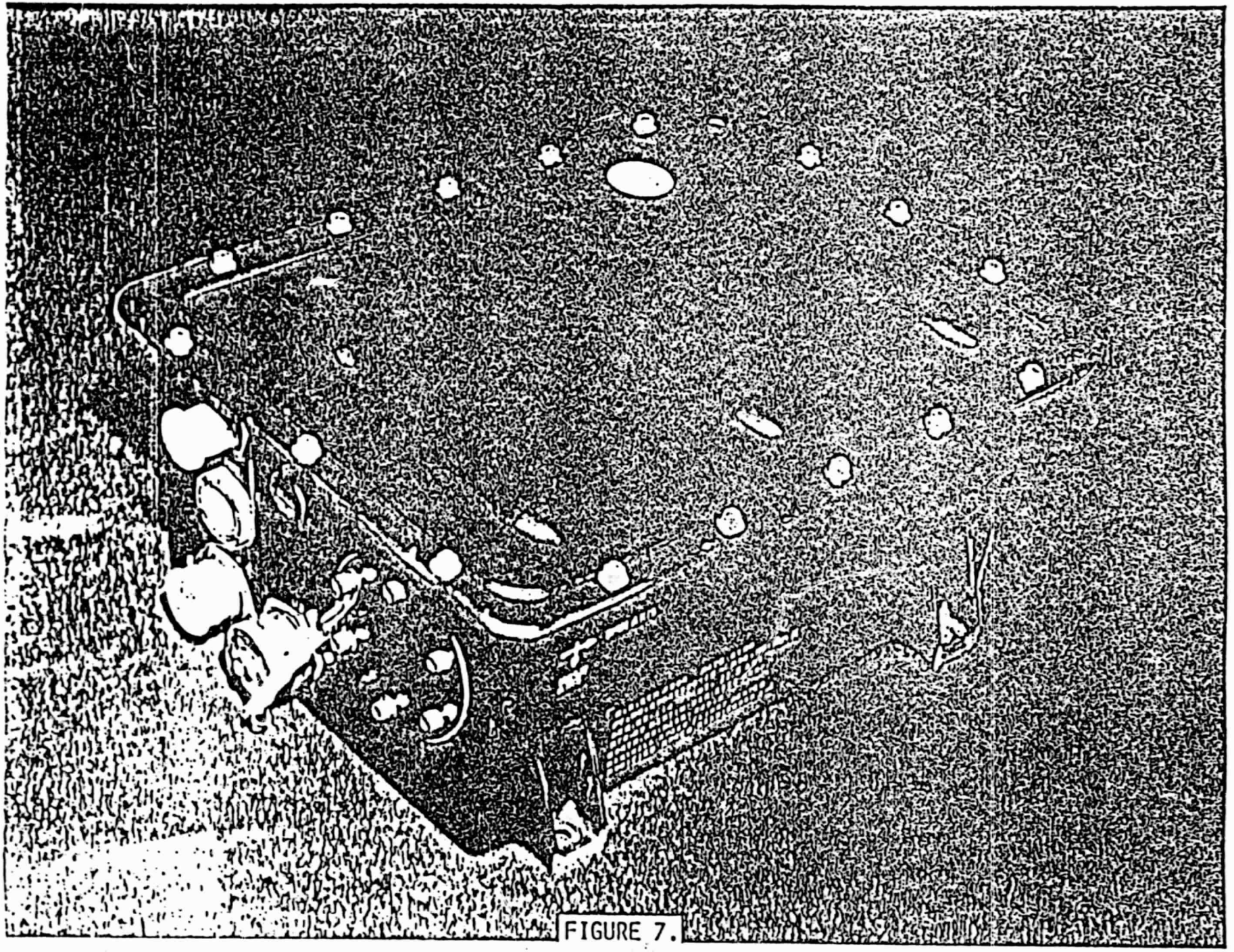

FIGURE 7.

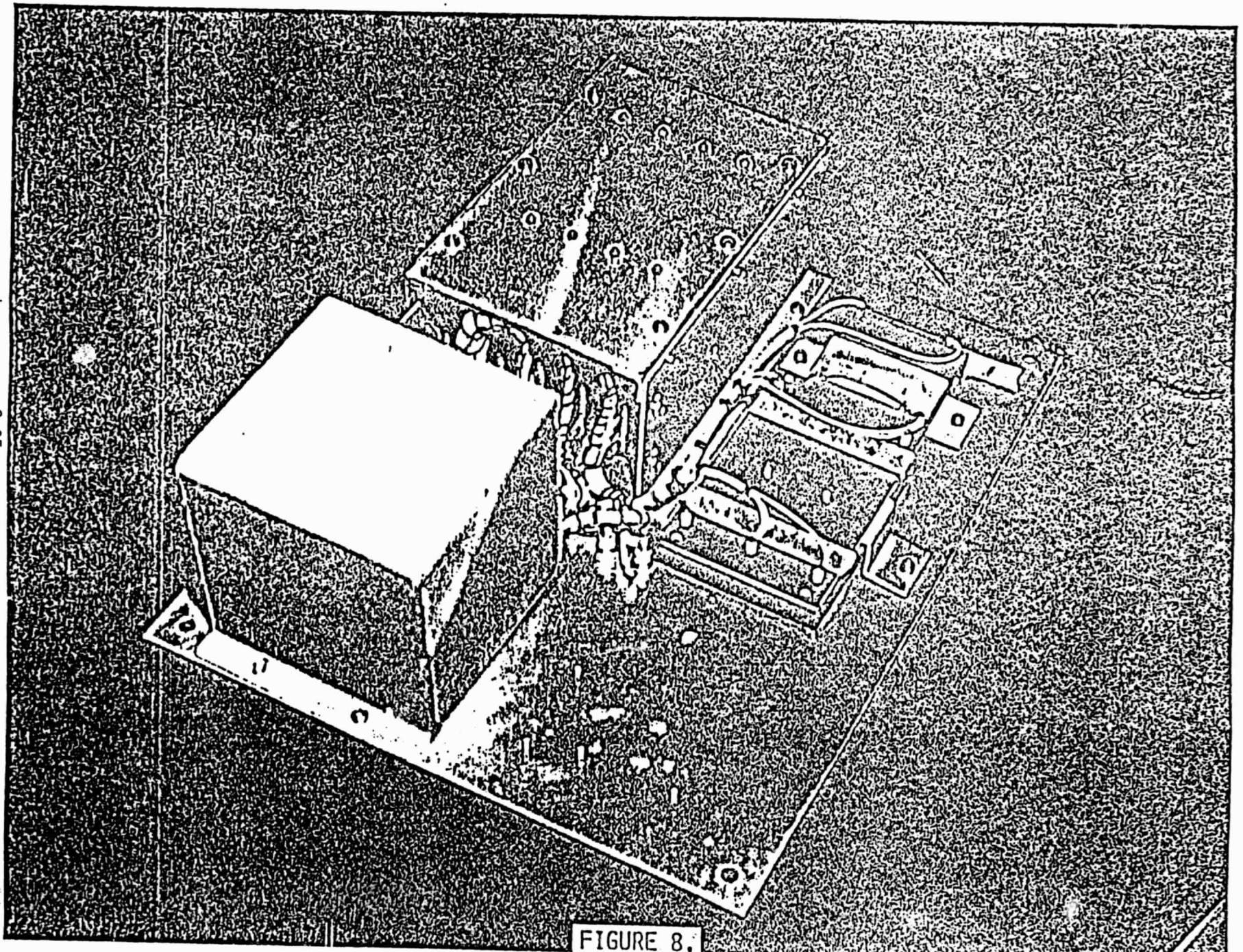

FIGURE 8.

FIGURE 9.

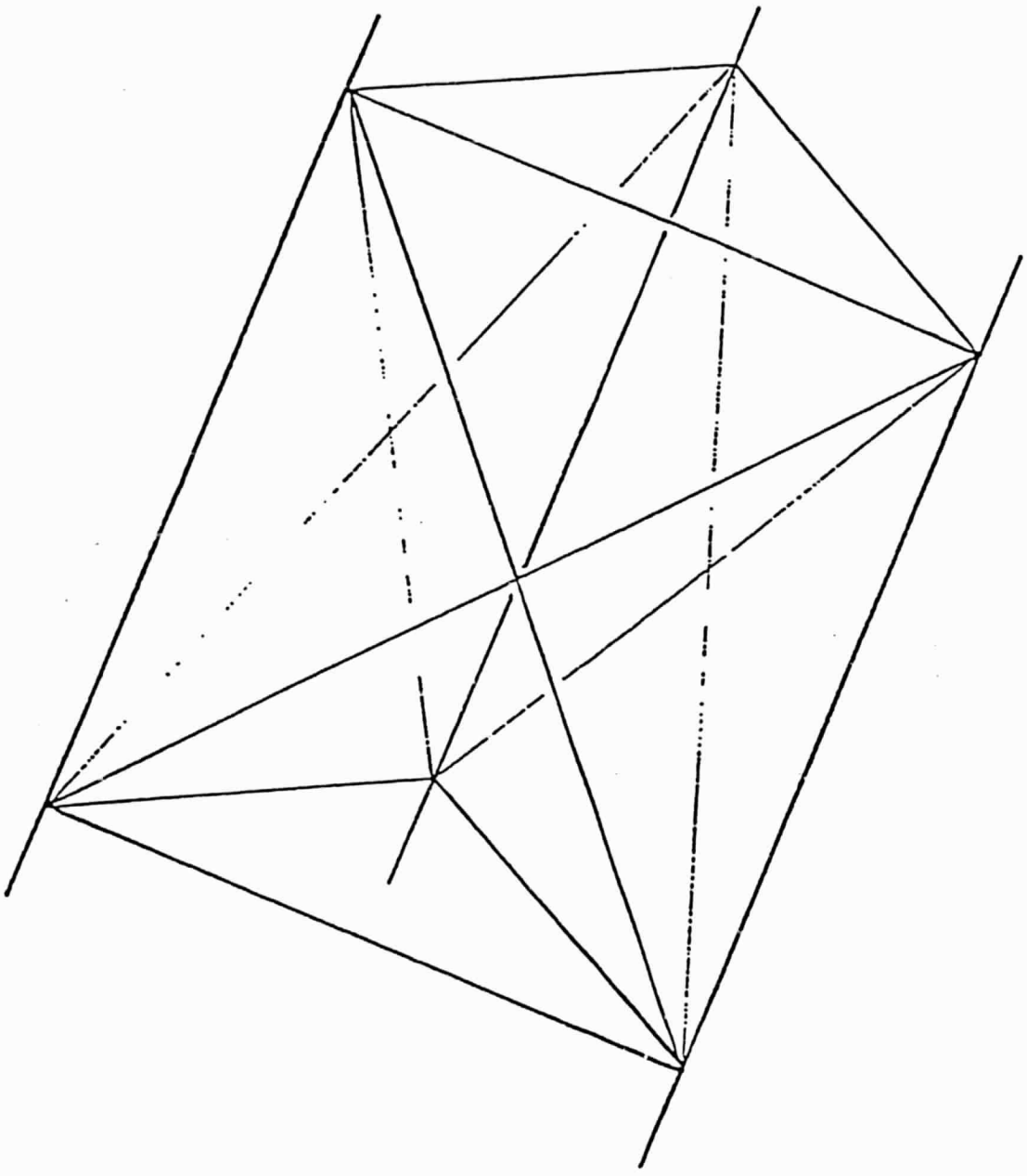

FIGURE 10.

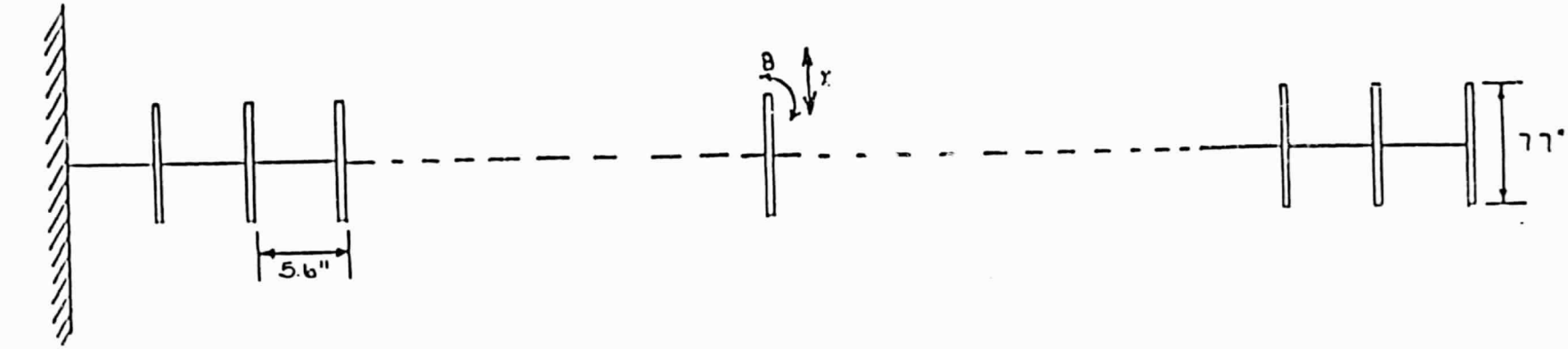

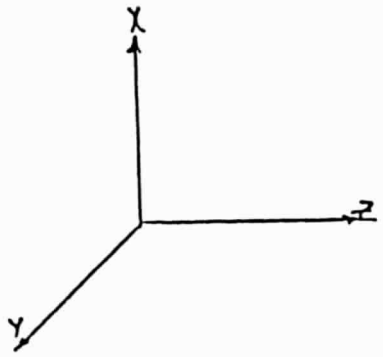

FIGURE 11.

FIGURE 12.

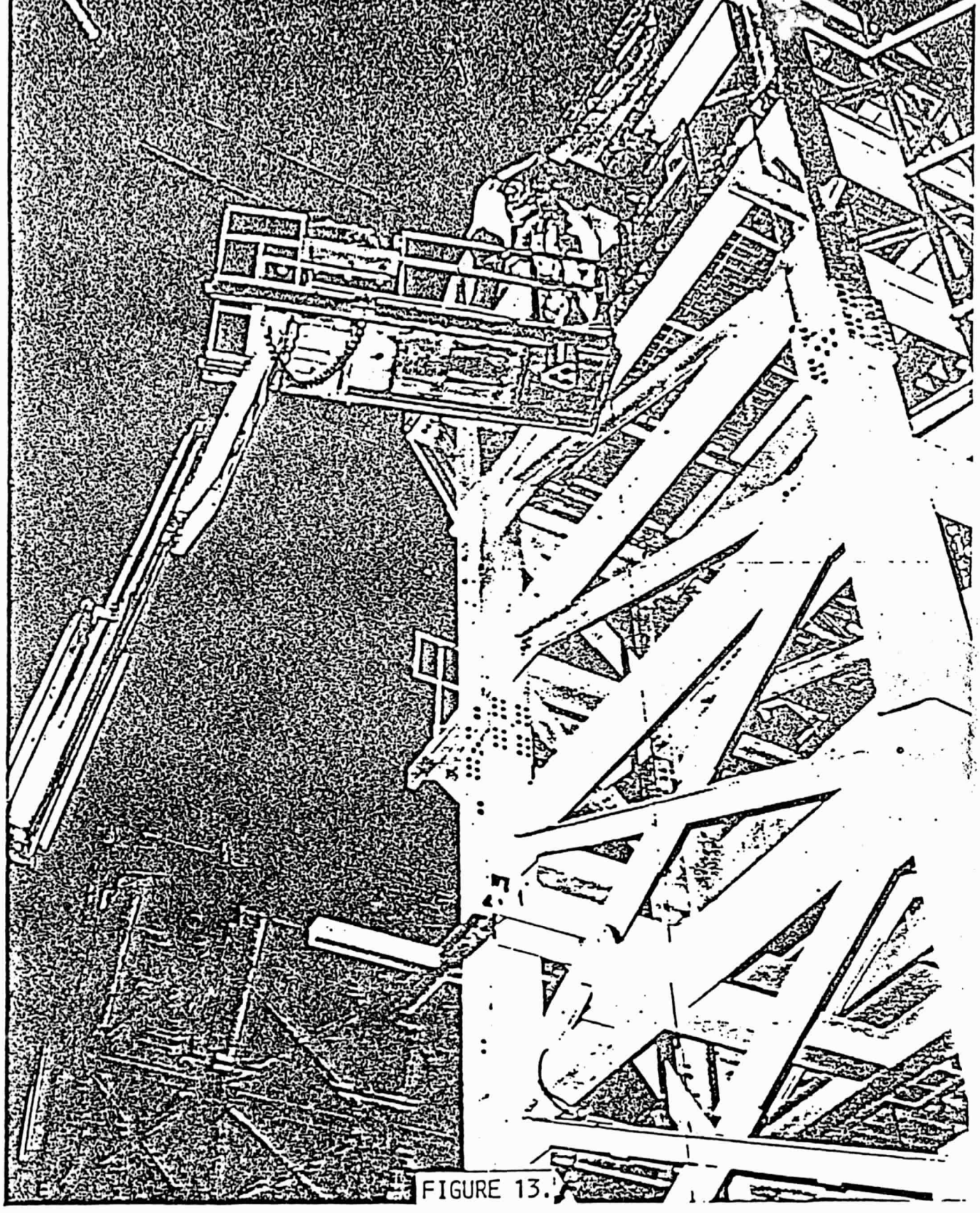

FIGURE 13.

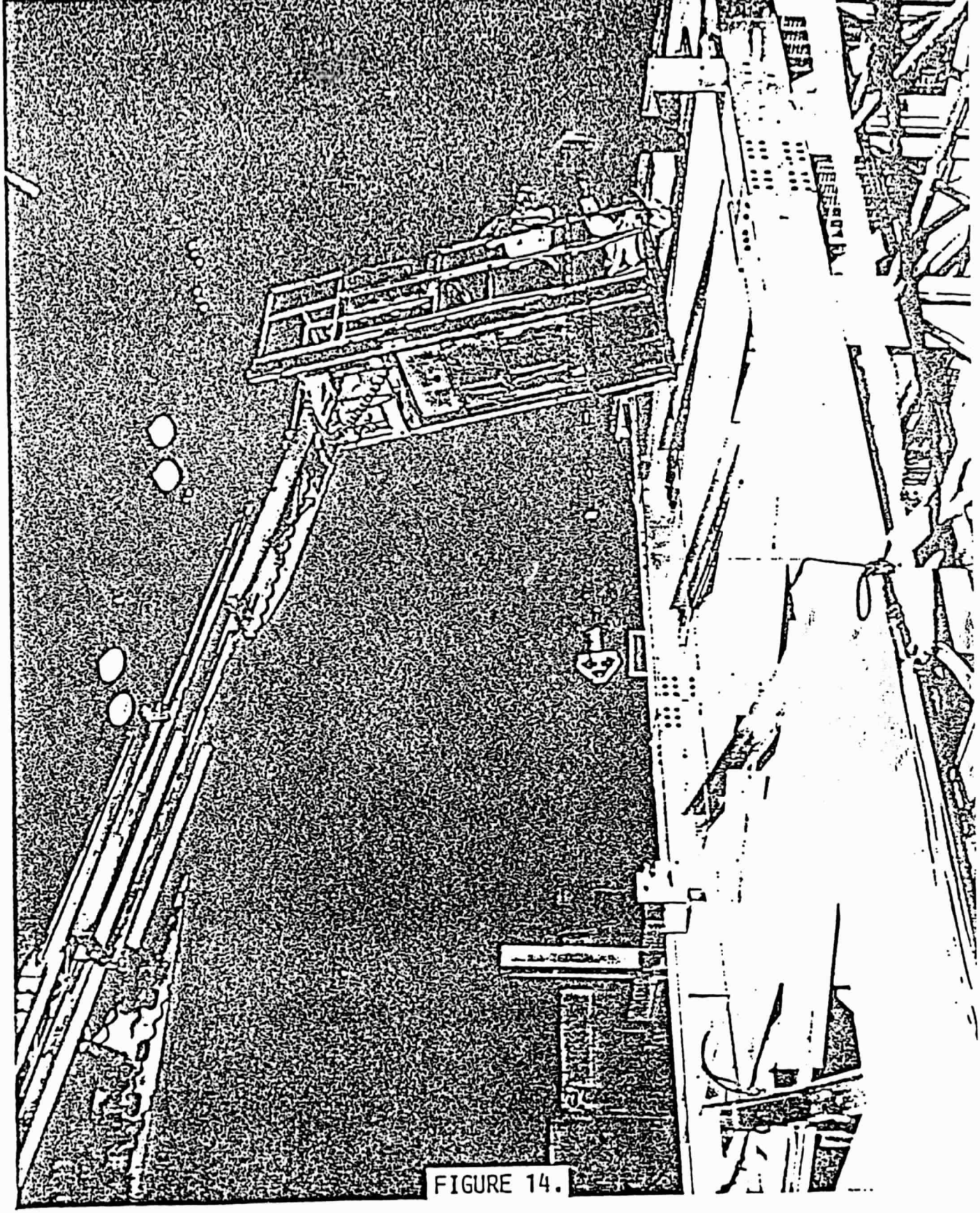

FIGURE 14.

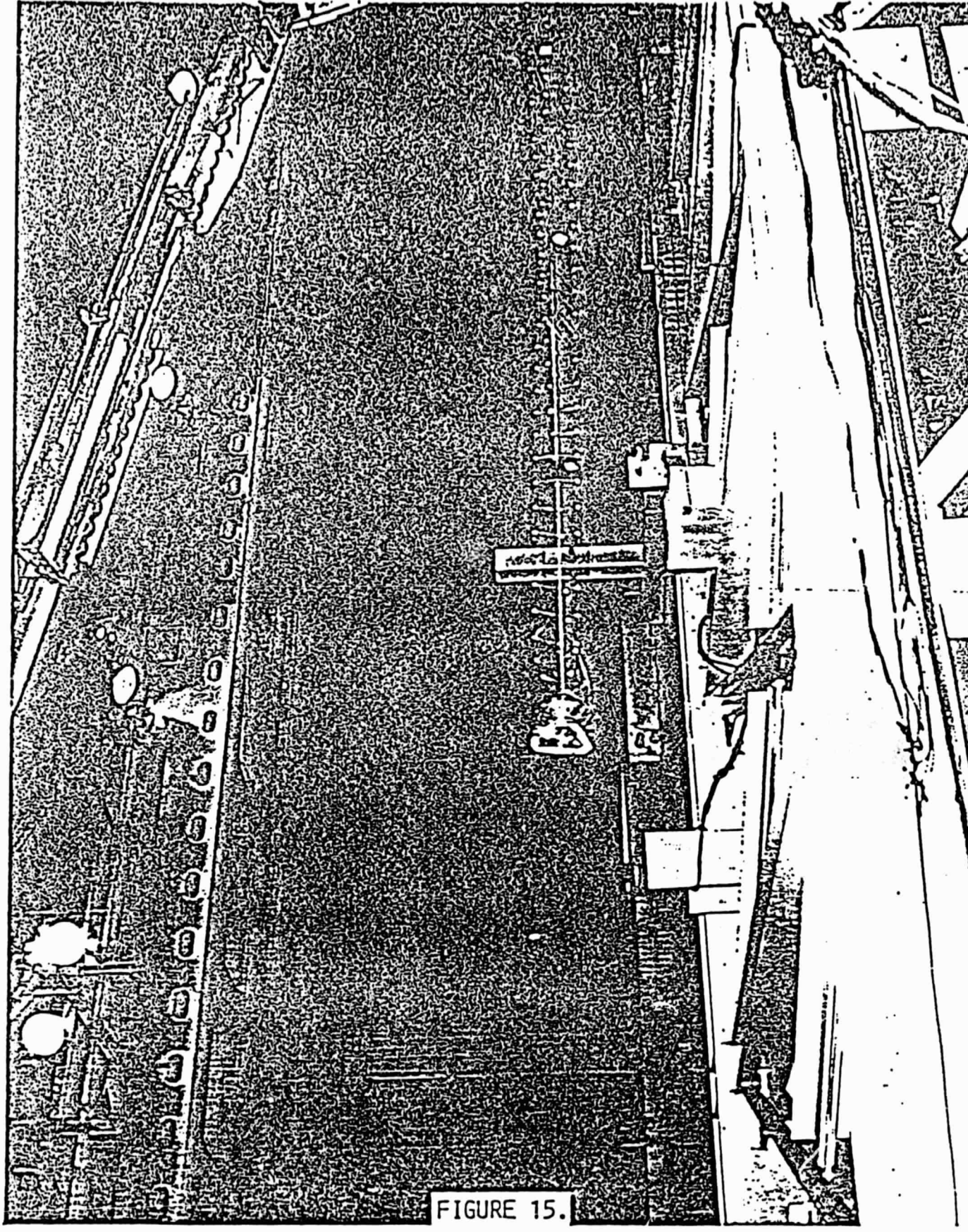

FIGURE 15.

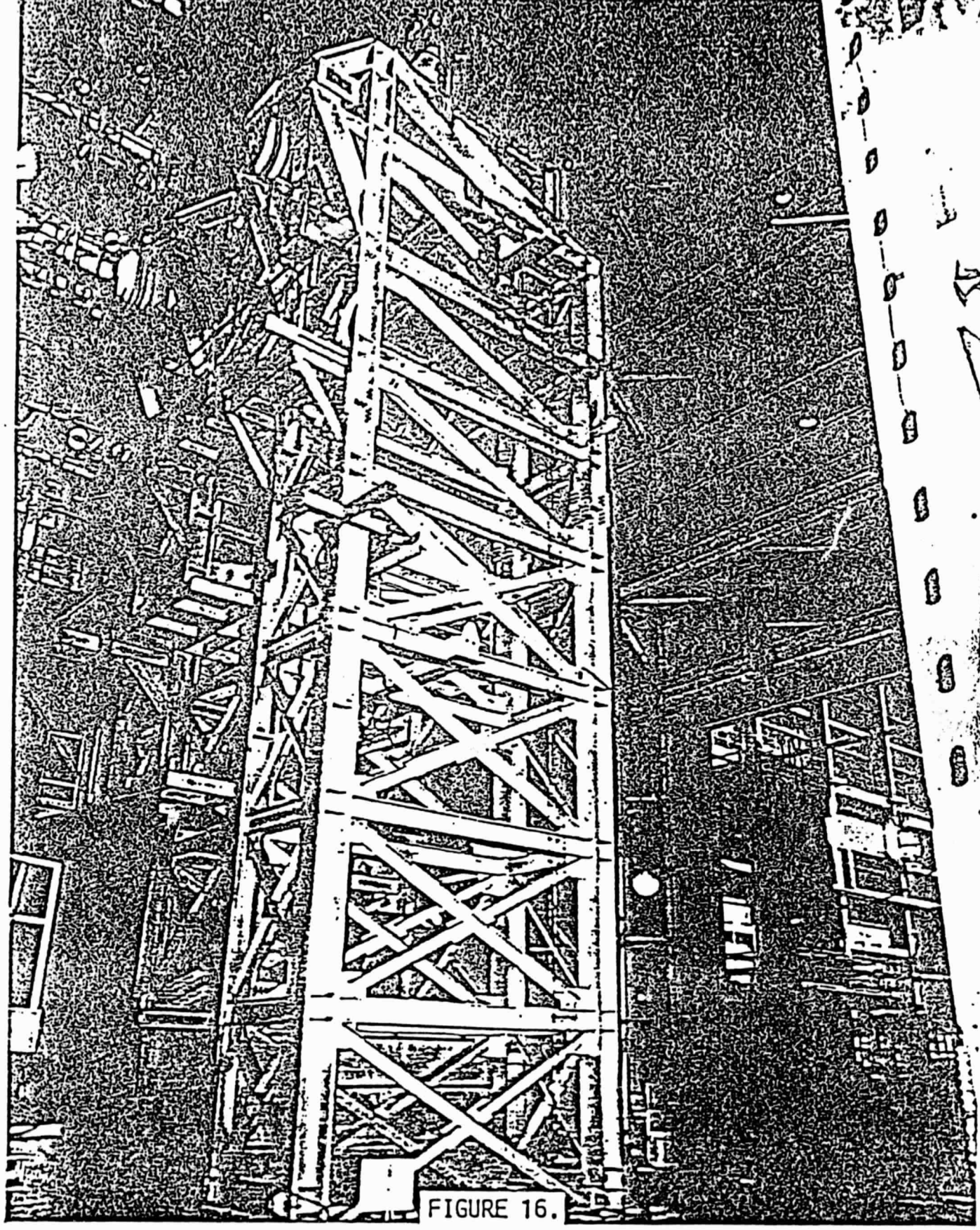

FIGURE 16.

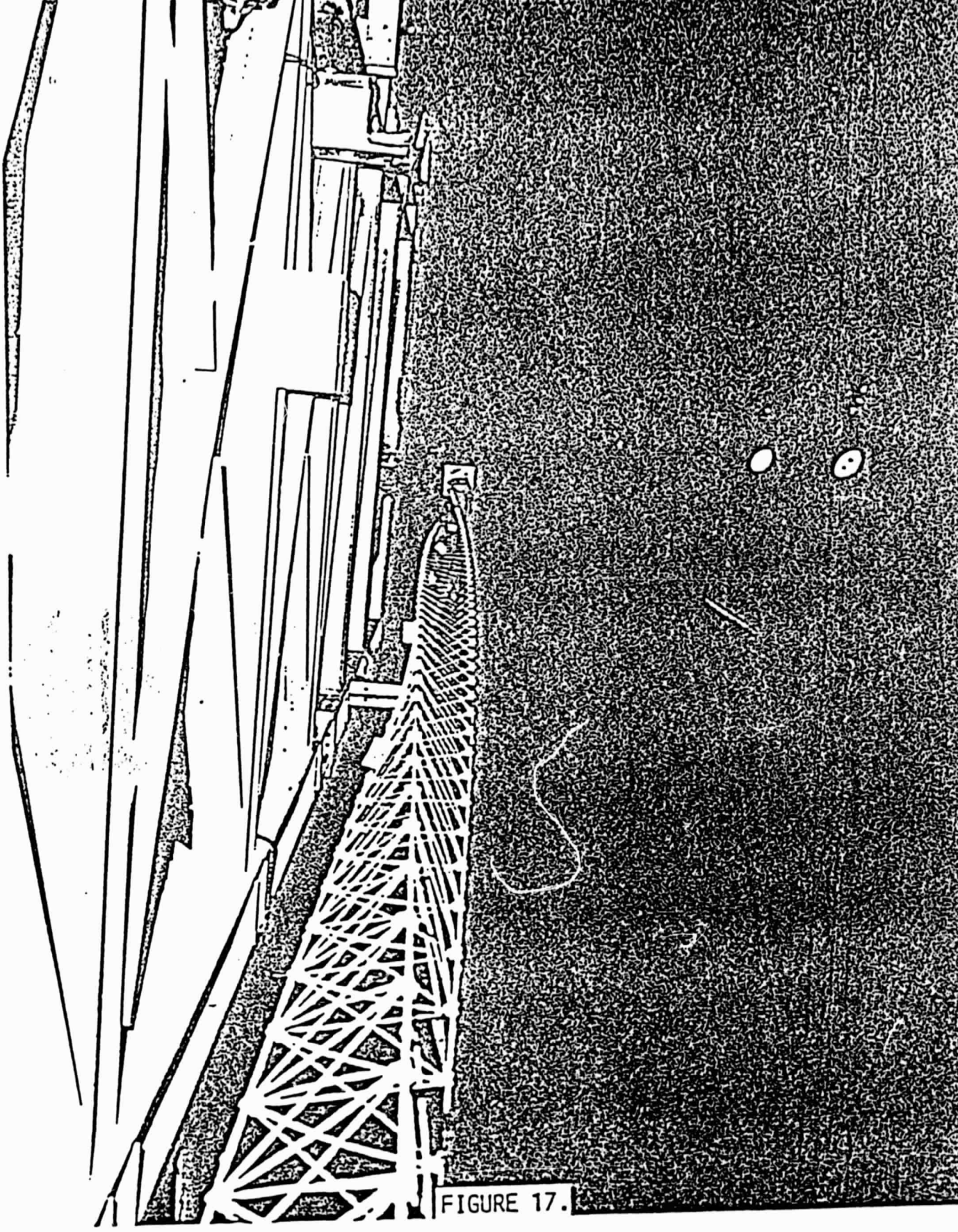

FIGURE 17.

APPENDIX H. ATTACHMENT FROM MR # 23 REVIEW OF TECHNICAL PAPERS

ATTACHMENT A. Review of Technical Papers

A.1 Introduction

A total of twelve (12) memos and papers by Dr. Henry Waites were supplied to Control Dynamics by NASA for the company's information and use in the study of large space structures. Ten (10) of these papers deal directly with control systems, such as observer designs or closed-loop pole placement methods. Of the ten papers there are three principle concepts treated: observers, closed-loop pole placement and a disturbance isolation technique.

Three of the ten papers were selected for critical review as they embodied the three basic concepts. The objectives of the review were:

(1) Check and verify the equations and derivations,

(2) Relate these new techniques to "standards" in the literature,

(3) Identify strengths and weaknesses of the methods,

(4) Determine suitable topics for further study using these methods.

A.2 Observer Techniques

Two Ovservers were compared in the first section: Dr. Waites' Technique as described in the AIAA paper "An Observer for a Deployable Antenna."[1] and the classic Luenberger[2] observer. Their block diagrams are depicted in Figures 1 and 2, respectively.

Dr. Waites' model circumvents the problem usually encountered with observers, the inputs (particularly the disturbances must constitute part of the input to the observer as can be seen in Figure 2. The Waites' model proposes to utilize the rate-of-the-state signals (as measured by accelerometers) that include the vehicle responses to all disturbances as well as the command inputs. Although this idea does indeed eliminate the need to know the characteristics of the disturbance inputs, it also imposes an additional constraint matrix which

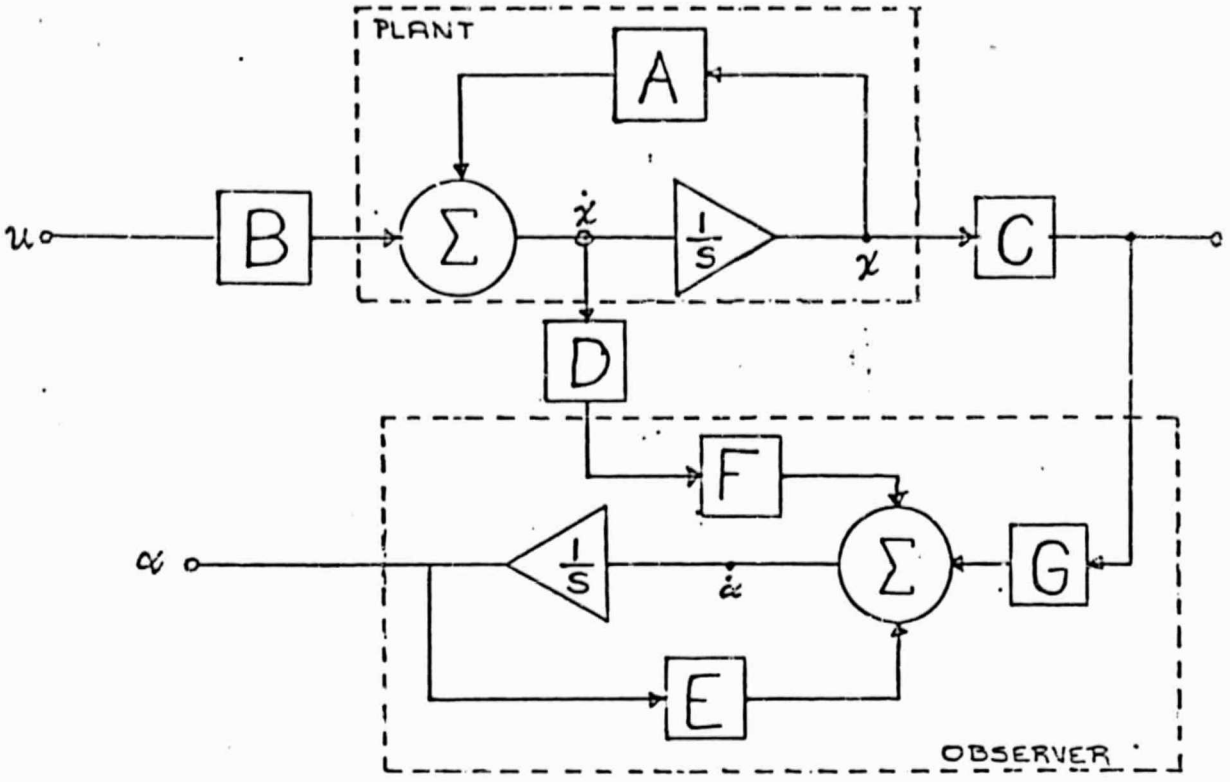

Figure 1, WAITES OBSERVER

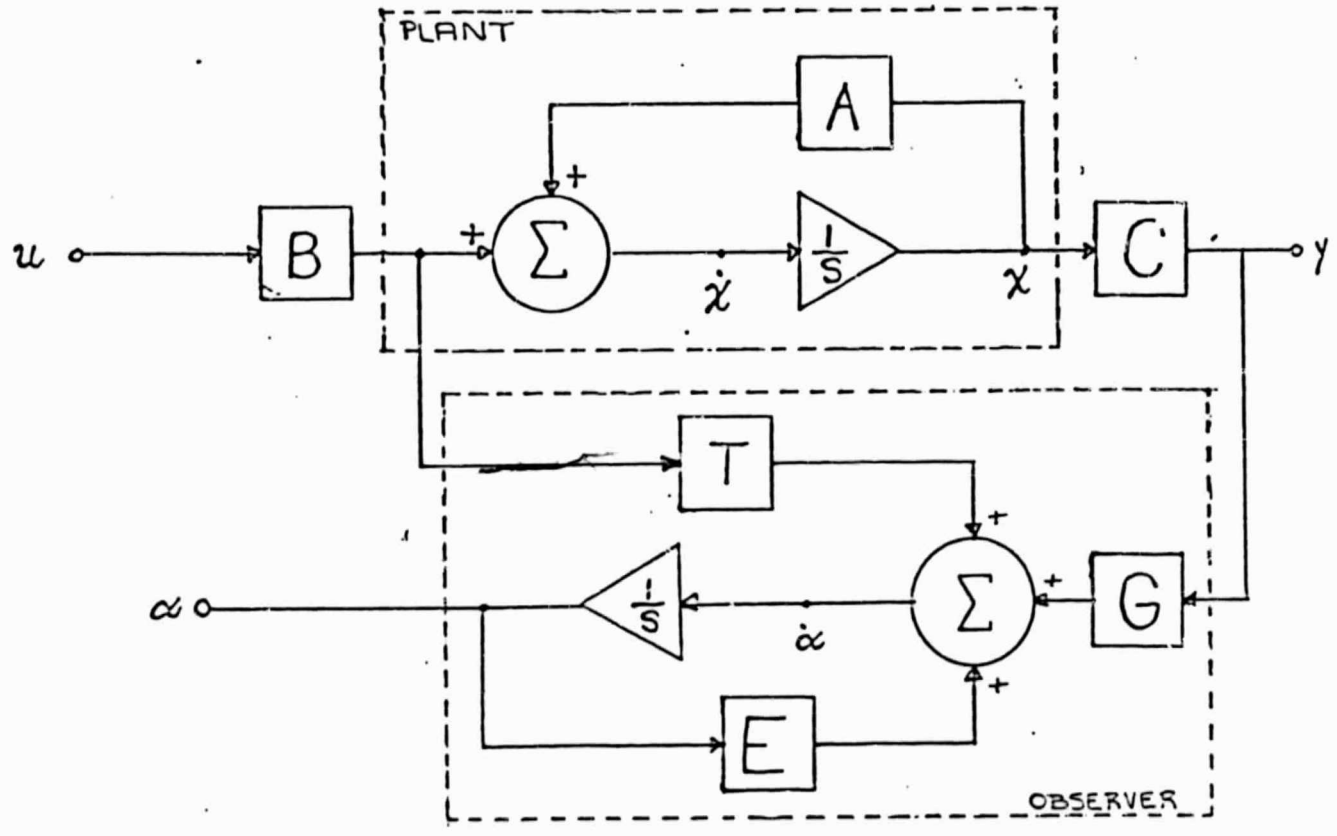

Figure 2, LUENBERGER OBSERVER

may result in a more sensitive system. The main advantage of the Waites' observer is that it provides a means of incorporating the disturbance inputs into the observer by direct measurement.

If time is available for future work, a topic for additional study is the sensitivity of the observer system to variations in sensor locations from the point of disturbance inputs.

A.3 Closed-Loop Pole Placement Methods

This section discusses two methods developed by Dr. Waites in memorandum ED/2-81-1, "Control Pole Placement Method." One is designated a control pole placement method with specified filters and the second is called a filter/control pole placement technique. The equations used by Waites can be expressed in block diagram form as shown in Figure 3. This one diagram is applicable to both methods. In the first method only the gain matrix F is unknown and is determined by Waites' method. The second technique requires the determination of both the gain matrix F and the filter matrix D.

The first step in both methods is to solve the closed-loop system equation of Figure 3 for the characteristic equation, given in matrix form as

$$\Delta(\lambda) = | \lambda I_m - A || \lambda I_p - D - EC(\lambda I_m - A)^{-1} BF | \qquad (10_a)$$

In method I matrices A, B, and C are known and matrices D and E are specified; that is the designer has to select the elements of these two matrices. The elements of D should be distinct from the values of the A matrix. Method II starts with the equation above but only the E matrix is specified. The second determinant of (10_a)

$$\Delta(\lambda i) = | \lambda i I_p - D - EC(\lambda i I_m - A)^{-1} BF |$$

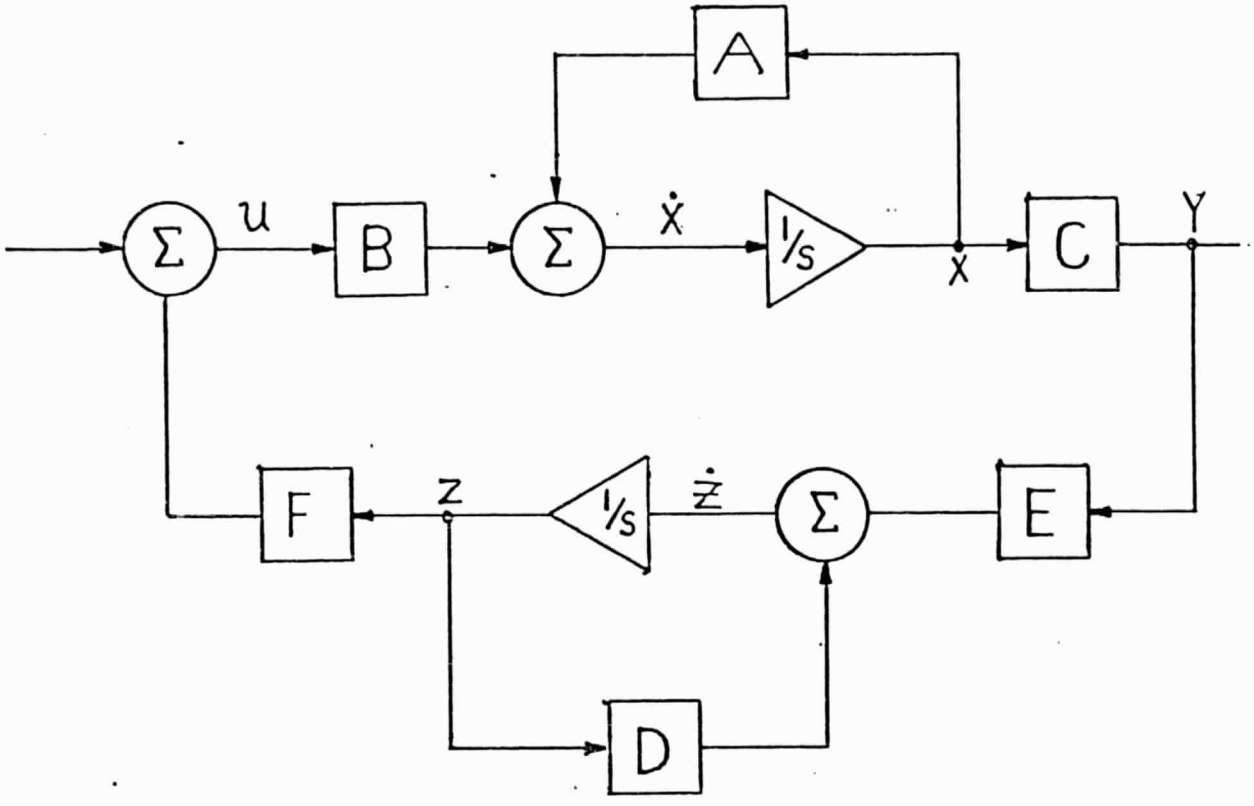

Figure 3. WAITES POLE PLACEMENT METHODS

SYSTEM EQUATIONS

$\dot{x} = Ax + Bu$

$y = Cx$

$\dot{z} = Dz + Ey$

$u = Fz$

is solved for any row, by equating that row to zero. This will require the designer to select a maximum of r + p λi's in order to solve for the resulting elements of D and F. As with almost any design technique, in order to use these methods a considerable amount of experience with the methods will be required. Also a solution for matrices D and F does not necessarily yield a state closed-loop system, as can be seen from Waites' simple example in the paper which has the unspecified closed-loop pole in the right half-plane.

Dr. Waites' derivation was examined extensively and is correct. As can be seen from the block diagram of Figure 3, the system equations yield a typical system with a filter and a couple of gain matrices in the feedback loop. In method I after the selection of a specific number of closed-loop poles the open-loop poles of the filter are selected arbitrarily and then solved for the gain matrix F.

In method II the closed-loop poles are selected and then the open-loop poles of the filter are found along with the elements of the gain matrix F. Some questions remain regarding this method, such as gain values, performance, and stability characteristics. These methods may provide techniques that can be used to rapidly establish a satisfactory control system since they were developed specifically for computer implementation; but as with most new design techniques, more experience using the methods may be necessary. An obvious area for further study of these techniques would be a computer oriented procedure to map the possible boundaries of the unassigned closed-loop poles as a function of the assigned poles. With such a procedure, more information would then be available regarding system stability and performance.

A.4 Disturbance Isolation Controller

The controller described in memorandum ED/12-81-5, "Disturbance Isolation Controller", is another application of observer theory. In developing the

example given in the memo, Dr. Waites defines a generic model. This model is shown with solid lines in Figure 4. The observer of Figure 4 appears to be a combination of a Luenberger and modified Waites observers. The dashed lines in the figure represent one possible implementation of the disturbance isolation feature for the example model.

An example is given in the memo to illustrate the control scheme. This example starts out with an eighteenth order unobservable system. By manipulating the equations the system is reduced to a twelve order observable system and arranged in state variable format.

To implement the disturbance isolation feature, three gain matrices are placed in the feedback loops as shown with dashed lines in Figure 4. These gain matrices are shown as K, U and T, where:

$K = [0\ 0\ -K_0\ -K_1]$

$U = [0\ (m_{32} - m_{31}\ dsm)\ 0\ 0]$, and

$P_T = [m_{31}\ m_{31}\ dsm\ 0\ ]$

(these symbols K, U and P_T are not used in Waites memo).

Waites uses the reduced order example model to develop the observer then he returns to the full-order model to demonstrate the disturbance isolation feature and this raises a question regarding the disturbance vector F. As can be seen from Figure 4, the input Z to the observer is the sum of Px and P_D F. The x signals are assumed to be measured with accelerometers but there is no apparent assumed method for measuring F. Regular disturbances like thruster firings can be characterized, but random disturbances such as astronaut movements are more difficult to model.

An area for possible further study would be to define a suitable system model, develop a disturbance isolation controller, and then conduct a system

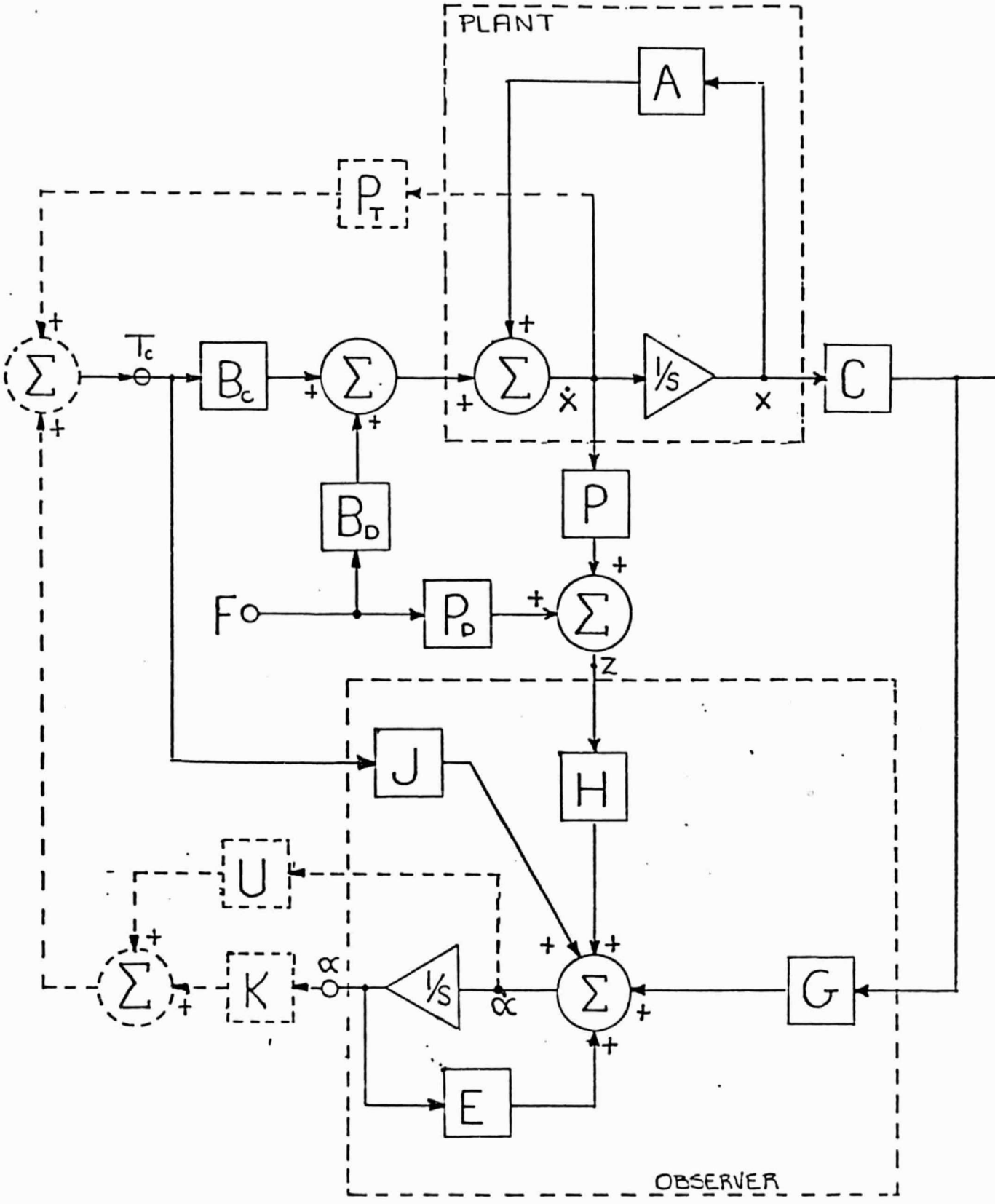

Figure 4 DISTURBANCE ISOLATION CONTROLLER

performance evaluation by characterizing the disturbance function with known and unknown components.

A.5 Summary

A characteristic of the methods reviewed that have not been discussed is the robustness of the techniques. That is, how will the closed-loop system perform for the expected uncertainties in the parameters of the system's state equations? The only way to answer such a question is with realistic case studies. Because of the apparent complexities of the Waites observer and the disturbance isolation controller, it is expected that these two methods will not exhibit as much robustness as the pole placement method.

REFERENCES

1. "An Observer For a Deployable Antenna," H. B. Waites, 2nd AIAA Conference on Large Space Platforms, Feb. 2-4, 1981, San Diego, California.

2. "An Introduction to Observers," David G. Luenberger, IEEE Transactions on Automatic Control, Vol. AC-16, No. 6, December 1971, pp. 130-136.

Papers and Memorandum by Dr. H. B. Waites

NO.	Title
AIAA 81-0453	An Observer For a Deployable Antenna, Feb. 2-4, 1981, 2nd AIAA Conference on Large Space Platforms
ED 12-81-1	Control Pole Placement Methods, March 2, 1981
ED 12-81-2	Sample-Data Control Pole Placement, March 20, 1981
ED 12-81-5	Disturbance Isolation Controller (DIC), March 25, 1981
ED 12-81-21	An Autonomous Nonlinear Observer, April 15, 1981
ED 12-81-23	Dynamic Chara. of Runge/Kutta . . ., April 15, 1981
ED 12-81-24	An Observer For All Seasons, June 1, 1981
ED 12-81-26	An Observer For a Linear System with noise, Aug. 28, 1981
ED 12-81-31	A Rate of the State Error Bound for a Nonlinear Nonautonomous Observer, Augu. 28, 1981
ED 12-81-34	A Determinant Identity, July 23, 1981
ED 12-81-60	Constraint Equations for Multiple Root Pole Placement, Preliminary
ED 12-81-61	Discretation for A Proportional - Integral - Derivative (PID) Sampled Data Control System, Preliminary

APPENDIX I. GROUND TEST EXPERIMENT FOR LARGE SPACE STRUCTURES

GROUND TEST EXPERIMENT FOR LARGE SPACE STRUCTURES

DANNY K. TOLLISON

CONTROL DYNAMICS COMPANY
HUNTSVILLE, ALABAMA

HENRY B. WAITES

MARSHALL SPACE FLIGHT CENTER
NATIONAL AERONAUTICS AND
SPACE ADMINISTRATION

ABSTRACT

In recent years a new body of control theory has been developed for the design of control systems for Large Space Structures (LSS). The problems of testing this theory on LSS hardware are aggravated by the expense and risk of actual "in orbit" tests. Ground tests on large space structures can provide a proving ground for candidate control systems, but such tests require a unique facility for their execution. The current development of such a facility at the NASA Marshall Space Flight Center (MSFC) is the subject of this paper.

INTRODUCTION

As the U.S. moves into the Shuttle era of space technology, there are numerous proposals from the scientific, civilian and Defense Communities which envision the use of Large Space Structures (LSS). By definition, a LSS is very flexible, lightly damped, and exhibits multiple vibrational modes of very low frequency. Many of the missions alluded to above require high performance from the LSS in areas such as precision pointing and preservation of vibration free image planes. To test the new and various schemes proposed for LSS control, Marshall Space Flight Center (MSFC) is establishing a LSS laboratory in which experimentation with LSS-like structures may be performed. The first experiment to be installed in the laboratory is being developed concurrently.

SYSTEM OVERVIEW

The Ground Test Verification (GTV) experiment is described by the drawing of Figure 1. The first test article will be the ASTROMAST beam as shown. The ASTROMAST is extremely lightweight (about 5 pounds) and approximately 45 feet in length and is constructed almost entirely of S-GLASS.

The test article will be mounted on the faceplate of the Advanced Gimbal System (AGS) engineering model which, along with an additional torque actuator in the azimuth, provides the control inputs for the system. The azimuth gimbal also provides a means of rotating the entire experiment manually to produce different test scenarios. The ASTROMAST will be gravity unloaded by a cord extending downward from the base excitation system of the ASTROMAST to the tip. The tension in this cord will be adjustable to provide a means of "tuning" the structure.

The AGS will be supported by the base excitation system of the beam containment structure which will be free to translate in the horizontal plane and will include hydraulic actuators to provide translational disturbance inputs to the test fixture. These disturbances will represent Astronaut push-off or RCS (Reaction Control System) thruster firing.

Six separately packaged inertial measurement assemblies comprise the control system sensors. Two of the packages, containing three axis translational accelerometers, are identical. One will be mounted on the mast tip, and the other on the AGS side of the base excitation system. Three other packages contain ATM (Apollo Telescope Mount) rate gyros and will be installed on the AGS faceplate. The sixth package, the Kearfott Attitude Reference System (KARS), will be placed at the mast tip along with the accelerometer package.

The signals from these instruments will be read by the COSMEC I data gathering and control system, and processed according to the control strategy under scrutiny. The control actuator signals will then be transmitted to the AGS as inputs to the dynamical system.

The COSMEC I will be interfaced to a Hewlett Packard HP9845C desktop computer which will store data as it is collected during a test run, and then provide post experiment data reduction and display off-line. The controller inputs and outputs (measurements and commands) can be recorded at each sample period or at some multiple of sample periods.

SUBSYSTEMS

The subsystems which comprise the LSS/GTV experiment fixture as described are currently in various stages of development at NASA MSFC. Thorough verification of each of the subsystems in controlled test environments comprises a significant part of the preliminary system testing. The subsystems will not only be tested individually, but will be tested in an integrated laboratory environment where each of the subsystems will interact with the others in a

manner much as if an actual test article were being used. Such testing is designed t ensure proper operation of the complete test fixture upon assembly.

ADVANCED GIMBAL SYSTEM

The Advanced Gimbal System (AGS) is a precision, two axis gimbal system designed for high accuracy pointing applications. The AGS gimbals serve the elevation plane and a third gimbal has been added to the system in the azimuth. The AGS receives torque commands from the COSMEC I data and control system in the form of analog inputs over the range of -10 to +10 volts. Because the AGS servo amplifier outputs a current which causes an applied torque proportional to the current, the control algorithms used in the COSMEC I must be designed to produce torque command signals. The AGS gimbal torquers can generate 37.5 ft.-lbs. of torque and the azimuth torquer can generate 13.8 ft.-lbs.

COMPUTATIONAL ELECTRONICS

The COSMEC I is an AIM 65 based (MC6502 processor) micro system which is used to handle data from the control system sensors, output commands to the control system actuators, transmit data for storage to the HP 9845C desk-top computer, and implement the control and inertial strapdown algorithms. The COSMEC I uses special hardware and software to allow the handling of a variety of devices (sensors,actuators,etc.) in real time. It also makes use of four hardware arithmetic processors to reduce computation time.

The COSMEC I "reads" a variety of types of sensor output signals via interface cards which are an integral part of the COSMEC I system. These cards allow the COSMEC I processor to interface with each of its peripherals in a similar manner.

The software used in the COSMEC I system may be separated into four basic groups: 1) utility software for handling the various hardware cards which interface to instruments, 2) software to implement the control algorithm, 3) software to implement the inertial strapdown algorithm, and 4) initialization and startup software to ready the instruments and equipment for a test.

The digital controller software for the first ground test experiment will implement a linear discrete multivariable controller having multiple inputs and outputs. The controller will be in state variable form and will be programme so that the system matrices are initial input data to the program and can be stored on tape and easily changed.

Because the inertial measurement instruments measure with respect to inertial reference space, there is a natural bias in the measurements due to the acceleration of gravity and earth's rotation. That is, in the earth based experiment the accelerometers measure about one g acceleration downward and the rate gyros measure about 15 deg/hr rotation while at rest with respect to the laboratory reference frame. The inertial strapdown algorithm provides a means of removing this bias from the measurement instruments.

INERTIAL MEASUREMENT ASSEMBLIES

Three different types of inertial measurement assemblies are planned for use on the Ground Test Verification structure in the first experiment: the Kearfott Attitude Reference System (KARS), the Apollo Telescope Mount (ATM) rate gyros, and two accelerometer packages developed by NASA. Each of the instrument packages generates signals in a particular form different from the other instruments as was mentioned in the section dealing with the COSMEC I interface cards. These different signal types are discussed in the following as each of the instruments is discussed individually.

The Kearfott Attitude Reference System (KARS) is an attitude measurement system designed for use in the U.S. Army remotely piloted vehicle. It provides measurement resolution of 13.9×10^{-3} deg/sec in the pitch and yaw axes (axes transverse to the ASTROMAST) and 25.0×10^{-3} deg/sec in the roll axis (axis along the length of the ASTROMAST). The dynamic range of the rate gyro outputs of the KARS is 40 deg/sec in pitch and yaw and 70 deg/sec in roll. Because of its light weight, (8.9 pounds) the KARS will be used as the mast tip rotation sensor in the first ground test experiment.

The output signals of the KARS are in the form of asynchronous digital pulses. One signal, the change in angular position in yaw for instance, requires two channels; one for pulses representing positive rotation and the other for pulses representing negative rotation. The COSMEC I system accumulates the pulses over a 20 millisecond period to produce measurements of the angular rate and position of the ASTROMAST tip.

The Apollo Telescope Mount (ATM) rate gyro packages are designed to measure small angular rates very precisely. Each package measures angular rate in one axis with resolution finer than 0.5×10^{-3} deg/sec and offers a dynamic range of ± 1.0 deg/sec. The ATM rate gyro packages will be mounted on the faceplate of the engineering AGS so that they will measure the rotation of the base of the test article.

The output signals of the ATM rate gyro packages are ±45 volt analogs and are handled by the analog to digital converter card of the COSMEC I system where they are converted to 12 bit binary words.

Two identical accelerometer packages will be used on the ground test experiment fixture in the first test. One package will be placed on the mast tip along with the KARS and the other on the test fixture base excitation system as shown in Figure 1. The accelerometers provide resolution finer than .0001 g and a dynamic range of ± 3 g with a bandwidth of 25 to 30 Hz.

The signals from the accelerometers are

different from either those of the KARS or the ATM rate gyros. As in the case of the KARS, two channels are required for each of the degrees of freedom of the accelerometer package, i.e., six channels per accelerometer package. One channel of each pair carries a 2.4 kHz. square wave synchronization signal and the other channel carries the acceleration information. Zero acceleration is represented by a signal identical to that of the synchronization channel, positive acceleration by an increase in frequency, and negative acceleration by a decrease in frequency as compared to the synchronization channel. As in the cases of the other instruments, these signals are monitored by a hardware card in the COSMEC I system.

BEAM CONTAINMENT STRUCTURE

The beam containment structure includes the base excitation system, the disturbance actuators and signal source(s), and power supply for the entire test fixture. This is essentially that equipment required of a laboratory to carry out dynamic testing of structures such as the ground test experiment. As depicted in Figure 1, the beam containment area can accommodate structures approaching 120 feet in height. Access is provided at various levels along the structure via catwalks. Also the control room for experimental operations is at a position about 50 feet above the floor of the test facility, thus making the experiment easily accessible.

The base excitation system for the GTV experiment incorporates a linear bearing arrangement which is designed to restrain the experiment as little as possible in the two translational degrees of freedom while allowing no rotation. Translation of the base of the AGS via the base excitation system provides the means of applying disturbances to the system. The base excitation system uses high pressure hydraulic system to effect force inputs to the structure.

SYSTEM MODELING AND PERFORMANCE

For purposes of system studies and controller design, an analytical model of the Ground Test Experiment is necessary. Modeling of the Ground Test Verification (GTV) experiment was carried out in two distinct stages. The first stage involved modeling the ASTROMAST itself as it would be tested in the first open loop modal test, i.e., the beam alone in a cantilevered position. (See Table 1 for a listing of the resulting modal frequencies.) This produced modal frequencies, mode shapes, and mass integrals which were used in the second stage of the modeling process to develop, through modal synthesis, a model of the entire GTV experiment including the AGS and the beam containment structure. The modal frequencies resulting from the analytical model of the complete experiment appear in Table 2.

To date, modal tests have been conducted on the ASTROMAST beam alone in a cantilevered configuration at Marshall Space Flight Center. So that gravity would have as little effect as possible on the test results, the ASTROMAST was cantilevered in a hanging position. When fully deployed, the ASTROMAST exhibits a longitudinal twist of about 280 degrees which contributes to coupling between the torsional and bending modes.

Measured modal frequencies resulting from the tests are shown in Table 3 along with the predicted modal frequencies and percentage errors. The errors are reasonable given the limited amount of knowledge about the percent composition of the S-GLASS composite and the unexpected twist which was not included in the mathematical model.

SUMMARY AND FUTURE DEVELOPMENT

Marshall space Flight Center is developing a Large Space Structure Ground Test Verification experiment facility having adequate fidelity and flexibility to accommodate the demands of LSS control theory testing. The first experiment is in the subsystem verification and integration phase with the first "all up" test targeted for spring 1984. This test employs the ASTROMAST, a lightweight S-GLASS composite deployable beam structure, as the test article and is cited to prove out centralized and distributed sensor control strategies.

Future plans for the facility include the test of more complicated structures and sensor/actuator arrangements. The first of these will be the addition of structural hardware to the existing ASTROMAST in order to produce a structure having more LSS-like characteristics.

MODE	FREQUENCY (HZ)
FIRST BENDING MODE	0.618
SECOND BENDING MODE	3.917
THIRD BENDING MODE	11.179
FIRST TORSIONAL MODE	6.877
SECOND TORSIONAL MODE	20.628
THIRD TORSIONAL MODE	34.373

Table 1. Modal Frequencies of Cantilevered ASTROMAST Beam Model in Bending and Torsion.

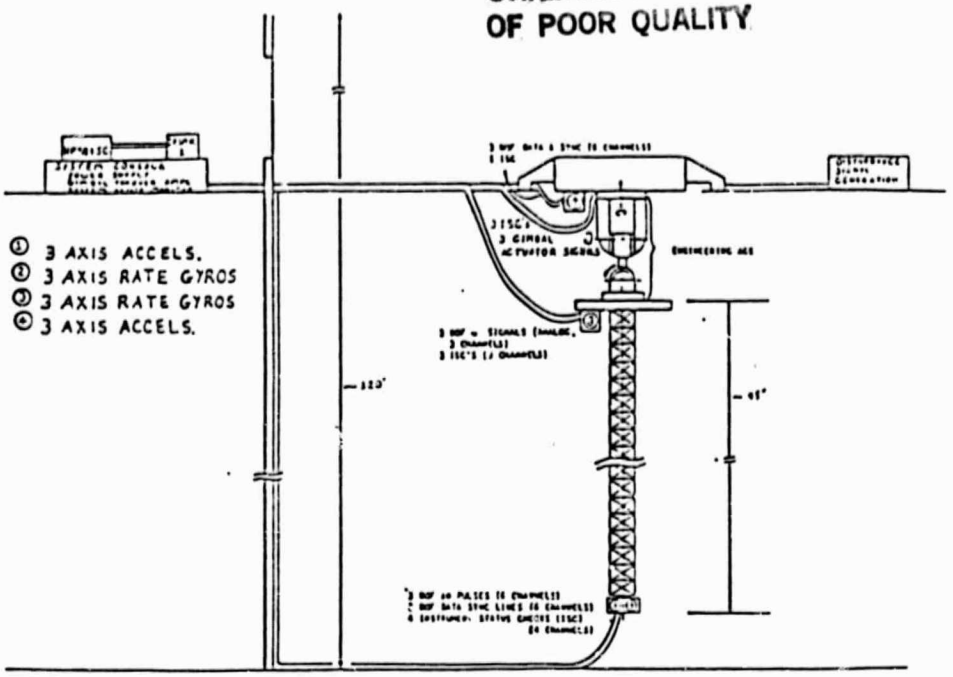

Figure 1. NASA Marshall Space Flight Center LSS/GTV Experiment.

MODE NUMBER	MODE FREQUENCY (Hz)
1	.94
2	1.16
3	1.80
4	3.25
5	3.71
6	9.21
7	9.23

Table 2. LSS/GTV Experiment Structure Mathematical Model Flexible Body Modes.

MODE FREQUENCIES (Hz)		MODE TYPE		% ERROR
Exp	Analytical	Exp.	Analytical	
.555	.618	b	b	11
3.43	3.92	b	b	14
4.02	6.88	t	t	71
8.83	11.2	b	b	27
12.23	20.6	t	t	68
15.71	34.4	b	t	119

Table 3. Summary of Analytical and Experimental Modal Frequencies and Mode Types. (b - bending, f - torsion)